To Dr. Collins,
with the compliments
of Salmeron.
Geneva, 12/5/59.

A CLOUD CHAMBER STUDY OF THE PRODUCTION OF STRANGE PARTICLES

-by-

R.A. SALMERON

submitted to the Victoria University of Manchester
as a thesis for the degree of Doctor of Philosophy

February, 1958

5363/E/p

PREFACE

In December 1950, a group from the Physics Department of the University of Manchester under the leadership of J.A. Newth installed a magnet cloud chamber at the Jungfraujoch Research Station (3500 m high), in Switzerland, with the aim of studying V-particles produced by cosmic radiation. In August, 1955, the control of the experiment passed to CERN, in Geneva. The author has been a member of the team since June 1953, and has spent fifteen months at the Jungfraujoch engaged in the running of the apparatus.

On the average four people have been working permanently on the analysis of the photographs which have been used for the study of many different problems.*) Since 1953 the author has participated in six works of the team((1)-(6)) and in an experiment which is now running. An attempt to obtain information about the production of strange particles had been made by the author in

---

*) A complete list of the works published by the group is given in reference (5).

collaboration with G.D. James.[1] That work, which consisted of the analysis of 19 photographs, was done at a time when very little was known about the production of strange particles, and can be regarded as a preliminary phase of the present work. This thesis, however, is the personal work of the author. Of the 72 photographs analysed, some have been measured with the help of Dr. A. Zichichi, and 4 have been extensively discussed by the whole group[4] after having been measured and interpreted by the author. The analysis of the 19 events reported in (1) has been neglected, and they have been remeasured and reanalysed by the author.

* * *

C O N T E N T S

		Page
PREFACE		i
INTRODUCTION		
1.	History	1
2.	The Aim of the Present Work	2
3.	Nomenclature	4
4.	Masses	5
5.	Known Hyperons and K-mesons	5
6.	Some Cases of Associated Production Experimentally Observed	7
CHAPTER I		
	THE EXPERIMENT AND THE MEASUREMENTS	
1.	The Apparatus	9
2.	The Experimental Arrangement	10
3.	Reconstruction of the Geometry of the Event	12
4.	Ionisation Estimates	13
5.	Measurement of Momentum	16

CHAPTER II

SUMMARY OF SOME THEORIES OF K-MESONS AND HYPERONS

		Page
1.	Introduction	19
2.	The Gell-Mann Model	20
3.	D'Espagnat and Prentki's Formalism of the Gell-Mann Model	27
4.	Sachs' Classification of the Fundamental Particles	30
5.	The Question of Conservation of Parity	34

CHAPTER III

DYNAMICS OF SOME REACTIONS IN WHICH HYPERONS AND K-MESONS ARE PRODUCED

1.	Introduction	36
	Part I - TWO-BODY REACTIONS	
2.	General Formulae	37
3.	Particular Cases of p_N and φ_{AN}	40
4.	Particular Reactions of the Type : $A + N \rightarrow Y + B$	41
5.	Relationship Between φ_Y and p_Y in the Extreme Relativistic Limit	42
6.	Maximum Angle of Emission of the Hyperon in the E.R.L.	44
7.	Minimum Momentum of the Hyperon in the E.R.L.	45

CHAPTER III (cont'd).

		Page
8.	The E.R.L. for Other Particles	46
9.	The Influence of the Fermi Energy of the Nucleon	50
10.	Endothermic and Exothermic Reactions	51
11.	K-mesons Produced in Two-Body Reactions	55
	Part 2 - n-BODY REACTIONS	
12.	Introduction	56
13.	Condition for the Maximum Momentum of a Secondary in the C.M.S.	58
14.	Nucleon-Nucleon Collisions	62
15.	Threshold Energies	64

CHAPTER IV

THE EXPERIMENTAL DATA

1.	Yield of the Jungfraujoch Experiment	66
2.	Selection of the Events	67
3.	Analysis of the Neutral V-particles	72
4.	Analysis of the Charged V-particles	76
5.	Identification of the non-decaying K-mesons	77
6.	Measurements Made on the Events	78
7.	Classification of the Events	79

CHAPTER V

EVENTS WHICH DO NOT CONSIST OF TWO IDENTIFIED K-MESONS

		Page
1.	Introduction	88
2.	Events in which Two Neutral V-Particles were Produced in the Plates	89
3.	Events in which Two Neutral V-particles were Produced above the Cloud Chamber	99
4.	The Cases of One Neutral V-particle Associated with One Charged V-particle	104
5.	Comments on the Other Events	108
6.	Conclusions	110

CHAPTER VI

EVENTS WHICH CONSIST OF TWO IDENTIFIED K-MESONS

1.	Introduction	112
2.	Events Observed in the Jungfraujoch Experiment	114
3.	Event VB 536	117
4.	Event SN 1534	124
5.	The Production Reactions	128
6.	Conclusion	134

CHAPTER VII

EVIDENCE FROM SINGLE V^0-PARTICLES

		Page
1.	Numbers of Λ^0- and θ^0-particles Produced in Carbon, Copper and Lead	135
2.	Normalisation of the Numbers of Events Produced in Carbon and Copper	139
3.	The Interactions produced by Secondary π-mesons and the bias in the observation of θ^0-mesons	141
4.	Conclusions	144

CHAPTER VIII

DISCUSSION

1.	Introduction	149
2.	The Number of Pairs (Λ^0 θ^0) Produced in the Copper Plate	152
3.	The Experimental Observation of the Production of Pairs of (K^+ $\overline{K}^0$)- and (K^0 $\overline{K}^0$)-mesons	152
4.	The ratio $\frac{N(\theta^0)}{N(\Lambda^0)}$ for Carbon, Copper and Lead	153
5.	The Spectrum of the θ^0-mesons in Cosmic Ray Experiments	153
6.	The Spectrum of the Λ^0-particles in Cosmic Ray Experiments	155
7.	The Positive Excess of K-mesons	157
8.	The High Energy of the Jungfraujoch "Double" Events	159

CHAPTER IX — Page

CONCLUSIONS 160

APPENDIX I ---------- 164

APPENDIX II ---------- 166

ACKNOWLEDGEMENTS ---------- 167

REFERENCES

* * *

INTRODUCTION

1. History

After the discovery of the V-particles by Rochester and Butler[7] in 1947, four years were needed to accumulate a minimum of experimental information which could show, at least vaguely, in which direction to look for the mechanism of production of these particles. In 1951, Nambu, Nishijima and Yamaguchi[8] made the brilliant remark that it is difficult to reconcile the long mean lifetime of the V-particles with their copious production if they are produced singly in nuclear interactions, and put forward the idea that V-particles are produced in association. As it will be seen in Chapter II, the idea was developed in other theoretical works by Pais, Gell-Mann, Nakano and Nishijima.

The first experimental observations of nuclear interactions which produced two associated V-particles were reported by Lal, Pal and Peters[9] in 1953; the events were found in nuclear emulsion in a cosmic ray experiment. In the same year, Fowler, Shutt, Thorndike and Whittemore[10] found in a diffusion cloud chamber an interaction, produced by a π^--meson from the cosmotron

beam, which gave evidence for associated production of a hyperon with a K-meson. Afterwards, other events were found in cosmic ray experiments: Dahanayake et al.[11] De Benedetti et al.[12] Thompson et al.[13] but it was the series of experiments made by Fowler et al[10] from 1953 to 1955 which definitely established the existence of associated production of strange particles. Since 1955 a large amount of information about the production of hyperons and K-mesons at energies not much greater than threshold energies has been obtained by several groups working with accelerators as, for instance, those quoted in references (14) to (28).

2. The Aim of the Present Work

The aim of the present work was to obtain information about the production of hyperons and K-mesons by analysing the photographs of the Jungfraujoch experiment which show more than one strange particle. In spite of the fact that properties of particles and of specific reactions in which particles are produced can be better studied with accelerators than with cosmic ray experiments, the reasons which justify this work are the following :

i) The average energy of the interactions which produced the V-particles of the Jungfraujoch experiment is greater than the

energy available with the accelerators that work at present, and well above the threshold for all the expected production processes.

ii) Several reactions that are expected to occur have never been observed in experiments made with accelerators, partly owing to the comparatively low available energy. Before this work started it was thought that examples of some of them could exist in the collection of photographs of the Jungfraujoch experiment. In fact, the two examples of $\overline{\theta^o}$-mesons(4) were found during the analysis of the events for this thesis.

iii) The Jungfraujoch experiment has 72 photographs which show more than one strange particle; in 47 of them the lines of flight of the strange particles are copunctual. Such a number of events is not negligible at the present stage of our knowledge of the subject.

iv) No other collection of cloud chamber photographs with a comparable number of events obtained in a cosmic ray experiment has been analysed on the lines presented in this work. In fact, very few attempts have been made to explain the production of all strange particles of a cosmic ray experiment. We find in the literature only reports of the work of Ballam et

al.,[35] Trilling and Leighton,[36] Reynolds and Treiman,[37] and reference (1).

3. Nomenclature

The nomenclature used in this thesis is that proposed by Amaldi et al.[29] A Υ -particle will represent a hyperon. Although in the original definition given by Amaldi et al. a K-meson is any particle with mass greater than the mass of the π -meson and less than the mass of the proton, in the last years the expression "K-meson" has been used in the literature to designate specifically the K-mesons with mass about 965 electronic mass. This is justified by the fact that no K-meson with mass significantly different from that has been proved to exist. In the present work "K-meson" or "heavy meson" will designate a particle with mass about 965 electronic mass, unless some remark is made. The expression "strange particle" will designate a K-meson or a hyperon. The anti-particle of a given particle will be indicated by the symbol of the particle with a bar over it.

4. Masses

For the purpose of calculations, the following values of masses have been used. *)

Particle	Mass in MeV/c^2
electron	0.511
$\mu^{\pm}$-meson	105.8
π^{o}-meson	135.0
$\pi^{\pm}$-meson	139.5
$K^{\pm}_{o}$-meson	493.4
proton and anti-proton	938.2
neutron and anti-neutron	939.5
Λ^{o}-particle	1115.0
$\Sigma^{\pm}_{o}$-particle	1190.0
Ξ^{-} -particle	1321.0

5. Known Hyperons and K-mesons

The existence of the hyperons and K-mesons listed below is firmly established. The decay modes mentioned have been experimentally observed. More than one sign written means that all the specified combinations of sign have been observed.

---

*) The most recent estimates of the masses of these particles were given by a special committee organized during the International Conference on Mesons and Recently Discovered Particles, Padua-Venice, September 1957.

	Particle	Decay Mode	
K-mesons	$K^+_{\pi 2}$	$\pi^+ + \pi^0$	
	$K^+_{\mu 2}$	$\mu^+ + \nu$	
	$K^{\pm}_{\pi 3}$	$\tau^{\pm} : \pi^{\pm} + \pi^+ + \pi^-$	
		$\tau^0 : \pi^+ + \pi^- + \pi^0$	
		$\tau' : \pi^+ + \pi^0 + \pi^0$	
	$K^{\pm}_{\mu 3}$	$\mu^{\pm} + \pi^0 + \nu$	
	K^+_e	$e^+ + \pi^0 + \nu$	
	θ^0_1	$\pi^+ + \pi^-$	(18)(30)
		$\pi^0 + \pi^0$	
	θ^0_2	$\pi^{\pm} + e^{\mp} + ?$	(16)
		$\pi^{\pm} + \mu^{\mp} + ?$	
		$\pi^+ + \pi^- + ?$	
Hyperons	Λ^0	$p + \pi^-$	(18)
		$n + \pi^0$	
	Σ^+	$p + \pi^0$	
		$n + \pi^+$	
	Σ^-	$n + \pi^-$	
	Ξ^-	$\Lambda^0 + \pi^-$	

There is only experimental evidence but not proof of the existence of the following particles and corresponding decay modes:

Particles	Decay Mode	
$K^-_{\pi 2}$	$\pi^- + \pi^0$	(31)
K^-_e	$e^- + \pi^0 + \nu$	(2)

6. Some cases of associated production experimentally observed

The following table gives some cases of associated production which have been experimentally observed. The existence of the first six reactions is firmly established, because all particles involved have been identified and the dynamics of the reactions verified. In the other cases, observed in cosmic ray experiments, all strange particles have been identified, but not all the other particles.

Reaction	Target Nucleon	Incident particle from	First observed by
$\pi^- + p \rightarrow \Lambda^0 + \theta^0$	Free	Accelerator	Fowler et al. (10)
$\pi^- + p \rightarrow \Sigma^0 + \theta^0$	"	"	"
$\pi^- + p \rightarrow \Sigma^- + K^+$	"	"	"
$\pi^+ + p \rightarrow \Sigma^+ + K^+$	"	"	Brown et al. (20)
$p + p \rightarrow \Sigma^+ + K^+ + n$	"	"	Block et al. (32)
$\pi^- + p \rightarrow \theta^0 + \bar{\theta}^0 + \pi^- + p$	"	"	Fowler et al. (34)
$? + ? \rightarrow \Xi^- + \theta^0 + \theta^0$	In a nucleus	Cosmic Ray	Sorrels et al. (33)
$? + ? \rightarrow K^+ + K^+ + K^- + (?)$	"	"	Lal et al. (9)
$n + p \rightarrow \theta^0 + \bar{\theta}^0 + p + n(+?)$	"	"	Cooper et al. (4)
$n + p \rightarrow K^+ + \bar{\theta}^0 + n + n(+?)$	"	"	"
$? + ? \rightarrow \Sigma^\pm + \gamma^+ + (?)$	"	"	Lal et al. (9)

CHAPTER I

THE EXPERIMENT AND THE MEASUREMENTS

1. The Apparatus

The apparatus of the Jungfraujoch experiment consists fundamentally of a cloud chamber and a magnet. Details of the construction and operation have been fully described by Newth.(38)

Initially a cloud chamber of dimensions 55 cm x 55cm x 15 cm was used, but later it was replaced by one measuring 55cm x 55cm x 25cm, with about 16 cm illuminated depth.

The magnet is an iron-core type, with copper coils cooled by air. The air-cooling has the advantage of allowing a simpler and cheaper construction than other cooling systems, but on the other hand has the disadvantage of making very difficult the temperature control of the cloud chamber. In order to stabilize the temperature, two water jackets were installed around the chamber (Fig. 1.1). The magnetic induction is on an average 5000 gauss, with a power consumption of about 30 kW, and is uniform to within $\pm 3\%$ in a volume of 60 cm x 60 cm x 30 cm.

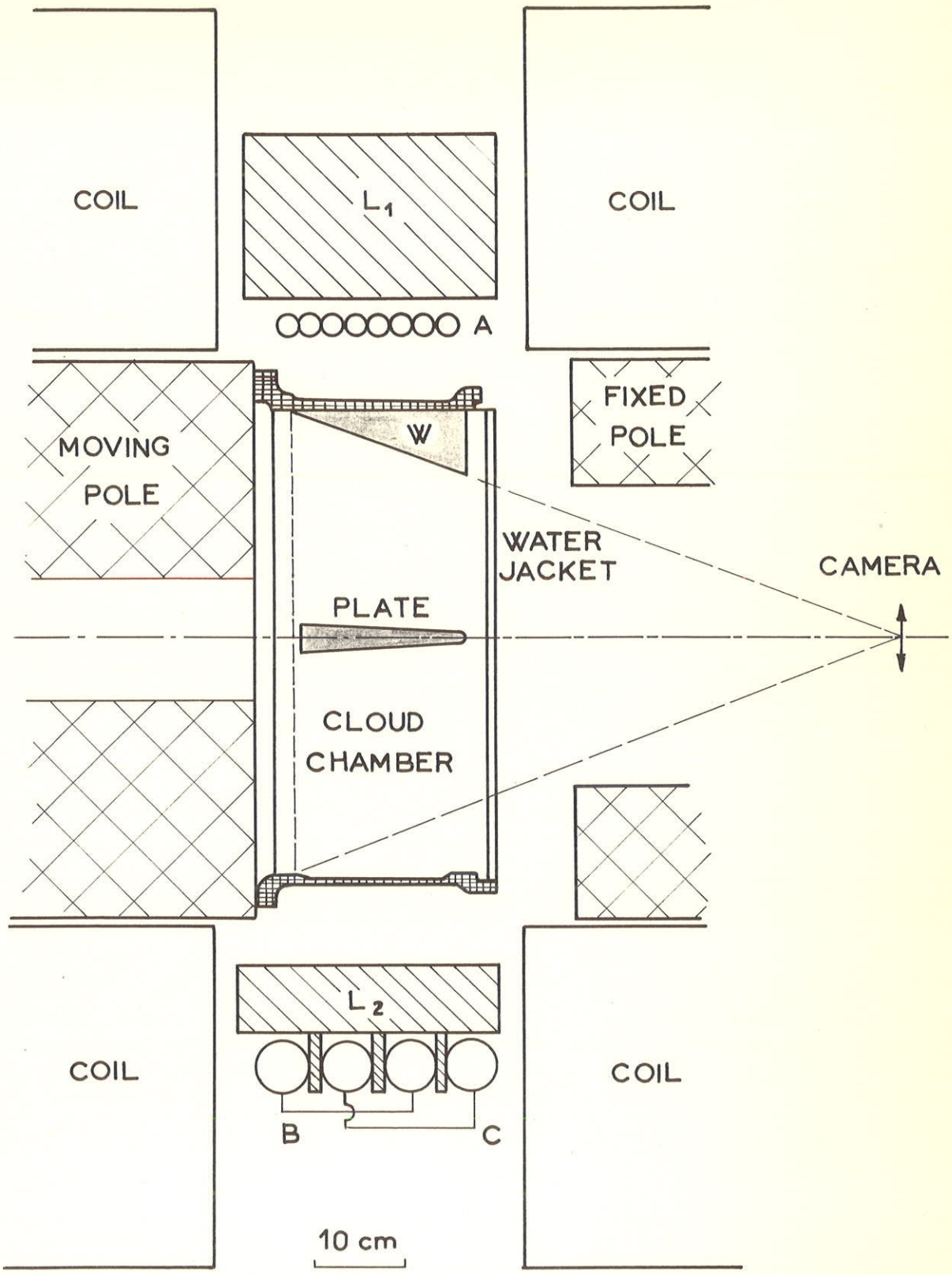
COIL
L1
COIL
A
FIXED
POLE
MOVING
POLE
W
WATER
JACKET
CAMERA
PLATE
CLOUD
CHAMBER
L2
COIL
COIL
B
C
10 cm

Figure 1.1

For the illumination, a flash tube 60 cm long is placed on each side of the chamber. The energy consumption is 4000 joules per tube per discharge. High sensivity recording film has been used for photography (Ilford 5G91). Stereoscopic photographs were taken with a camera which has two large-angle lenses (Leitz Hektor f = 2.8 cm, 1 : 6.3) placed 8.8 cm apart, used with aperture f/9. The mean demagnification is 1/19.

2. The Experimental Arrangement

Since the observation made by Armenteros et al.[39] that V-particles are associated with penetrating showers, in most cloud chamber experiments designed to the study of such particles the triggering of the chamber has been made by a penetrating shower counter selection system. In the Jungfraujoch experiment the selection system was the following (Fig. 1.1):

a) A block of lead L_1, 30 cm high, was placed above the cloud chamber at an average distance of 17 cm from the useful illuminated volume.

b) During part of the time, below this lead block two large proportional counters were placed in parallel. The pulses given by these counters were discriminated in such a way that only

pulses corresponding to an ionisation equal to or greater than four times the minimum ionisation were accepted. During part of the time the two proportional counters were replaced by eight Geiger-Müller counters in parallel, and the pulses given by these counters were accepted only when three or more counters were triggered (tray A).

c) Below the cloud chamber a block of lead L_2, 10 cm high, was placed, and below this lead four large Geiger-Müller counters making two sets of two counters in parallel (trays B and C). The cloud chamber was triggered every time that there was a coincidence between trays A, B and C. With this selection system an average of seven photographs per hour were taken, and 70% of them showed penetrating shower. Details of the proportional counters and of the selection system have been described by Buchanan.(40)(41).

Cosmic ray particles were then used as projectiles which produced nuclear interactions in the lead block L_1. Because many secondary particles produced in these interactions are very energetic and many high energy cosmic ray particles go through L_1 without interacting, in order to increase the number of interactions close to the illuminated volume of the cloud chamber a lead wedge

W with average thickness 5 cm was put at the top of the chamber. The run with the lead targets placed at L_1 and W corresponds to a first phase of the experiment.

In a second phase, a copper plate 1.2 cm thick was placed across the middle of the chamber. Many V-particles produced in this plate have been photographed.

During the second phase, the work which the author had made in collaboration with G.D. James[1] showed that the production of V-particles can be better studied when they are produced in a material of low mass number placed inside the cloud chamber. As a consequence, in a third phase of the experiment the copper plate was replaced by a carbon plate 2.5 cm thick, and the lead wedge by a carbon wedge geometrically similar to the first.

3. Reconstruction of the Geometry of the Event

An optical method was used for the reconstruction. In the Jungfraujoch experiment the plane of the photographic film is parallel to the front glass of the cloud chamber, i.e. the lenses axis are perpendicular to the front glass and to the film. A stereoscopic projector was constructed with two lenses similar to the lenses used in the camera, and separated by the same distance as the two camera lenses (8.8 cm). The two photographs

are simultaneously projected onto a movable screen placed perpendicularly to the lenses axis. The position of a point of the track in space, given by the intersection of the two images of the track, is then marked on the secreen. The points on the screen represent the orthogonal projection of the event on a plane parallel to the front glass, i.e. gives two coordinates for every point. A scale which reads for every point the distance from the screen to the lenses gives a third coordinate.

Two drawings with scale 1 : 1 are then made : the orthogonal projection on the plane of the screen and the orthogonal projection on a plane perpendicular to the first. After having the two orthogonal projections of the event, the angle between two lines (as the decay angle of a V-event) or the angles between two planes can be calculated by the classical methods of analytical geometry. The displacement of the points due to the expansion of the chamber is taken into account. With our optical system the position of a point on a track can be determined with an average error of 1 mm x 1 mm x 2 mm. The error in the decay angle of a V-event is in most cases less than 2^{o}.

4. Ionisation Estimates

With a cloud chamber immersed in a magnetic field, the mass of a particle may be determined by the combined measurements

of its momentum and its ionisation. For a given electrical charge the ionisation of a particle is a function of its velocity and of the density of the gas of the chamber.

The measurement of ionisation requires the measurement of the number of ions formed along 1 cm of the path of the particle. Two techniques have been developed during the past few years to measure in a magnet cloud chamber the relative ionisation, i.e. the ratio between the ionisation of a particle and that of another particle at minimum ionisation: the drop counting technique (Barker et al.,[42] Fretter et al.,[43]) and the photometric method (Butterworth[44]). Both methods allow the measurement of the relative ionisation with an error that is in most cases less than 20%. This accuracy in the measurement of ionisation is very high, and only has a meaning when the momentum of a particle can be measured with corresponding high accuracy, for instance when a momentum of the order of 1 GeV/c can be measured within an error of about 5%.

Neither of the two techniques has been used in the Jungfraujoch experiment, for the following reasons:

a) The use of drop counting would require to stop the experiment (in order to prepare the cloud chamber and the photographic system for the technique), at a time when the

experiment was running at high efficiency, and would require the use of 16 times more recording film than is normally used (Newth[38]).

b) The use of the photometric method would require the construction of special measuring apparatus, and as the measurement of the ionisation corresponding to one single track requires several hours of work, one physicist would have to be permanently displaced to do this work. Moreover, with the wide photographic angle used for the Jungfraujoch cloud chamber the conditions of photography vary greatly from side to side of the chamber. This makes necessary the measurement of reference tracks close to the track of interest.

c) As will be described below, one of the handicaps of the Jungfraujoch apparatus is the relatively low accuracy in momentum measurement: a further effort would then have to be made in order to improve the accuracy in momentum measurement, otherwise the accuracy in ionisation measurement would be meaningless.

As a consequence of this situation the ionisation of a particle was never measured in the Jungfraujoch experiment. It was always estimated between two limits, by a visual comparison

of the structure of the track with the structure of tracks of particles supposed to be at minimum ionisation on the same photograph. For this comparison a straight track was supposed to be at minimum ionisation and an electron with momentum between about 30 and 80 MeV/c at 1.3 times minimum.

5. Measurement of Momentum

Two methods have been employed for the measurement of the curvature of tracks.

a) The photograph was projected on a screen and the curvature of the track was compared with that of standard curves. This method was only used when the track was long (more than 15 cm in space), had small dip (angle between the direction of the track and a plane parallel to the front of the chamber) and the quality of the photograph was good.

b) A second method was the measurement of the curvature of the track image on the film with a travelling microscope. This has the great advantage of allowing an accurate measurement of curvature whatever the dip of the track may be and a better judgement of the quality of the individual tracks as far as distortions are concerned.

Due to the fact that the image of the track is the conical projection of the track on the film, and not its orthogonal projection, a correction must be applied to the measured curvature. The magnitude of this correction is a function of the dip and length of the track and of its position relatively to the lens axis. This correction was sometimes calculated by applying an approximate formula due to Barker,(45) but when the dip of the track was large (greater than 30°) or the photograph showed some particularly interesting feature, a more elaborate method due to the author was applied. The author's method has the advantages of determining the correction factor with great accuracy and of allowing a systematic study of the qualities of the track. (Unpublished)

Generally in a cloud chamber immersed in a magnetic field, the most important source of error in momentum measurement is the distortion of the tracks as a consequence of thermal convection of the gas. This is due to temperature gradients inside the cloud chamber, which appears essentially because the cooling of the coils is not equally efficient in all parts. This situation is still worse when the coils are air-cooled, as is the case with the Jungfraujoch magnet. The distortion of the track is related to the maximum detectable momentum, which is an

index of the quality of a magnet cloud chamber as a detecting instrument. In the Jungfraujoch cloud chamber the maximum detectable momentum is 4 GeV/c for a vertical track 25 cm long. No experiment has ever been made with this cloud chamber to study the variation of the maximum detectable momentum as a function of the track length. The pessimistic assumption has been made that the maximum detectable momentum varies with the square of the track length. It must be emphasized that the relatively low value of the maximum detectable momentum imposed the method of analysis of the photographs which is described in Chapter IV.

Besides distortion, the other sources of error on momentum are the scattering of the particle by the gas of the cloud chamber, the uncertainty in the magnetic induction and the diffusion of the ions along the trajectory of the particle. All errors on momentum have been calculated and combined according to the method described by Blackett.(46)

* * *

CHAPTER II

SUMMARY OF SOME THEORIES OF K-MESONS AND HYPERONS

1. Introduction

The first attempts to explain the production and the decay of K-mesons and hyperons were made in 1951 by some groups of Japanese theoreticians.[8][47] Among these, Nambu, Nishijima and Yamaguchi deserve great merit for calling attention to the important problem of reconciling the abundance of production of those particles with their long mean lifetimes. As a possible solution to this problem they suggested that in collisions between pions and nucleons, or between nucleons and nucleons, K-mesons could be produced in association, rather than singly. Pais in 1952,[48] laid emphasis on the idea of associated production and began a series of studies on these lines.[49] In 1953, Gell-Mann[50] and, independently, Nakano and Nishijima[51] proposed a scheme to systematise the production and decay of heavy mesons and hyperons. The ideas of Pais, Gell-Mann, and Nakano and Nishijima, gradually refined with the accumulation of

experimental results, allowed Gell-Mann[52] to formulate a model of the new unstable particles which has been very successful. A summary of this model is given below, as well as of the ideas on this subject of d'Espagnat and Prentki,[53] and Sachs.[54]

Goldhaber[55] developed a theory, based on a compound hypothesis for hyperons and heavy mesons. The results are the same as those of the Pais, Gell-Mann and Nishijima model.

Salam and Polkinghorne,[56] and Schwinger[57] made theories which in some aspects give results different from those expected in the Pais, Gell-Mann and Nishijima model. As recent experimental facts disagree with these theories, they will not be discussed here.

2. The Gell-Mann model

In what follows we give a summary of the Gell-Mann model. The word "meson" will designate only π - and K-mesons; the μ -mesons will be called muons. The K-mesons and hyperons have the general denomination of "strange" particles and all the other particles that of "ordinary" particles. The nucleons and hyperons will be called "baryons", and their anti-particles "anti-baryons".

i) Following Pais, the interactions of the fundamental particles are classed as strong (or fast), electromagnetic, and weak (or slow). The strong interactions are those responsible for nuclear forces and the production of mesons and hyperons. They cannot occur with muons, electrons and neutrinos.

Electromagnetic interactions are those through which the photon is linked to all charged particles, real or virtual.

The weak interactions are those responsible for β - decay, the slow decays of hyperons and K-mesons, the decay of the muon and the absorption of the muon in matter.

ii) It is postulated that in any interaction or transformation of the fundamental particles the number of baryons minus the number of anti-baryons (the "baryonic number") is kept constant.

iii) Peaslee[58] had suggested that the principle of charge independence, which is believed to hold for pions and nucleons, may extend to hyperons and heavy mesons. Gell-Mann postulates that for strong interactions the principle of charge independence holds.

iv) If charge independence holds for strong interactions, the immediate consequence is that the strongly interacting particles are divided into charge multiplets. Each charge multiplet is characterised by an isotopic spin I, common to all members of the multiplet. Each member of the multiplet is characterised by its electrical charge, i.e. by the third component I_3 of the isotopic spin. The multiplicity of the multiplet is given by $2I + 1$. If the isotopic spin of the charge multiplet is 0, the multiplet is a singlet formed by only one particle, for example the Λ^0-particle. If the isotopic spin is $\frac{1}{2}$, the multiplet is a doublet, formed by one charged and one neutral particle, for example the nucleons and presumably the Ξ-particle. If the isotopic spin is 1, the multiplet is a triplet, formed by one positive, one neutral and one negative particle, for example the pions. The isotopic spins of the several multiplets were chosen empirically, having in mind only that experimental results must be interpreted, but no correlation was assumed "a priori" between the isotopic spin and the spin angular momentum of a particle: there are fermion multiplets with integral I and boson multiplets with half-integral I.

v) Strangeness : We know that for nucleons the relationship between electrical charge and the third component of the isotopic spin is:

$$Q = e\,(I_3 + \tfrac{1}{2}) \qquad (1)$$

and for pions it is:

$$Q = e\,I_3 \qquad (2)$$

Expressions (1) and (2) can be combined in a single expression, valid for all "ordinary" particles:

$$Q = e\,(I_e + \frac{\mathcal{N}}{2}) \qquad (3)$$

where $\mathcal{N}$ is the number of nucleons minus the number of anti-nucleons.

Gell-Mann calls "centre of charge" of a given multiplet the arithmetic mean of the charges of the members of the multiplet. Expression (3) shows that for the "ordinary" particles the centre of charge of the multiplet is given by $\frac{\mathcal{N}'e}{2}$ or, that it is given by the number $\mathcal{N}'$ in units of $\frac{e}{2}$. For instance, in the nucleon doublet ($\mathcal{N}' = +1$) the centre of charge is $+\frac{e}{2}$; in the anti-nucleon doublet ($\mathcal{N}' = -1$) it is $-\frac{e}{2}$; in the pion triplet ($\mathcal{N}' = 0$) it is 0.

Gell-Mann considers the centre of charge of the nucleon doublet ("ordinary" baryons) as the "normal" centre of charge of baryon multiplets, and the centre of charge of π-mesons as the

"normal" centre of charge of mesons. He then generalizes expression (3) in order to have an expression of Q as a function of I_3 which is not only valid for pions and nucleons but also for K-mesons and hyperons. He postulates that Q is a function not only of I_3 and $\mathcal{N}'$, but also of a new quantum number S (called "strangeness") and has the form:

$$Q = e\left(I_3 + \frac{\mathcal{N}}{2} + \frac{S}{2}\right) \qquad (4)$$

where $\mathcal{N}$ is the number of baryons minus the number of anti-baryons. The number S is zero for "ordinary" particles, and different from zero for the "strange" particles. A definite value of S is assigned to every multiplet. Table 2.1 lists the several multiplets and the corresponding values of Q, I and S. It must be emphasized that these values have been chosen empirically to fit the experimental results. A detailed justification of the choice is found in reference (52).

For every multiplet S establishes the relationship between Q and I_3. As a characteristic of the multiplet S measures the "displacement" of the centre of charge of the multiplet relative to the "normal" position of the centre of charge, in units of $\frac{e}{2}$. Apart from this, no physical meaning has been attributed to the strangeness.

TABLE 2.1

Charge, isotopic spin and strangeness of fermions and bosons in the Gell-Mann scheme

	Multiplet	Q			I	S	Q (I_3)
		-1	0	+1			
Fermions	Ξ	-	-		$\frac{1}{2}$	-2	$Q = I_3 - \frac{1}{2}$
	Σ	-	-	-	1	-1	$Q = I_3$
	Λ		-		0	-1	$Q = I_3$
	N		-	-	$\frac{1}{2}$	0	$Q = I_3 + \frac{1}{2}$
Bosons	K		-	-	$\frac{1}{2}$	+1	$Q = I_3 + \frac{1}{2}$
	π	-	-	-	1	0	$Q = I_3$

Q is the electrical charge, in units of e, of the members of the multiplet. I and S are the isotopic spin and the strangeness of the multiplet. The last column gives Q as a function of I_3. To each of these multiplets corresponds the multiplate of the anti-particles, which has equal and opposite strangeness.

vi) As Q, I_3 and $\mathcal{N}$ change sign under charge conjugation, expression (4) shows that S also changes sign. Then, the strangeness of a particle is equal and opposite to the strangeness of its anti-particle. Then for every multiplet given in Table 2.1 there is a multiplet of the corresponding anti-particles.

vii) S is an additive number. The strangeness of a collection of particles is the algebraic sum of the values of the strangeness of the particles.

viii) The conservation laws of the three types of interaction:

In addition to the classical laws of conservation (energy, momentum, angular momentum, charge), Gell-Mann, following a suggestion of Pais, differentiates between the three types of interaction in the additional laws of conservation that are obeyed. The additional conservation laws are:

a) Strong interactions : I, I_3, $\mathcal{N}$ and consequently S are conserved.

b) Electromagnetic interactions : I_3, $\mathcal{N}$ and consequently S are conserved.

c) Weak interactions : $\mathcal{N}$ is conserved.

The question of conservation of parity - not considered by Gell-Mann, Pais and Nishijima - is discussed in Section 5.

ix) The law $\Delta S = \pm 1$ for weak interactions :

Gell-Mann and Pais,[5] having noticed that in the decay of several hyperons and K-mesons I_3 varies by $+\frac{1}{2}$ or $-\frac{1}{2}$, proposed as general rule for weak interactions, $\Delta I_3 = \pm\frac{1}{2}$. Expression (4) shows that, in terms of strangeness, this rule is equivalent to :

$$\Delta S = \pm 1 \qquad (5)$$

3. d'Espagnat and Prentki's formalism of the Gell-Mann Model

d'Espagnat and Prentki[53] succeeded in making a Lagrangian formalism of the interactions of baryons, K-mesons and pions in such a way that, as a consequence of the postulated properties of the Lagrangians three good quantum numbers result naturally associated to hypothetical sets of particles :

i) I_3, the third component of the isotopic spin.

ii) $\mathcal{N}$, the number of baryons minus the number of anti-baryons which are contained in each particle.

iii) U, a new quantum number, which is defined below.

In the two spaces which they consider, the ordinary space and the isotopic space, the identification of the known particles with the hypothetical particles to which I_3, $\mathcal{N}$ and

U belong can be made in such a way as to fit the properties that have been experimentally found.

Identification of the particles

a) In the ordinary space - In this space the number $\mathcal{N}$ is the basis for the classification of the particles into three groups:

- fermions : particles with $\mathcal{N} = +1$, identified with N, Λ, Σ, Ξ.
- anti-fermions : particles with $\mathcal{N} = -1$, identified with $\bar{N}, \bar{\Lambda}, \bar{\Sigma}, \bar{\Xi}$.
- bosons : particles with $\mathcal{N} = 0$, identified with π, K, $\bar{K}$.

b) In the isotopic space - For analogy with what $\mathcal{N}$ represents in the ordinary space, U is defined in the isotopic space as the number of isofermions minus the number of anti-isofermions, and it is the basis for the classification of the particles into three groups:

- isofermions : particles with U = +1, identified with N, K, Ξ.
- anti-isofermions : particles with U = -1, identified with $\bar{N}$, $\bar{K}$, Ξ.
- isobosons : particles with U = 0, identified with π, Λ, Σ, $\bar{\Lambda}$, $\bar{\Sigma}$.

Each particle is then classified twice. For instance, the Λ^{o}-particle is fermion and isoboson.

d'Espagnat and Prentki call their formalism "Mathematical formulation of the Gell-Mann model", since they concluded that the strangeness S turns out to be the difference between U and $\mathcal{N}$:

$$S = U - \mathcal{N} \tag{6}$$

and that the conservation laws for the three types of interaction are identical to those of the Gell-Mann model. The conservation laws are:

- Strong interactions : I, I_3, Q, $\mathcal{N}$ and U are conserved.
- Electromagnetic interactions : I_3, Q, $\mathcal{N}$ and U are conserved.
- Weak interactions : Q and $\mathcal{N}$ are conserved.

Since $\mathcal{N}$ is conserved in both models, it follows from (6) that Gell-Mann's rule for weak interaction, $\Delta S = \pm 1$, is equivalent to:

$$\Delta U = \pm 1 \tag{7}$$

4. Sachs' Classification of the Fundamental Particles

In an attempt to correlate the modes of production, modes of decay and the interactions of the fundamental particles, Sachs[54] also proposed to assign to each particle a quantum number which he called "attribute" (represented here by "a"). No physical interpretation was given to "a", but the following properties of "a" are postulated:

i) A definite value of "a" exists for every fundamental particle.

ii) "a" is additive, i.e. the value of "a" for any collection of particles is the algebraic sum of the value of "a" of all the particles.

iii) Transitions having $\triangle a = 0$ are very fast.

iv) Transitions having $\triangle a = \pm 1$ are slow, of the order of the observed decay rates of the fundamental particles.

v) Transitions having $|\triangle a| > 1$ are so slow as to be unobserved.

In addition to the five postulates, Sachs assumes the validity of the usual conservation laws, including the conservation of $\mathcal{N}$ (the baryonic number).

Isotopic spin : In assigning isotopic spin to the several particles he found necessary, in order to fit the experimental

results, to follow the suggestion of Nishijima and Gell-Mann that there need not be a direct connection between the isotopic spin and the spin angular momentum of a particle; that is to say, he assumes that fermions and bosons can both have integral or semi-integral isotopic spin. He postulates the following "odd-even" rule which connects "a" with I (and not with I_3) :

> "Fermions have half-integral isotopic spin when "a" is even, and integral isotopic spin when "a" is odd. The converse holds for bosons."

In addition he assumes the normal relationship between charge and I_3, i.e. that :

$$Q = e\, I_3 \quad \text{for integral I}$$

and $$Q = e\,(I_3 \pm \tfrac{1}{2}) \quad \text{for half-integral I.}$$

The values of "a" and I which Sachs assigns to the several particles are listed in Table 2.2. We see that

i) the values of I are exactly the values which Nishijima and Gell-Mann had proposed;

ii) with the exception of the electron, the neutrino and the muon, for every particle the value of "a" is equal and opposite to the value of the strangeness proposed by Gell-Mann.

TABLE 2.2

Values of I, $\mathcal{N}$, U , S and "a" for the various particles

Particle	I	U	$\mathcal{N}$	S = U-$\mathcal{N}$	"a" = -S
N	$\frac{1}{2}$	+1	+1	0	0
Λ	0	0	+1	-1	+1
Σ	1	0	+1	-1	+1
Ξ	$\frac{1}{2}$	-1	+1	-2	+2
π	1	0	0	0	0
K	$\frac{1}{2}$	+1	0	+1	-1
$\bar{N}$	$\frac{1}{2}$	-1	-1	0	0
$\bar{\Lambda}$	0	0	-1	+1	-1
$\bar{\Sigma}$	1	0	-1	+1	-1
$\bar{\Xi}$	$\frac{1}{2}$	+1	-1	+2	-2
$\bar{K}$	$\frac{1}{2}$	-1	0	-1	+1
μ^+		0	0	0	$-\frac{1}{2}$
e^+		0	0	0	$-\frac{1}{2}$
ν		0	0	0	$-\frac{1}{2}$
μ^-		0	0	0	$+\frac{1}{2}$
e^-		0	0	0	$+\frac{1}{2}$
$\bar{\nu}$		0	0	0	$+\frac{1}{2}$

5363

If it were not for the electron, the neutrino and the muon, Sachs model would be exactly the Gell-Mann model. But when those three particles are considered the following differences arise between the two models :

i) Whereas Gell-Mann proposes S = 0 for these three particles, Sachs proposes a = $-\frac{1}{2}$ for the positon, the positive μ-meson and the neutrino, and a = $+\frac{1}{2}$ for the negaton, the negative μ-meson and the anti-neutrino.

ii) As a consequence of the values of "a" for electron, neutrino and muon, the allowed decay modes of charged K-mesons are more restrictive in the Sachs model than in the Gell-Mann model. For instance, in the Gell-Mann model the decay of the K^+_2 can be

$$\text{either} \qquad K^+_{\mu 2} \rightarrow \mu^+ + \nu$$

$$\text{or} \qquad K^+_{\mu 2} \rightarrow \mu^+ + \overline{\nu};$$

since in both $|\Delta S| = 1$; in the Sachs model only the second is allowed, because in only the second is $|\Delta a| = 1$; in the first $|\Delta a| = 0$.

Sachs showed that if the proposed rules for the attribute and the isotopic spin hold, by examining the decay modes of the

charged K-mesons the two following conclusions arise :

i) The anti-neutrino must exist.

ii) The Fermi (beta-decay) coupling is a characteristic of the neutrino, and in that sense is not "universal".

As a final remark it is interesting to point out that Sachs model does not explain the very small probability of the pion beta decay as long as the pion is assumed to have a =0.

5. The Question of Conservation of Parity

Since the Gell-Mann model was formulated, a further development took place, arising from the study of the decays of the τ- and θ-mesons. It was shown by Lee and Yang[59] that the evidence for conservation of parity in weak interactions was not good. They suggested experiments to test parity conservation in weak interactions. An experiment made by Wu et al.[60] proved that parity is not conserved in β-decay, and an experiment made by Garwin et al.[61] proved that it is not conserved in the reactions :

$$\pi^+ \rightarrow \mu^+ + \nu$$

$$\mu^+ \rightarrow e^+ + 2\nu$$

At present there is no evidence for violation of parity conservation in strong interactions. It is taken as a further difference between strong and weak interactions that parity is conserved in the former and is not conserved in the latter.

* * *

CHAPTER III

DYNAMICS OF SOME REACTIONS IN WHICH HYPERONS AND K—MESONS ARE PRODUCED

1. Introduction

The dynamics of reactions in which strange particles are produced are in general easily studied in accelerator experiments, because the direction and energy of the primary of the interaction are well known. The situation is very different in cosmic ray experiments. The primary of the interaction in most of the cases is not known, its direction and energy being never directly known. The only way of studying the production process is to start from the dynamical measurements made on the observed particles and try to reconstruct the reactions in which the V—particles could have been produced. An example of this method of work was given by Thompson et al.(13)

In this chapter we shall study in detail the dynamical characteristics of some reactions in which hyperons and K-mesons are produced. The results will be applied to the interpretation

$$\pi^- + p \rightarrow \Lambda^0 + \theta^0$$

or $$K^- + p \rightarrow \Xi^- + \pi^+ \text{ , etc.}$$

In cosmic ray experiments the target N is in general a nucleon contained in a complex nucleus (carbon, iron, copper, lead, etc.) and therefore possesses some Fermi energy. The dynamical analysis of the reactions will take into account the Fermi energy of the nucleon, in order to allow us to understand what effects the Fermi momentum of the nucleon has on the dynamical characteristics of the produced strange particles. General formulae will be deduced including the Fermi momentum and the formulae corresponding to a free nucleon will be deduced as particular cases of the general ones.

In the laboratory system of reference (L.S.), let p be the momentum of the incident particle A;

E_N the kinetic energy of the nucleon (Fermi energy), and

p_N the corresponding momentum;

P the vector sum of p and p_N;

φ_{AN} the angle between p and p_N (i.e. angle between the direction of the incident particle and that of the moving nucleon);

p_Y the momentum of the hyperon;

p_B the momentum of particle B;

φ_Y the angle between p_Y and P;

φ_B the angle between p_B and P.

The centre of mass of the system will move in the L.S. along the direction of P, with velocity

$$\beta = \frac{P}{(m_A^2 + p^2)^{\frac{1}{2}} + (m_N^2 + p_N^2)^{\frac{1}{2}}} \quad \text{and} \quad \gamma = (1 - \beta^2)^{-\frac{1}{2}}$$

In the centre of mass system of reference (C.M.S.), let θ^* be the angle of emission of the hyperon, i.e. the angle between the line of flight of the hyperon and the direction of P;

p^* the momentum of the hyperon, and of particle B;

$E_Y^* = (m_Y^2 + p^{*2})^{\frac{1}{2}}$ $\qquad$ $E_B^* = (m_B^2 + p^2)^{\frac{1}{2}}$

Figure 3.1 shows the quantities used to describe the reaction in the two frames of reference.

We have then :

$$p_Y = \left[\gamma^2 (\beta E_Y^* + p^* \cos\theta^*)^2 + (p^* \sin\theta^*)^2\right]^{\frac{1}{2}}$$

$$p_B = \left[\gamma^2 (\beta E_B^* - p^* \cos\theta^*)^2 + (p^* \sin\theta^*)^2\right]^{\frac{1}{2}} \qquad (2)$$

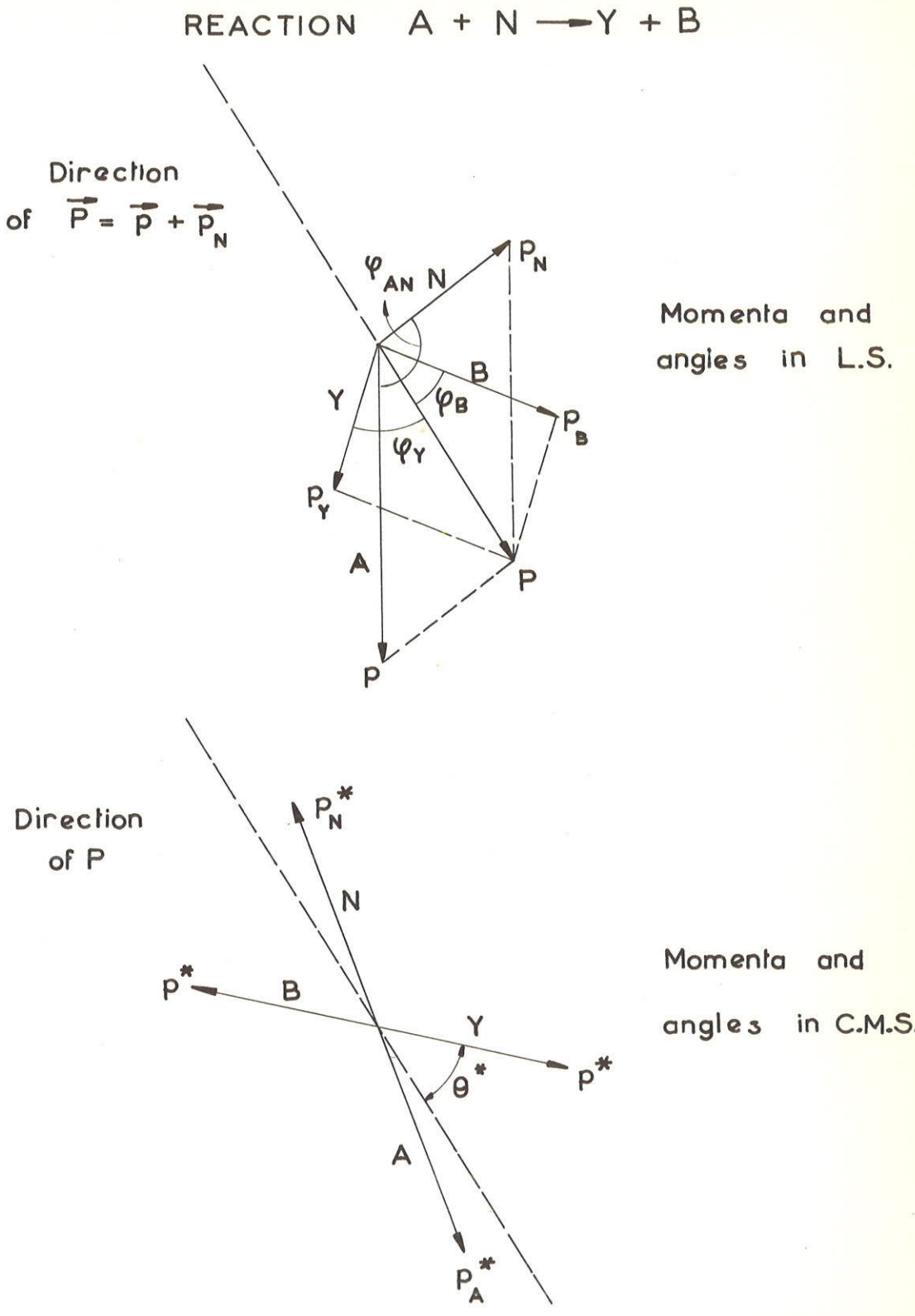
REACTION A + N → Y + B
Direction of $\vec{P} = \vec{p} + \vec{p}_N$
φ_{AN} N
P_N
B
φ_B
Y
φ_Y
P_B
P_Y
A
P
P
Momenta and angles in L.S.
Direction of P
P_N^*
N
P^*
B
Y
P^*
θ^*
A
P_A^*
Momenta and angles in C.M.S.

Figure 3.1

$$tg\varphi_Y = \frac{p^* \sin\theta^*}{(\beta E_Y^* + p^* \cos\theta^*)}, \qquad tg\varphi_B = \frac{p^* \sin\theta^*}{(\beta E_B^* - P^* \cos\theta^*)} \quad (3)$$

For a given set of values of p_N and φ_{AN}, only two of the six quantities p, p_Y, φ_Y, p_B, θ^* and γ_B must be known in order to determine completely the dynamics of the interaction in the L.S. and in the C.M.S. (the masses of the particles are supposed to be known).

3. Particular Cases of p_N and φ_{AN}

For a given value of the momentum p of the incident particle, the values to be expected for p_Y, φ_Y, p_B and φ_B will be studied in the following particular cases :

case a) : $p_N = 0$ (Free nucleon) ;

case b) : p_N non-zero and $\varphi_{AN} = 180^\circ$ ↓ p, ↑ p_N

case c) : p_N non-zero and $\varphi_{AN} = 0^\circ$ ↓ p, ↑ p_N

case d) : p_N non-zero and $\varphi_{AN} = 90^\circ$ → p_N, ↓ p

As the V-particles which are studied in this work were produced in copper, carbon and lead, we have chosen for the Fermi energy of the nucleon the maximum value $E_N = 25$ MeV (see

Rossi[62]), which corresponds to p_N = 218 MeV/c. This value will give the maximum influence of the Fermi energy of the nucleon on the dynamics.

4. Particular Reactions of the Type A + N → Y + B

We have considered, for the purpose of analysing the photographs, the following two-body reactions :

$$\pi^- + N \rightarrow \Lambda^0 + K \qquad \text{(I)}$$

$$\pi^- + N \rightarrow \Sigma^- + K \qquad \text{(II)}$$

$$K + N \rightarrow \Lambda^0 + \pi \qquad \text{(III)}$$

$$K + N \rightarrow \Sigma + \pi \qquad \text{(IV)}$$

For the four reactions each of the cases a), b), c) and d) for p_N and φ_{AN} was studied, and diagrams relating p_Y and φ_Y, p_B and φ_B were plotted. These diagrams are Figures I to 24 of Appendix I. Figures 1 to 8 show the variation of φ_{Λ^0} as a function of p_{Λ^0}, and of φ_K as a function of p_K for curves of constant p and curves of constant θ^*. Figures 9 to 16 show the variation of φ_Σ as a function of p_Σ and of φ_K as a function of p_K also for curves of constant p and constant θ^*. Figures 17 to 20 show the behaviour of the Λ^0-particle in reaction (III) and Figures 21 to

24 that of the Σ -particle in reaction (IV). The reasons why the curves have been calculated for the Λ^{o}-particle and also for the Σ -particle are given below.

It is important to notice that, in all the figures of Appendix I, θ^{*} represents the angle of emission of the hyperon in the C.M.S. For instance, if a Λ^{o}-particle and a K-meson are produced according to reaction (I), $\varphi_{\Lambda^{o}}$ and $p_{\Lambda^{o}}$ will determine in Figure 1 a point which corresponds to one fixed value of p and one fixed value of θ^{*}. Then, φ_{K} and p_{K} will determine in Figure 2 a point which corresponds to the same values of p and θ^{*} of the case of the Λ^{o}-particle.

5. Relationship Between φ_{Y} and p_{Y} in the Extreme Relativistic Limit

Let us assume that a hyperon is produced in a collision of a particle A (incident particle) with a particle N (target particle) which does not need to be at rest. It is important to know the relationship between the angle of emission and the momentum of the hyperon in the L.S. when the energy of the incident particle becomes very large. As we shall see this relationship is important because it represents the limit of the possibility for the hyperon to be produced in any endothermic reaction in which particle N is target.

In the following we shall assume that particle N is a nucleon, although for the reasoning this is not necessary. We shall also assume that only the energy of the incident particle becomes infinitely large, but that the energy of the target N remains finite.

The total momentum available in the L.S. is :

$$P^2 = p^2 + p_N^2 + 2pp_N \cos \varphi_{AN}$$

and the momentum of particle B can be written

$$p_B^2 = p_Y^2 + P^2 - 2Pp_Y \cos \varphi_Y$$

Conservation of energy gives :

$$(m_A^2 + p^2)^{\frac{1}{2}} + (m_N^2 + p_N^2)^{\frac{1}{2}} = (m_Y^2 + p_Y^2)^{\frac{1}{2}} + (m_B^2 + p_B^2)^{\frac{1}{2}}$$

Solving these equations for $\cos \varphi_Y$ and passing to the limit when $p \longrightarrow \infty$, we conclude :

$$\lim_{p \to \infty} \cos \varphi_Y = (\cos \varphi_Y)_\infty = \frac{1}{p_Y} \left[(m_Y^2 + p_Y^2)^{\frac{1}{2}} - (m_N^2 + p_N^2)^{\frac{1}{2}} + p_N \cos \varphi_{AN} \right] \quad (4$$

Let us define δ as :

$$\delta = (m_N^2 + p_N^2)^{\frac{1}{2}} - p_N \cos \varphi_{AN} \quad (5$$

Then expression (4) can be written :

$$(\cos \varphi_Y) = \frac{1}{p_Y} \left[(m_Y^2 + p_Y^2)^{\frac{1}{2}} - \delta \right] \qquad (6)$$

Expression (4) or (6) is the relationship between the momentum and the angle of emission of the hyperon in the L.S. for very high values of the momentum of the incident particle (extreme relativistic limit, E.R.L.). It is interesting to note that this relationship depends neither on the nature of the incident particle A nor on the nature of particle B which was produced with the hyperon. For a given mass of the hyperon it depends on the mass, momentum and direction of the target particle.

In the particular case of a free nucleon,

$$\delta = m_N$$

and

$$(\cos \varphi_Y)_\infty = \frac{1}{p_Y} \left[(m_Y^2 + p_Y^2)^{\frac{1}{2}} - m_N \right] \qquad (6')$$

6. Maximum Angle of Emission of the Hyperon in the E.R.L.

The derivative of expression (6) relative to p_Y is :

$$\frac{d(\cos \varphi_{Y})_{\infty}}{dp_Y} = \frac{\delta}{p_Y^2} - \frac{m_Y^2}{p_Y^3}\left(1 + \frac{m_Y^2}{p_Y^2}\right)^{-\frac{1}{2}}$$

Equating this expression to zero and solving for p_Y we obtain

$$p_Y = \left[\left(\frac{m_Y^2}{\delta} \right)^2 - m_Y^2 \right]^{\frac{1}{2}} \qquad (7)$$

This is the value of p_Y which corresponds to the maximum allowed angle of emission of the hyperon in the L.S. in the E.R.L. To obtain the value of the maximum angle of emission in the E.R.L., $(\varphi_{Y})_{\infty\ max}$, we must substitute this value of p_Y in (6), and we obtain:

$$\cos\ (\varphi_{Y})_{\infty\ max} = \left[\frac{m_Y^2}{\delta} - \delta \right] \left[\left(\frac{m_Y^2}{\delta} \right)^2 - m_Y^2 \right]^{-\frac{1}{2}} \qquad (8)$$

7. Minimum Momentum of the Hyperon in the E.R.L.

Expression (6) gives us a way of determining the minimum allowed momentum of the hyperon in the E.R.L., which corresponds to the hyperon emitted at 180° in the C.M.S. and at 0° in the L.S. Making $\cos(\varphi_{Y})_{\infty} = +1$ in (6) and solving the resulting

Table 3.1

Values of δ for different cases

Case	φ_{AN} (Degrees)	δ (MeV)
a	--	938.2
b	180	1182.2
c	0	745.2
d	90	963.2

Values of the parameter δ for several directions of the moving nucleon, assuming Fermi momentum equal to 218 MeV/c. Note that in cases a, c and d, δ is less than the mass of any hyperon, and in case b it is less than the mass of the Σ^- and of the Ξ^--hyperon but greater than the mass of the Λ^0-particle. In all cases it is greater than the masses of the K-meson and π^--meson, and only in case c it is less than the mass of the proton.

value of δ for a free nucleon and for the three directions of the nucleon's Fermi momentum.

To show the influence of the mass of the particle which is produced in the E.R.L., curves representing equation (6) for constant values of δ are given in Figures 3.2 and 3.3. The curves were calculated under the assumption that the target particle is a nucleon. Figure 3.2 gives the E.R.L. for Λ^{o}-, Σ and Ξ-particles, K- and π-mesons and proton for cases a and b of the Fermi momentum. Figure 3.3 gives the E.R.L. for the same particles for cases c and d of the Fermi momentum.

It is important to notice the limitations in minimum momentum and in maximum angle of emission which exist for hyperons in the E.R.L. To stress these limitations, which can be seen from Figures 3.2 and 3.3, the values of the minimum momentum and maximum angle of emission in the E.R.L. are listed in Table 3.2 for Λ^{o}-, Σ - and Ξ-particles, K- and π-mesons and proton.

In the E.R.L. there is no limitation for the angle of emission of the K- or the π-meson, and the proton is only limited in cases a and c.

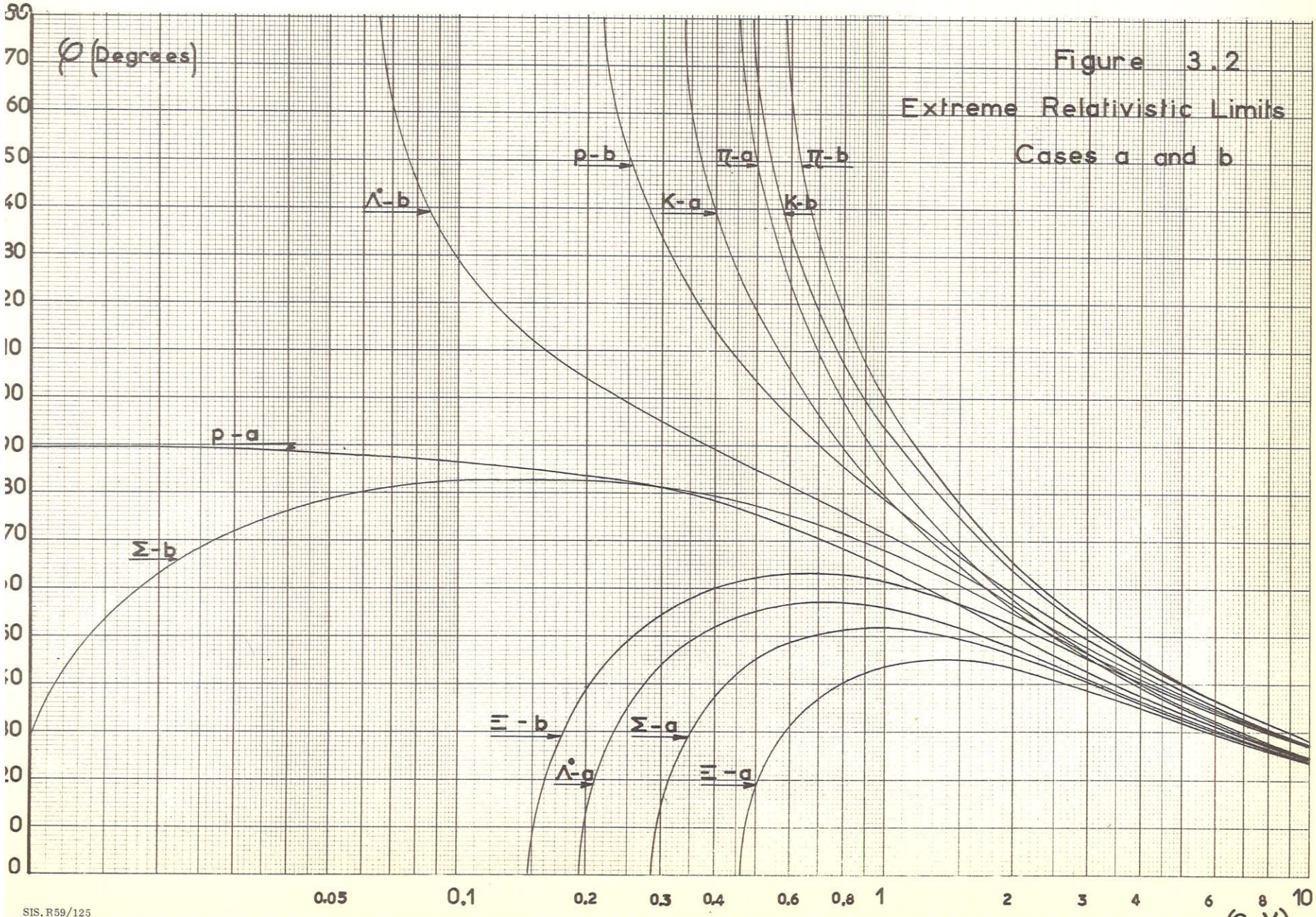
φ (Degrees)
Figure 3.2
Extreme Relativistic Limits
Cases a and b
p - b
π - a
π - b
Λ° - b
K - a
K - b
p - a
Σ - b
Ξ - b
Σ - a
Λ° - a
Ξ - a
80
70
60
50
40
30
20
10
0
0.05
0.1
0.2
0.3
0.4
0.6
0.8
1
2
3
4
6
8
10

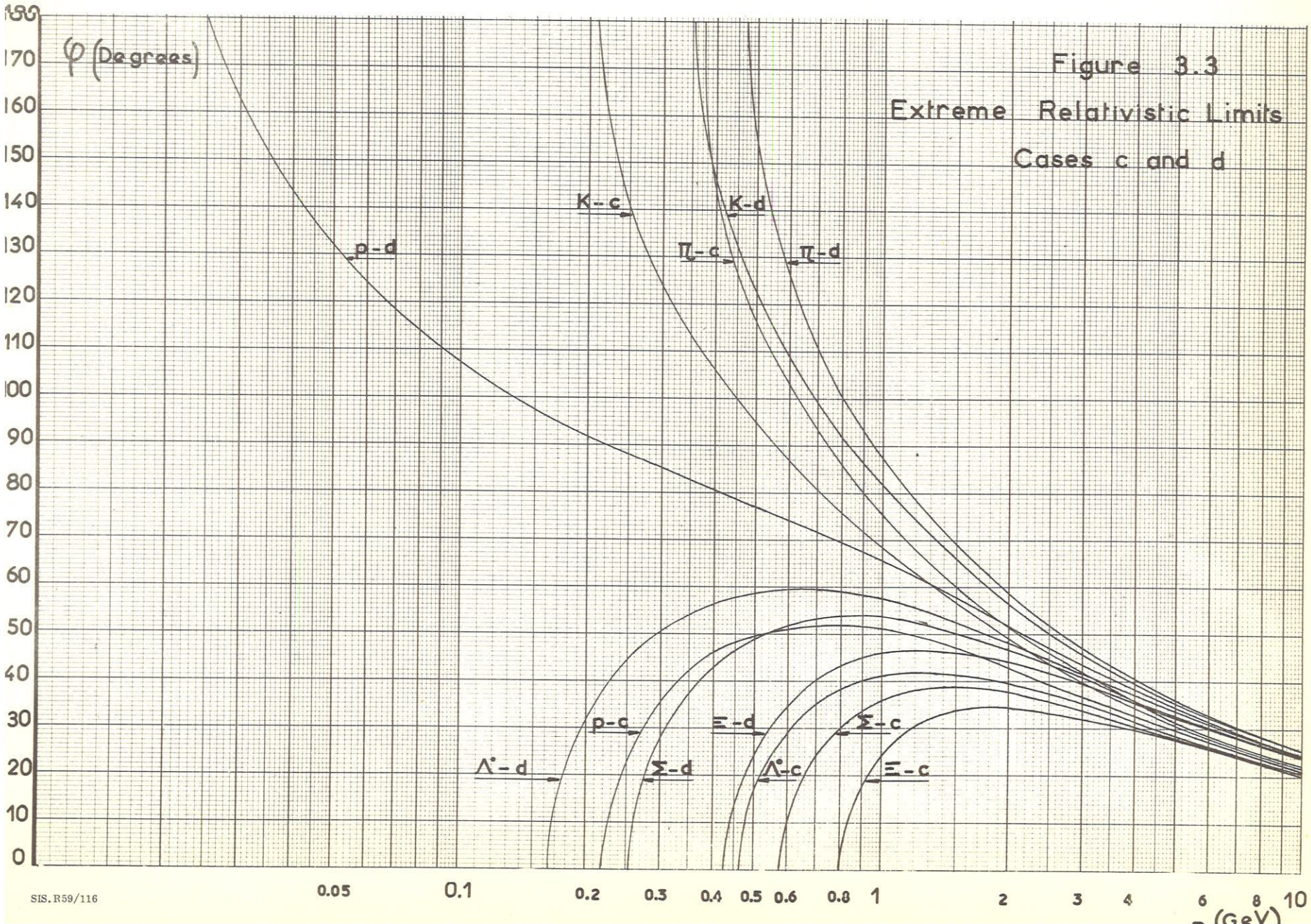

Figure 3.3
Extreme Relativistic Limits
Cases c and d

TABLE 3.2

Values of minimum momentum and maximum angle of emission in the extreme relativistic case

Case	Minimum Momentum ($\frac{MeV}{c}$)						Maximum Angle of Emission (Degrees)					
	Λ^o			K	p		Λ^o			K	p	
a	193	286	461	339	0	459	57	52	46	180	90	180
b	65	9	148	488	218	582	180	83	64	180	180	180
c	461	578	798	209	218	373	42	39	35	180	53	180
d	163	253	424	355	25	472	60	54	47	180	180	180

Minimum allowed momentum and maximum allowed angle of emission in the extreme relativistic limit for Λ^o-, Σ- and Ξ-hyperon, K-meson, proton and π-meson. Cases a, b, c and d are the four cases of the nucleon's Fermi momentum. These values apply to any collision of any particle with a nucleon.

9. The Influence of the Fermi Energy of the Nucleon

For a given particle, the maximum angle of emission and the minimum momentum in the E.R.L. are functions of the parameter δ. Equations (8) and (9) show that, when the mass of the particle is greater than δ, $(p)_{min}$ and $\cos(\varphi)_{\infty\,max}$ are positive; in the E.R.L. the particle does not reach 90° and is always emitted forwards in the L.S. When the mass of the particle is less than δ, $(p)_{min}$ and $\cos(\varphi)_{\infty\,max}$ become negative, and the particle is emitted backwards in the L.S. This fact is well illustrated by combining the values quoted in Tables 3.1 and 3.2. For instance, the Λ°-particle, which has mass 1115 MeV/c, has $(\varphi_{Y})_{\infty\,max}$ equal to 57°, 42° and 60° in cases a, c and d, in which δ is less than the mass; but the Λ°-particle is emitted at 180° in the L.S. in case b because then δ is greater than the mass. Because the mass of the Σ-particle (1190 MeV/c) and that of the Ξ-particle (1321 MeV/c) are greater than δ in any of the four cases of the Fermi momentum, these hyperons can never be emitted backwards in the L.S. in the E.R.L. In no circumstances can a Σ-hyperon be emitted at an angle greater than 83° nor a Ξ-hyperon be emitted at an angle greater than 64° in the E.R.L. of the collision of any particle with a nucleon.

10. Endothermic and Exothermic Reactions

There are fundamental differences in the allowed ranges of the angle of emission and momentum of a hyperon, according to whether it was produced in an endothermic or exothermic reaction.

i) Endothermic reaction

In an endothermic reaction, as for instance

$$\pi^+ + N \rightarrow \Lambda^0 + K \quad \text{or} \quad \Sigma + K$$

at threshold the C.M.S. has already some velocity in the L.S. and the hyperon is emitted forward in the L.S. at an angle of 0°. When the energy of the primary increases, the velocity of the C.M.S. in the L.S. increases, but the velocity of the hyperon in the C.M.S. also increases. For a given value of the energy of the primary there is a minimum value of the momentum of the hyperon, corresponding to $\theta^* = 180^\circ$, a maximum value of the momentum, corresponding to $\theta^* = 0^\circ$, and a maximum allowed angle of emission in the L.S. When the energy of the primary increases the maximum angle of emission is shifted to higher values and the minimum momentum to lower values, and they tend to the values given by the E.R.L.

The E.R.L. for a particle, corresponding to given conditions of a target particle N, represents the limit of the possibility for the particle to be produced in any endothermic reaction in which the target is particle N in the same conditions.

The curves of Figure 3.2 corresponding to nucleon at rest (case a), divide the plane "angle of emission-momentum" into two regions: the first, between the curve, the axis of momentum and eventually the axis of angle of emission, in which the particle can be produced in an endothermic reaction in which the target is a nucleon at rest. The second, in which the particle can never be produced in an endothermic reaction where the target is a nucleon at rest. The curves of E.R.L. have identical meaning for cases b, c and d of the nucleon's Fermi momentum. Figures 1 to 16 of Appendix I show clearly the division of the plane (φ, p) into an allowed and a forbidden region for Λ^{o}- and Σ -particles and K-mesons produced in collisions in which a nucleon is target. Cases a, b, c and d for the same particle show how striking is the influence of the Fermi energy of the nucleon in the limitation between the allowed and the forbidden region.

It is also important to note how the comparatively small differences in the masses of the several hyperons make the limits between allowed and forbidden region so different for them. In fact, the differences in the dynamical characteristics of the hyperons do not occur only at very high energies but also at energies not much above the threshold for two-body reactions. It is very illustrative to compare, for instance, cases b) of reactions (I) and (II), represented in Figures 3 and 11 of Appendix I; already for a π^--meson of momentum 2 GeV/c the Λ^0- and the Σ - hyperons have very different dynamical characteristics. It was, in fact, due to the differences which arise from small mass differences that we decided to make diagrams for Λ^0-particle and for Σ -particle separately.

ii) Exothermic reaction

An exothermic reaction can occur with zero kinetic energy of the two initial particles, a situation in which the C.M.S. coincides with the L.S. Consequently the secondaries of the interaction can be emitted at any angle in the L.S. This is the case, for example, of the Λ^0- and Σ -particles produced in the reactions:

$$K + N \rightarrow \Lambda^0 + \pi^- \qquad \text{(III)}$$

$$K + N \rightarrow \Sigma + \pi^- \qquad \text{(IV)}$$

and of the Λ^{o}-particle produced in the reaction:

$$\Sigma + N \rightarrow \Lambda^{o} + N \qquad (V)$$

The E.R.L. for the emission of a particle is the same if the particle is produced in an endothermic or in an exothermic reaction (for the same mass and vector momentum of the target particle). Nevertheless it does not represent the same physical limitations in the two types of reaction. In an exothermic reaction at low energies the E.R.L. is not a boundary between allowed and forbidden angles of emission or momenta of the particle in the L.S., and therefore it has not the same interest as it has in the case of endothermic reactions. At high energies where the mass difference between secondary and primary particles is small compared with their total energy, the difference between exothermic and endothermic reactions becomes unimportant. The E.R.L. then has the same significance as a boundary for both types of reaction.

The difference between endothermic and exothermic reactions is important in the production of low energy particles. Let us consider, for example, the Λ^{o}-particle produced in reactions in which the target particle is a free nucleon. The E.R.L. determines that in any endothermic reaction occurred with

a free nucleon as target, the Λ^{o}-particle cannot be emitted in the L.S. at an angle greater than 57^{o} or with momentum less than 195 MeV/c. But in any exothermic reaction, as for instance (III) or (V), there is always some energy range of the primary of the interaction in which the Λ^{o}-particle can be emitted at any angle or with any low momentum in the L.S.

These properties are shown in Figures 17 to 24 of Appendix I, where the dynamics of reactions (III) and (IV) are given in detail. It is interesting to compare the relative position of the E.R.L. in Figures 17 to 24, which correspond to two exothermic reactions, with its relative position in Figures 1 to 16, which correspond to two endothermic reactions.

11. K-mesons Produced in Two-Body Reactions

If we accept the conservation of strangeness in strong interactions, in a two-body reaction a K-meson can only be produced associated with a hyperon. Reactions (I) and (II) are precisely the only two-body reactions that can produce K-mesons. The characteristics of K-mesons produced in (I) and (II) are given in detail in Figures 1 to 16 of Appendix I, and in Figures 3.2 and 3.3.

have been deduced in the case of two-body are also valid in the case of n-body reactions.

Let us assume, for example, the interaction:

$$p + p \rightarrow \Lambda^{\circ} + K^{+} + p \qquad (VI)$$

What is the maximum momentum that the Λ°-particle can have at a given angle in the L.S., for a given momentum of the incident proton ? Problems of this type arise not only in the interpretation of data of experiments already performed, but also in the planning of experiments. These limitations occur because the momenta of all secondaries are bound by conservation of energy and momentum.

In order to calculate the limitations of momentum in the L.S. of a particle produced in a particular reaction with a particular energy of the primary, we must know the value of the maximum allowed momentum of that particle in the C.M.S. and the conditions for this maximum to occur. This maximum value and the conditions for it to occur will be deduced by using a method developed by the author.

13. Condition for the Maximum Momentum of a Secondary in the C.M.S.

Let us assume that, in a collision of a particle A with a nucleon, n particles are produced:

$$A + N \longrightarrow B + C + \ldots + M \qquad (10)$$

Call $m_1, m_2, \ldots, m_n$ the masses of B, C, ... , M and $p_1, p_2, \ldots, p_n$ their momenta in the C.M.S. What is the distribution of the momenta $p_1, p_2, \ldots, p_n$, when one of them, p_1 for instance, is a maximum, for a given energy of the incident particle A ?

For a given energy of the incident particle A, the total energy E in the C.M.S. is a constant such as:

$$(m_1^2 + p_1^2)^{\frac{1}{2}} + (m_2^2 + p_2^2)^{\frac{1}{2}} + \ldots + (m_n^2 + p_n^2)^{\frac{1}{2}} = E \qquad (11)$$

There is an infinity of sets $p_1, p_2, \ldots, p_n$ which satisfy equation (11). When p_1 is a maximum, $p_2, p_3, \ldots, p_n$ have the same direction and are opposite to p_1:

$$p_2 + p_3 + \ldots + p_n - p_1 = 0 \qquad (12)$$

For a given value of E, when p_1 is a maximum, the following quantity is a minimum:

$$f(p_2, \ldots, p_n) = (m_2^2 + p_2^2)^{\frac{1}{2}} + \ldots + (m_n^2 + p_n^2)^{\frac{1}{2}} = E - (m_1^2 + p_1^2)^{\frac{1}{2}} \tag{13}$$

As $f(p_2, \ldots, p_n)$ is a function of $p_2, \ldots, p_n$, which are bound by condition (12), its minimum can be found by the method of the Lagrangian multipliers. Let us multiply the left hand side of (12) by a constant λ and construct the function:

$$F(p_2, \ldots, p_n) = (m_2^2 + p_2^2)^{\frac{1}{2}} + \ldots + (m_n^2 + p_n^2)^{\frac{1}{2}} + \lambda (p_2 + \ldots + p_n - p_1)$$

Then we know that the system of equations:

$$\frac{F}{p_2} = 0 \quad \text{or} \quad p_2 (m_2^2 + p_2^2)^{-\frac{1}{2}} + \lambda = 0$$

$$\frac{F}{p_n} = 0 \quad \text{or} \quad p_n (m_n^2 + p_n^2)^{-\frac{1}{2}} + \lambda = 0$$

$$p_2 + \ldots + p_n - p_1 = 0$$

has as solution the values of $p_2, \ldots, p_n$ which correspond to the minimum of $f(p_2, \ldots, p_n)$. Solving the equations for $p_2, \ldots, p_n$ we find:

$$p_2 = \frac{m_2}{m_2 + m_3 + \ldots + m_n} p_1$$

$$\text{----------} \qquad (14)$$

$$p_n = \frac{m_n}{m_2 + m_3 + \ldots + m_n} p_1$$

Conclusion

When p_1 is maximum, the momentum of any other particle is a fraction of p_1 equal to the ratio of the mass of that particle to the sum of the masses of all particles except that corresponding to p_1.

Expressions (14) can be written in a different way. We have:

$$\frac{p_1}{m_2 + m_3 + \ldots + m_n} = \frac{p_2}{m_2} = \beta_2 \gamma_2$$

$$\text{----------}$$

$$\frac{p_1}{m_2 + m_3 + \ldots + m_n} = \frac{p_n}{m_n} = \beta_n \gamma_n$$

i.e. when one particle has maximum momentum, the other particles have equal $\beta\gamma$.

Example

Let us assume that in reaction (VI) the incident proton has momentum 5 GeV/c and the target proton is at rest, and ask what are the momenta of the secondaries in the L.S. when the momentum of the Λ^0-particle is maximum in the L.S.

The C.M.S. will move in the L.S. with $\beta = 0.830$ and $\gamma = 1.79$. The total energy of the two protons in the C.M.S. is E = 3.36 GeV. Calling p_Λ^* the maximum momentum of the Λ^0-particle in the C.M.S., and p_K^* and p_p^* the corresponding momenta of the K-meson and secondary proton, we have, according to (14):

$$p_K^* = \frac{m_K}{m_K + m_p} p_\Lambda^* = \frac{493}{493 + 938} p_\Lambda^* = 0.344\, p_\Lambda^*$$

$$p_p^* = \frac{m_p}{m_K + m_p} p_\Lambda^* = \frac{938}{493 + 938} p_\Lambda^* = 0.656\, p_\Lambda^*$$

The conservation of energy gives:

$$(m_\Lambda^2 + p_\Lambda^{*2})^{\frac{1}{2}} + (m_K^2 + p_K^{*2})^{\frac{1}{2}} + (m_p^2 + p_p^{*2})^{\frac{1}{2}} = 3.36$$

Using the numerical values and solving the equations assuming that in the C.M.S. the Λ^0-particle is emitted at 0° and the K-meson and the proton at 180°, we obtain:

In the C.M.S.		In the L.S.	
$(p_\Lambda^*)_{max}$	= 1.10 GeV/c	$(p_\Lambda)_{max}$	= 4.29 GeV/c
p_K^*	= 0.38 "	p_K	= 0.24 "
p_p^*	= 0.72 "	p_p	= 0.47 "

the three particles being emitted forwards in the L.S.

In this example we can calculate, for instance, that the maximum momentum which the Λ^0-particle can have when emitted at an angle of 25° in the L.S. is 2.60 GeV/c.

The example shows that in spite of the fact that some of the primary energy is used to create particles, a secondary particle can have a momentum of the same order of magnitude as the momentum of the primary of the interaction.

14. Nucleon-Nucleon Collisions

Because the number of baryons must be conserved, the nucleon-nucleon collisions which produce hyperons and/or K-mesons

are all n-body reactions and endothermic. The two following remarks must be made.

i) Section 13 shows that very fast or very slow hyperons and K-mesons can be produced in nucleon-nucleon collisions. The condition for any of them to have maximum energy in the C.M.S. is given by expressions (14).

ii) By examining the way in which formula (6) was deduced it becomes clear that the relation between momentum and angle of emission of a particle in the E.R.L. is a characteristic of the particle (for a fixed condition of the nucleon's Fermi momentum). That relation does not depend on the type of interaction in which the particle was produced, nor on whether it was a two-body or n-body reaction. Figures 3.2 and 3.3 are valid also when the particles are produced in a nucleon-nucleon collision. As nucleon-nucleon reactions which produce hyperons and/or K-mesons are endothermic, the remark which was made about the meaning of the E.R.L. for two-body reactions (Section 10) is also valid for them. That is to say, the E.R.L. represents the absolute limit of momentum and angle of emission of particles produced in nucleon-nucleon collisions. For instance, a Σ -hyperon produced in any nucleon-nucleon collisions can never be emitted in

the L.S. at an angle greater than 83° nor can it have momentum less than 9 MeV/c.

These remarks apply, for example, to the reactions :

$$N + N \rightarrow Y + K + N$$

$$N + N \rightarrow K + \bar{K} + N + N$$

$$N + N \rightarrow \Xi + K + K + N$$

$$N + N \rightarrow Y + \bar{Y} + N + N$$

15. Threshold Energies

Table 3.3 gives the threshold energies of several reactions.

* * *

TABLE 3.3

Thresholds for several reactions

Reaction	Kinetic energy, in GeV	
	Free nucleon	Case b
$\pi + N \rightarrow \Lambda^0 + K$	0.76	0.58
$\pi + N \rightarrow \Sigma + K$	0.89	0.68
$N + N \rightarrow \Lambda^0 + K + N$	1.57	1.10
$N + N \rightarrow \Sigma + K + N$	1.78	1.30
$\pi + N \rightarrow K + \bar{K} + N$	1.36	1.06
$N + N \rightarrow K + \bar{K} + N + N$	2.49	1.84
$\pi + N \rightarrow \Xi + K + K$	2.21	1.73
$N + N \rightarrow \Xi + K + K + N$	3.73	2.82
$\pi + N \rightarrow \Lambda^0 + \bar{\Lambda}^0 + N$	4.72	3.76
$\pi + N \rightarrow \Sigma + \bar{\Sigma} + N$	5.22	4.30
$N + N \rightarrow \Lambda^0 + \bar{\Lambda}^0 + N + N$	7.10	5.63
$N + N \rightarrow \Sigma + \bar{\Sigma} + N + N$	7.78	6.20

The table gives the values of the minimum kinetic energy of the incident particle in the L.S. needed for the reaction to occur. The values given in the second column were calculated on the assumption of a collision with a free nucleon, those in the third column on the assumption of case b of the nucleon's Fermi momentum.

CHAPTER IV

THE EXPERIMENTAL DATA

1. Yield of the Jungfraujoch Experiment

The events analysed in this work were selected from among 120,000 photographs obtained during more than five years' running of the experiment. As was mentioned in Section 2 of Chapter I, they correspond to three different phases of the experiment. In the first phase, the V-particles were produced in the lead block L_1 placed above the cloud chamber and in a lead wedge W placed at the top of the cloud chamber. In the second phase, a copper plate was put across the middle of the cloud chamber, and in the third phase a carbon wedge and a carbon plate were put in place of the lead wedge and copper plate (Figure 1.1). Of course, during the second and the third phase, V-particles continued to be produced above the cloud chamber. The numbers of neutral and charged V-particles observed during the three phases of the experiment are given in Table 4.1. There is a total of 72 photographs which show more than one strange particle. However, in 25 of these events the lines of flight are not copunctual with

a nuclear interaction; therefore only 47 "associated events" are listed in Table 4.1.

2. Selection of the Events

For the present thesis only the 72 photographs which show more than one strange particle were considered. The first work done was to select, among them, those in which the strange particles came from a point in the target where a nuclear interaction occurred. For this purpose, the spatial relation of the interaction and of the strange particles was reconstructed by using the stereoscopic reprojection method described in Chapter I. In this way, using the tracks emerging from the interaction, the position of the interaction in the target was determined; and, in a similar way the lines of flight of the strange particles were determined. When these lines of flight were consistent with passing through the interaction within the experimental errors, the strange particles were classed as "geometrically associated" or "copunctual". When this condition was not satisfied the strange particles were classed as "geometrically non-associated" or "non-copunctual".

The association of neutral V-particles, one with another, was considered established when the individual decay-events were

Table 4.1

Yield of the Jungfraujoch experiment

Origin of the event	Neutral V-decays	Charged V-decays	Photographs with 2 or 3 "copunctual" strange particles	Corresponding total number of photographs
Above the cloud chamber	1411	153	35	120,000
Copper plate	51	3	8	35,135
Carbon plate or wedge	28	4	4	18,877
Totals	1490	160	47	120,000

Numbers of neutral V-decays, charged V-decays and cases of two or three "copunctual" strange particles observed during the three phases of the Jungfraujoch experiment.

TABLE 4.2

Types and frequencies of the events with "copunctual strange particles.

Type of event	Origin and frequency				Total
	Above the chamber	Copper plate	Carbon		
			Plate	Wedge	
V^o-decay + V^o-decay	21	4	2	2	29
V^o-decay + V^o-decay + V^o-decay	2	0	0	0	2
V^o-decay + $V^{\pm}$-decay	8	2	0	0	10
V^o-decay + V^o-decay + $V^{\pm}$-decay	1	0	0	0	1
$V^{\pm}$-decay + $V^{\pm}$-decay	1	0	0	0	1
V^o-decay + non-decaying K^+	2	1	0	0	3
$V^{\pm}$-decay + non-decaying K^+	0	1	0	0	1
Total	35	8	2	2	47

The first column gives the different types of association observed among the 47 events which consist of two or three "copunctual" strange particles. Columns 2 to 5 give the frequencies of each type of association relative to the four possible positions of the origin of the strange particles.

TABLE 4.3

Frequencies of the various cases of non-associated V-events

	V^0 from above	V^0 from plate	$V^{\pm}$ from above	$V^{\pm}$ from plate
V^0 from above	12	-	-	-
V^0 from plate	3	0	-	0
$V^{\pm}$ from above	4	1	0	-
$V^{\pm}$ from plate	2	0	1	0

Cases of two strange particles which appear on the same photograph and are geometrically non-associated. The columns indicate the origin of one strange particle, the rows indicate the origin of the other. V^0 stands for neutral V-decay, $V^{\pm}$ stands for charged V-decay.

long lived neutral K-meson which decays with a mean lifetime of $\sim 10^{-8}$ sec.*) (see, for instance, Lande et al.,(64) Chinowsky et al.,(16) Fitch et al.,(25)); its decay schemes are not well established, but it does certainly decay into three particles. It is not yet proved whether the long lived neutral K-meson can decay into two particles. Due to this fact and the long mean lifetime of this particle relatively to that of the θ_1^o-meson, all neutral K-mesons of our analysis were supposed to be θ_1^o-mesons.

To summarize, it was assumed that among the analysed events there are only two types of neutral V-particles : Λ^o-hyperons and θ_1^o-mesons.

A Λ^o-particle can be identified either by measuring the Q-value of the decay process, or by a heavily ionising proton. A θ_1^o-meson can be identified only by measuring the Q-value. It is well known that a measured Q-value of a Λ^o- or a θ_1^o-particle can only be reliable if the momenta of the two decay products can be very accurately measured, within about 5% error. In order to measure in a magnet cloud chamber a momentum of 1 GeV/c with an error of 5%, the maximum detectable momentum of the cloud chamber must be 21 GeV/c, and to measure with the same accuracy a momentum

---

*) The long lived neutral K-meson is presumably the θ_2^o-meson proposed by Gell-Mann and Pais.(65)

of 2 GeV/c the maximum detectable momentum must be 42 GeV/c. It will be emphasized later that the strange particles considered in this work are fast, the majority with momenta of several GeV/c. As the maximum detectable momentum of the Jungfraujoch cloud chamber is only 4 GeV/c, the Q-value of most of the events cannot be measured. Only in two or three cases could this measurement be made.

The classification of the V^o-particles into Λ^o- and θ_1^o-particles was then made in the following way:

i) When the positive secondary was slow (momentum less than 450 MeV/c), if its momentum and ionisation were consistent with those of a proton and not consistent with those of a light meson the V^o-particle was considered a Λ^o-particle. If its momentum and ionisation were consistent with those of a light meson and not consistent with those of a proton, the V^o-particle was considered a θ_1^o-meson.

ii) In a few cases the Λ^o-particle was excluded because the product of the sine of the decay angle by the momentum of the negative decay product, with at least one standard error, was greater than 118 MeV/c (Astbury[66]).

iii) When the negative decay product showed well measurable curvature, its momentum was measured. Then the momentum of the positive decay product was calculated from the decay angle and momentum of the negative, both assuming a Λ°- and a θ_1°-decay. The results were compared with the observed ionisation. If the positive was consistent with a proton and not consistent with a light meson, the V°-particle was considered a Λ°-hyperon. If the positive was consistent with a light meson, and not consistent with a proton, the V°-particle was considered a θ_1°-meson.

iv) As the V°-events were coplanar with the interaction, the line of flight of the V°-particle was drawn from the origin of the interaction to the apex of the V°-event. The decay angle and the angles between the line of flight and the charged secondaries were measured, and with these angles an analysis of the event based on the α and ϵ parameters of Podolanski and Armenteros[67] was made. The (α , ϵ) analysis was made twice: once assuming that the V°-particle was a Λ°-hyperon, then assuming that it was a θ_1°-meson. The calculated momentum of the positive secondary was combined with the observed ionisation. Again, if the positive secondary was consistent with a proton and not consistent with a light meson, the

V^o-particle was considered a Λ^o-hyperon, and if conversely, the V^o-particle was considered a θ_1^o-meson.

Whenever it was possible to apply more than one of the described criteria to the same event, this was done.

When it was not possible to exclude the Λ^o- or the θ^o-decay, both possibilities were assumed for the V^o-particle. These cases appear in Tables 4.4, 4.5 and 4.8 as Λ^o- and θ^o-decays.

4. Analysis of the Charged V-particles

The momentum of the primary particle of our charged V-events could not in general be directly measured. When the momentum of the charged secondary could not be measured, a lower limit to its value, equal to the corresponding maximum detectable momentum, was established. The decay angle was always measured. The ionisations of the primary and of the charged secondary were estimated.

The measurements which could be made are usually not enough to decide whether a charged V-particle is a K-meson or a hyperon. For this reason, each charged V-particle was analysed on the assumption that it is a K-meson and also on the assumption that it is a hyperon.

When assuming that the V-particle is a K-meson, the momentum of the K-meson could only be determined on the assumptions of the two-body decay modes : $K_{\pi 2} \rightarrow \pi + \pi^{o}$ and $K_{\mu 2} \rightarrow \mu + \nu$. The momentum of the K-meson could not be determined on the assumptions of three-body decay modes.

When assuming that the charged V-particle is a hyperon, the three following decay modes were considered : $\Sigma^{+} \rightarrow p + \pi^{o}$, $\Sigma^{\pm} \rightarrow n + \pi^{\pm}$ and $\Xi^{-} \rightarrow \Lambda^{o} + \pi^{-}$.

In all cases the momentum of the primary was obtained from the momentum of the secondary and the decay angle by using the curves calculated by H.S. White[68]. The ionisation of the primary was sometimes used to fix a lower limit to its momentum.

5. Identification of the non-decaying K-mesons

Three events were found in which a non-decaying K^{+}-meson is associated with another strange particle. The three K-mesons were identified from momentum and ionisation. In a magnet cloud chamber it is difficult to identify a K^{+}-meson which does not decay; due to uncertainties attached to ionisation estimates the track of a supposed K^{+}-meson could in fact be the track of a proton. However, the identification of the

One event which showed one negative V-particle and two neutral K-mesons was considered separately. The measurements made on this event are given in Tables 4.10 and 4.11.

* * *

Table 4.4

Measurements of the events of the type neutral V-particle plus neutral V-particle

SDS.R59/1s4

Event	V_a^o Momentum (GeV/c) and identity		V_b^o Momentum (GeV/c) and identity		ϕ (Deg.)	n_s	n_h	Minimum E (GeV)	ψ_a (Degrees)	ψ_b (Degrees)	ψ_{ab} (Degrees)	Origin
	Λ^o	θ^o	Λ^o	θ^o								
SG 75	0.67 ± 0.12			2.00 ± 0.20	15 ± 2	0	0	2.4	48 ± 10	37 ± 10	83 ± 8	
SN 1756	$0.59^{+0.08}_{-0.10}$			0.57 ± 0.05	27 ± 2	3	2	2	29 ± 8	42 ± 12	70 ± 7	P - Cu
TD 1183	$0.70^{+0.25}_{-0.18}$			0.83 ± 0.05	41 ± 1	1	0	3	90 ± 12	33 ± 8	64 ± 10	P - Cu
TF 901	$0.82^{+0.21}_{-0.14}$			1.48 ± 0.07	10 ± 2	6	1	8	30 ± 13	43 ± 10	13 ± 5	
TH 1018	$0.69^{+0.06}_{-0.09}$			1.15 ± 0.10	24 ± 2	2	2	3.3	88 ± 4	40 ± 5	58 ± 3	P - Cu
TS 200	0.47 ± 0.07			0.26 ± 0.02	67 ± 1	0	1	0.6	50 ± 4	62 ± 4	88 ± 6	P - C
NJ 42		2.70 ± 0.20		$5.10^{+0.20}_{-0.70}$	8 ± 2	2	0	12	20 ± 5	80 ± 2	86 ± 5	
TF 1561		1.08 ± 0.06		$1.70^{+0.10}_{-0.20}$	42 ± 1	1	3	6.5	84 ± 5	61 ± 20	28 ± 20	P - Cu
VB 536		1.40 ± 0.07		$2.55^{+0.32}_{-0.18}$	5 ± 1	0	1	3.9	72 ± 3	20 ± 2	55 ± 2	P - C
VB 913		$4.30^{+0.53}_{-0.30}$		2.30 ± 0.15	10 ± 2	4	0	14.5	29 ± 10	86 ± 16	56 ± 16	W - C
TF 221	0.44 ± 0.04		$1.30^{+0.25}_{-0.15}$		25 ± 2	6	1	8	47 ± 13	38 ± 9	82 ± 12	
MJ 29	$3.00\div4.00$	$4.70^{+1.00}_{-0.50}$		2.35 ± 0.35	15 ± 2	3	0	11	53 ± 5	82 ± 5	46 ± 5	
OC 31	$0.86\div2.30$	$1.84\div2.30$		$3.37^{+0.05}_{-0.15}$	35 ± 2	6	0	19	0 ± 5	10 ± 5	10 ± 5	
OC 56	$1.60\div5.06$	$2.40\div5.00$		$3.55\div4.30$	10 ± 2	6	0	13	10 ± 10	80 ± 10	85 ± 5	
RH 338	1.11 ± 0.05	0.98 ± 0.03		$4.00\div5.00$	19 ± 2	1	0	9	89 ± 8	88 ± 13	19 ± 11	
RT 851	$\geqslant 2.00$	$\geqslant 2.00$		$\geqslant 1.50$	8 ± 2	2	2	7	13 ± 5	30 ± 5	43 ± 2	
SH 232	$1.25\div4.20$	3.70 ± 0.50		4.30 ± 0.40	7 ± 2	4	0	10	14 ± 5	89 ± 2	89 ± 5	
SK 162	$1.25^{+0.10}_{-0.15}$	1.22 ± 0.05		1.60 ± 0.10	22 ± 3	1	0	5	29 ± 9	44 ± 10	21 ± 8	
SZ 414	$2.50\div6.40$	$6.60^{+1.00}_{-1.20}$		1.32 ± 0.10	10 ± 4	3	2	10	35 ± 16	74 ± 10	40 ± 11	
TC 1226	$0.90\div6.50$	$4.60\div6.60$		$4.00\div5.00$	4 ± 1	4	0	13	66 ± 20	44 ± 24	21 ± 21	
NU 11	$0.97\div1.99$	$1.48\div2.04$	$0.71\div1.42$	$1.39\div1.45$	5 ± 5	8	0	8	4 ± 2	10 ± 5	11 ± 5	
PH 161	$4.80^{+2.67}_{-1.20}$	$9.98^{+1.33}_{-1.60}$	$3.10\div4.50$	$4.30\div5.50$	10 ± 2	20	0	40	10 ± 5	85 ± 5	85 ± 5	
RH 1066	$1.20\div12.40$	$5.00\div11.00$	3.47 ± 0.28	2.75 ± 0.25	16 ± 2	5	0	8	73 ± 14	64 ± 12	18 ± 16	
RJ 451	2.48 ± 0.15	1.73 ± 0.10	$\geqslant 2.00$	$\geqslant 2.00$	17 ± 2	3	0	7	49 ± 5	72 ± 6	33 ± 6	
SF 1841	$\geqslant 2.00$	$\geqslant 2.00$	$\geqslant 2.00$	$\geqslant 2.00$	0 ± 4	7	0	25	-	-	-	
SQ 1209	-	-	-	-	~ 0	1	0	5	-	-	29 ± 24	
TF 611	$\geqslant 2.00$	$\geqslant 2.00$	$\geqslant 4.00$	$\geqslant 4.00$	2 ± 2	3	0	15	-	-	-	
TK 809	$1.20^{+0.30}_{-0.10}$	1.44 ± 0.10	1.44 ± 0.40	1.80 ± 0.20	17 ± 5	3	0	5	46 ± 15	64 ± 13	71 ± 6	W - C
TI 1204	$1.85^{+0.60}_{-0.35}$	$3.40^{+0.20}_{-0.10}$	$0.70\div1.50$	$2.15\div2.65$	4 ± 1	2	0	6	80 ± 12	82 ± 9	18 ± 6	

The first two columns give the momentum and identity of one of the V^o-particles. When the value of the momentum is written in the column headed "Λ^o" and nothing is written in the column headed "θ^o", the V^o-particle was identified as a Λ^o-hyperon. (Example, V_a^o of event SG 75.) When the value of the momentum is written in the column headed "θ^o" and nothing is written in the column headed "Λ^o" the V^o-particle was identified as a θ^o-meson with the criteria described in the text. (Example, V_a^o of event NJ 42.) When values of the momentum appear in both columns, the V^o-particle could not be identified as a Λ^o- or as a θ^o-particle and was analysed under both hypothesis. The third and fourth columns give the momentum and identity of the other V^o-particle. ϕ is the angle between the lines of flight of the two V^o-particles. n_s is the number of fast charged particles associated with the interaction which produced the two V^o-particles. n_h is the number of heavily ionising particles associated with the interaction. E is the lower limit of the visible energy of the interaction. ψ_a and ψ_b are the angles that each plane of decay makes with the plane containing the lines of flight of the two V^o-particles. ψ_{ab} is the angle between the planes of decay of the two V^o-particles. In the column headed "Origin", P stands for plate, W for wedge, Cu for copper and C for carbon, and when nothing is written the event was produced in lead. Photograph SQ 1209 shows bad distortions and no measurement can be made apart from the ones which are quoted.

Table 4.5

Measurements of the events of the type
neutral V-particle plus charged V-particle

Event	Neutral V-particle		Charged V-particle						ϕ (Deg.)	n_s	n_h	Minimum E (GeV)
	Momentum (GeV/c) and identity		Sign	Momentum (GeV/c) for several assumed identities								
	Λ°	θ°		$K_{\pi 2}$	$K_{\mu 2}$	$\Sigma^\pm \to n + \pi^\pm$	$\Sigma^+ \to p + \pi^\circ$	$\Xi^- \to \Lambda^\circ + \pi$				
RC 941		1.33 ± 0.06	+	0.95÷2.00	0.95÷2.90	2.30÷ 3.95	-	-	25 ± 3	10	1	15
RG 425		$1.53^{+0.06}_{-0.10}$	±	0.36÷0.48	0.36÷0.70	0.80÷ 1.05	-	0.80 ± 0.05	15 ± 4	> 10	3	12
RK 829	$0.90^{\pm 0.25}_{0.20}$		±	0.80÷6.50	0.80÷6.50	⩾ 0.80	⩾ 0.80	⩾ 0.80	3 ± 1	2	0	4
SJ 388	$1.26^{+0.05}_{-0.16}$	$1.20^{+0.06}_{-0.10}$	+	$0.77^{+0.10}_{-0.26}$	$1.05^{+0.15}_{-0.30}$	$1.55^{+0.25}_{-0.75}$	-	0.80÷1.30	14 ± 1	2	0	3.5
SL 101	0.63 ± 0.08		+	$1.02^{+0.18}_{-0.50}$	$1.40^{+0.40}_{-0.35}$	0.83÷ 2.60	-	-	32 ± 3	2	0	2.5
SL 496		$5.00^{+1.00}_{-0.50}$	+	-	0.35 ± 0.10	-	-	-	59 ± 4	4	4	9
SU 908		$4.00^{+0.60}_{-0.20}$	±	0.75÷2.30	0.64÷3.20	2.10÷ 4.60	0.60÷1.10	-	18 ± 1	1	0	5.5
SZ 984	$2.40^{+0.50}_{-1.10}$	$2.60^{+0.60}_{-0.20}$	+	0.70÷0.80	0.70÷1.15	0.80÷1.80	-	0.80÷1.10	33 ± 5	0	0	2.5
TB 249		$2.74^{+0.38}_{-0.14}$	±	2.10÷6.00	1.85÷7.50	⩾ 5.50	1.77÷2.30	-	23 ± 2	3	0	7
TE 286	$0.98^{+0.04}_{-0.08}$	0.89 ± 0.04	±	4.00÷4.50	4.00÷7.00	4.00÷10.00	-	-	46 ± 2	> 10	3	20

The first two columns give the momentum and identity of the neutral V-particle with the same convention used for the V°-particles of Table 4.4. The third column gives the sign of the charged V-particle. Columns 4 to 8 give the momentum of the charged V-particle under several assumed decay schemes; these momenta were obtained from the momentum of the charged secondary and the decay angle by using the curves calculated by H.S. White.(68). A line means that the corresponding decay scheme cannot occur with the observed decay angle and momentum of secondary. ϕ is the angle between the lines of flight of the two V-particles. n_s and n_h are the number of fast charged particles and of heavily ionising particles as-

TABLE 4.6

Measurements of the events of the type

neutral V-particle plus charged V-particle

- Angles between planes -

Event	ψ_o (Degrees)	ψ_{cv} (Degrees)	$\psi_{o,cv}$ (Degrees)	Origin
RC 941	45 ± 7	28 ± 8	22 ± 4	
RG 425	6 ± 12	25 ± 20	26 ± 18	
RK 829	20 ± 17	38 ± 17	21 ± 6	
SJ 388	69 ± 2	5 ± 2	74 ± 2	
SL 101	30 ± 3	83 ± 5	58 ± 4	
SL 496	10 ± 6	41 ± 9	38 ± 9	P - Cu
SU 908	61 ± 5	4 ± 4	60 ± 4	
SZ 984	22 ± 10	-	-	
TB 249	0 ± 5	32 ± 7	30 ± 6	P - Cu
TE 286	28 ± 2	22 ± 2	47 ± 2	

ψ_o is the angle between the decay plane of the V^o- particle and the plane determined by the two lines of flight. ψ_{cv} is the angle between the decay plane of the charged V-particle and the plane determined by the two lines of flight. $\psi_{o,cv}$ is the angle between the two decay planes. In the column headed "Origin" the convention used in Table 4.4 was followed.

Table 4.7

Measurements of the three events of the type neutral V-particles plus non-decaying positive K-meson

Event	Neutral V-particle		K^+-meson		ϕ (Deg.)	n_s	n_h	Minimum E (GeV)	ψ_o (Degrees)	Origin
	Momentum (GeV/c) and identity		Momentum (GeV/c)	Ionisation estimate						
	Λ°	θ°								
SC 507	$0.61^{+0.19}_{-0.14}$		0.29 ± 0.02	2 ÷ 5	60 ± 3	2	1	2	28 ± 4	
SN 1534		1.09 ± 0.05	0.22 ± 0.02	3 ÷ 6	69.5 ± 2	0	0	3.8	20 ± 7	P - Cu
SY 91	$0.60^{+0.12}_{-0.10}$		0.17 ± 0.02	4 ÷ 8	66 ± 2	8	1	7	47 ± 5	

The first two columns give the momentum of the neutral V-particles. In events SC 507 and SY 91 the V°-particle was identified as a Λ°-hyperon; in event SN 1534 it was identified as a neutral K-meson and the quoted momentum was calculated under the assumption that it is a θ_1°-meson. The third and fourth columns give the momentum and ionisation of the K^+-meson. The meaning of ϕ, n_s, n_h and E is the same as in Table 4.4. ψ_o is the angle between the decay plane of the V°-particle and the plane determined by the lines of flight of the V°-particle and K^+-meson.

Table 4.8

Measurements of the events with three neutral V-particles

Event	V_a^o		V_b^o		V_c^o		n_s	n_h	Minimum E (GeV)
	Momentum (GeV/c) and identity		Momentum (GeV/c) and identity		Momentum (GeV/c) and identity				
	Λ°	θ°	Λ°	θ°	Λ°	θ°			
TD 255	$\geqslant$ 0.90	$\geqslant$ 0.75	$\geqslant$ 0.90	$\geqslant$ 0.75		$2.45^{+0.20}_{-0.10}$	1	0	8
TN 140	2.50÷4.40	4.60÷6.40		$1.81^{+0.09}_{-0.06}$	1.50÷6.20	6.50÷8.00	2	0	7

The first six columns give the momentum and identity of the three neutral V-particles with the same convention used for the V^o-particles of Table 4.4. The meaning of n_s, n_h and E is the same as in Table 4.4.

Table 4.9

Angles, in degrees, of the events with three neutral V-particles

Event	ϕ_{ab}	ϕ_{ac}	ϕ_{bc}	ψ_a^b	ψ_b^a	ψ_{ab}	ψ_a^c	ψ_c^a	ψ_{ac}	ψ_b^c	ψ_c^b	ψ_{bc}
TD 255	6 ± 1	32±1	28±1	54±14	54±14	10±10	11±15	13±7	10±10	7±12	4±4	10±10
TN 140	30± 1	7±1	23±1	64±13	79±15	30±8	63±14	83±22	21±14	79±18	83±24	23±16

ϕ_{ab}, ϕ_{ac} and ϕ_{bc} are the angles between the lines of flight of V_a^o and V_b^o, V_a^o and V_c^o, V_b^o and V_c^o. ψ_a^b is the angle between the decay plane of V_a^o and the plane determined by the lines of flight of V_a^o and V_b^o. ψ_b^a is the angle between the decay plane of V_b^o and the plane determined by the lines of flight of V_a^o and V_b^o. ψ_{ab} is the angle between the decay planes of V_a^o and V_b^o. The meaning of the other angles is obvious.

Table 4.10

Measurements made on the event
RQ 31 of the type : $V^- + \theta^o + \theta^o$

θ_a^o Momentum (GeV/c)	θ_b^o Momentum (GeV/c)	Negative V-particle: Momentum (GeV/c) for several assumed identities				n_s	n_h	Minimum E (GeV)
		$K_{\pi 2}$	$K_{\mu 2}$	$\Sigma^- \to n + \pi^-$	$\Xi^- \to \Lambda^o + \pi^-$			
$8.40^{+1.20}_{-1.80}$	0.88 ± 0.05	1.00÷6.50	0.85÷10.00	2.60÷10.00	4.00÷10.00	10	0	37

The first two columns give the momenta of the two neutral K-mesons under the assumption that they are θ_1^o-mesons. Columns 3 to 6 give the momentum of the negative charged V-particle under several decay schemes. n_s, n_h and E have the same meaning as given in other tables.

Table 4.11

Angles, in degrees, of the event RQ 31

ϕ_{ab}	$\phi_{a,cv}$	$\phi_{b,cv}$	ψ_a^b	ψ_b^a	ψ_{ab}	ψ_a^{cv}	ψ_{cv}^a	$\psi_{a,cv}$	ψ_b^{cv}	ψ_{cv}^b	$\psi_{b,cv}$
46 ± 3	20 ± 2	66 ± 3	59 ± 13	31 ± 5	83 ± 13	44 ± 11	39 ± 5	14 ± 14	51 ± 6	37 ± 4	71 ± 7

ϕ_{ab}, $\phi_{a,cv}$ and $\phi_{b,cv}$ are the angles between the lines of flight of V_a^o and V_b^o, V_a^o and charged V-particle, V_b^o and charged V-particle. The nine angles ψ have similar meanings to those described in the caption to Table 4.9.

CHAPTER V

EVENTS WHICH DO NOT CONSIST OF TWO IDENTIFIED K-MESONS

1. Introduction

The events presented in Tables 4.4. to 4.11. will be divided into two groups: one containing all cases in which the strange particles are not two identified K-mesons; they will be analysed in this chapter. A second group contains only the events in which both particles are identified K-mesons; they will be analysed in the next chapter.

We shall analyse separately the events that show two neutral V-particles and those that show one neutral and one charged V-particle. At the end of the chapter we shall comment briefly on the events which show three neutral V-particles, on those that show one neutral V-particle and one non-decaying K^+-meson, and on event RQ 31.

There are 29 events which show two neutral V-particles. The results of the measurements made on them are given in Table 4.

Table 5.1 gives a survey of the 29 events, classed according to the position of the interaction in which they were produced and the identity of the V^o-particles. In this table "K^o" and "Λ^o" mean that the particle was identified as a K^o-meson or as a Λ^o-hyperon respectively, according to the criteria described in section 3 of chapter IV; "V^o" means that the particle could not be identified.

As a consequence of the mean lifetimes of the Λ^o-hyperon and θ_1^o-meson, the probability for these particles to decay in the illuminated volume of the cloud chamber is much greater when they are produced in the plates than when they are produced above the cloud chamber. Due to this fact we shall consider separately the events produced in one and in the other region.

2. Events in which two neutral V-particles were produced in the plates.

i) The reaction $\pi^- + p \rightarrow \Lambda^o + \theta^o$

From the six events produced in the plates, two are of the type $K^o + K^o$ and four of the type $\Lambda^o + K^o$: SN 1756 TD 1183 and TH 1018, produced in copper and TS 200 produced in carbon. Let us examine whether these four events could have

TABLE 5.1

Origins and frequencies of the 29 events which show two "copunctual" neutral V-particles

Origin	K^o K^o	Λ^o K^o	Λ^o Λ^o	V^o K^o	V^o Λ^o	V^o V^o	Totals
Above the illuminated volume	2	2	1	9	0	9	23
Plates	2	4	0	0	0	0	6
Totals	4	6	1	9	0	9	29

The table gives the frequencies of the several types of events, classed according to the identification of the particles. K^o means that t V^o-particle was identified as a K^o-meson and Λ^o means that the V^o-particl was identified as a Λ^o-hyperon, according to the criteria described in se tion 3 of chapter IV; V^o means that the particle could not be identified. The majority of the events with origin above the illuminated volume of the cloud chamber were produced in the lead block L_1; few of them were produc in the wedges.

Note that in the six events produced in the plates all the V^o-particles were identified.

Plate 1

EVENT TH 1018 - A and B are the decay products of the Λ^{o}-hyperon, C and D those of the θ^{o}-meson. The two V^{o}-particles were produced in a nuclear interaction in the copper plate. The event is described in the text. E and F are the decay products of a third V^{o}-particle (non-identified) which is not associated with the first two.

5363

been produced in the simplest reaction which leads to the creation of a Λ^{o}-hyperon associated with a K^{o}-meson, namely:

$$\pi^{-} + p \rightarrow \Lambda^{o} + K^{o} \qquad (1)$$

This reaction was studied in detail in chapter III and its dynamics are represented in diagrams 1 to 8 of Appendix I. In each event, from the measured momenta $p_{\Lambda^{o}}$ and $p_{K^{o}}$, and angle ϕ between the lines of flight, we can calculate the angles of emission $\varphi_{\Lambda o}$ and $\varphi_{K^{o}}$ in the L.S., on the several assumptions about the nucleon's Fermi momentum. The values of $p_{\Lambda o}$, $\varphi_{\Lambda o}$, $p_{K^{o}}$ and $\varphi_{K^{o}}$ of the four events, compared with diagrams 1 to 8 of Appendix I show that three of the events fit the dynamics of reaction (1): SN 1756 and TD 1183 with case d of the nucleon's Fermi momentum, TH 1018 with case c. The elements of the dynamics in the L.S. and in the C.M.S. are given in Table 5.3.

ii) Probability of seeing the decays of the Λ^{o} and the Θ^{o} particles produced in reaction (1).

If the probability of seeing the decays of both the Λ^{o}- and the Θ^{o}-particles produced according to reaction (1) is known, then the observed number of pairs (Λ^{o}, Θ^{o}) produced in that reaction will indicate how many have been produced.

TABLE 5.2

Calculated limits of the probability to observe in the Jungfraujoch cloud chamber the decays of the particles produced in the interaction $\pi^- + p \rightarrow \Lambda^0 + \theta^0$

θ^* (Degrees)	p (GeV/c)	Events produced in the lead block L_1 - Upper limits			Events produced in the plates - Lower limits		
		Λ^0	θ^0	$\Lambda^0 + \theta^0$	Λ^0	θ^0	$\Lambda^0 + \theta^0$
0	1	6	0.2	0.009	35	38	13
	1÷1.5	14	0	0	26	11	2
	1.5÷3	24	0	0	21	25	5
90	1	3.2	0.1	0.005	35	36	14
	1 ÷ 3	13	13	0.6	21	18	3.4
	1	2.1	2.4	0.05	35	35	13
	1 ÷ 3	1.8	22	0.5	30	21	6

The probabilities are given as percentages of the number of interactions produced. For events produced in the lead block L_1 the columns headed Λ^0, θ^0 and $\Lambda^0 + \theta^0$ give respectively the upper limits of the probabilities to observe the decays of only the Λ^0-particle, only the θ^0-particle, and of both particles. For events produced in the plates, the figures are the lower limits of those probabilities. θ^* is the angle of emission of the Λ^0-particle in the C.M.S., p is the momentum of the incident π-meson. In this calculation the nucleon was assumed at rest. In the calculation of the probabilities the decay of the θ_1^0-particle into two π^0-mesons was not taken into account.

TABLE 5.3

Measurements of the 4 events which fit the dynamics of the reaction : $\pi^- + p \rightarrow \Lambda^\circ + \theta^\circ$

Event	ϕ (Deg.)	Momentum $\left(\frac{GeV}{c}\right)$		φ_{Λ° (Deg.)	φ_{θ° (Deg.)	p $\left(\frac{Gev}{c}\right)$	θ^* (Deg.)	Case
		Λ°	θ°					
SG 75	15 ± 2	0.67 ± 0.12	2.00 ± 0.20	11 ± 1	4 ± 1	2.3 ± 0.3	170 ± 5	c
SN 1756	27 ± 2	$0.59^{+0.08}_{0.10}$	0.57 ± 0.05	11 ± 2	16 ± 2	0.95 ± 0.05	130 ± 10	d
TD 1183	41 ± 1	$0.70^{+0.25}_{0.18}$	0.83 ± 0.05	23 ± 2	18 ± 2	1.1 ± 0.1	140 ± 10	d
TH 1018	24 ± 2	$0.69^{+0.06}_{0.09}$	1.15 ± 0.10	15 ± 2	10 ± 2	1.7 ± 0.2	150 ± 5	d

The first event was produced above the illuminated volume of the cloud chamber; the other three, in the copper plate.

ϕ is the angle between the lines of flight of the two V°-particles. φ_{Λ° and φ_{θ° are the angle between the lines of flight of the Λ° and the θ°-particle, respectively, with the direction of the total momentum in the L.S. p is the momentum of the incident π^--meson. θ^* is the angle of emission of the Λ°-hyperon in the C.M.S. The last column indicates the direction of the nucleon's Fermi momentum according to the convention adopted in chapter III. The Fermi energy of the nucleon was taken as 25 MeV. φ_{Λ°, φ_{θ°, p and θ^* were obtained from diagrams 5 to 8 of Appendix I.

It is impossible to make the exact calculation of that probability in a cosmic-ray experiment, because many elements which would have to be well-known are not, such as the exact energy and direction of the primary π-meson, the angle of emission of the Λ^{o}- or θ^{o}-particle in the C.M.S., the point of the target where the interaction occurred (the masses and the mean lifetimes of the particles are supposed to be known). Nevertheless, by making reasonable assumptions about the primary momentum and about the angle of emission of the particles in the C.M.S., limits of that probability can be calculated. The geometrical uncertainties are greater when the interaction occurs outside the cloud chamber than when it occurs inside.

Due to the large thickness of the lead block L_1 placed above the cloud chamber (Fig. 1.1), only an upper limit of the probability for both the Λ^{o}- and the θ^{o}-particles to decay in the illuminated volume of the chamber can be calculated, corresponding to interactions which occurred at the bottom of the block. When the interactions occur in the plate in the middle of the chamber, on the contrary, a lower limit of that probability can be calculated. Table 5.2 gives the result of the calculation for several energies of the π-meson

and several angles of emission in the C.M.S., assuming collision with a free nucleon and primary direction making the angle not greater than 30° to the vertical. The table lists for events produced in the block L_1 the upper limit of the probabilities to see only the Λ^0-decay, only the Θ^0-decay and both decays; for events produced in the plate the upper limit of those probabilities are given. The calculation was not carried out for π^--mesons of momentum greater than 3 GeV/c, because the π^--meson has to be a secondary of an interaction and the average energy of such π^--mesons is expected to be between 1 and 2 GeV (Camerini et al. (69)).

iii) The CERN-Jungfraujoch group experiment on V^0-particles produced in copper and carbon.

The CERN-Jungfraujoch group (6) made a comparative study of the single neutral V-particles produced in the copper and carbon plates. The numbers of Λ^0- and Θ^0-particles produced in those plates and observed to decay in the chamber were determined, and then, correcting for the probability of observation, the numbers of Λ^0- and Θ^0-particles produced in those materials were calculated. The results are reproduced in Table 5.4, where the corresponding numbers of observed single charged V-particles are also quoted. The number produced was

obtained by dividing the number observed by the probability of observation. The probability of observation was calculated for every particular V^o-particle taking into account the measured momentum, the mean lifetime, the position of the decay point and of the line of flight in the cloud chamber. The mean lifetimes used were 3.0×10^{-10} sec for the Λ^o-particle and 1.0×10^{-10} sec for the θ^o-particle.

The data of Table 5.4 show that the "measured" probability of observation of the decay of a single Λ^o- or θ^o-particle produced in the plate is $\sim$ 50%. It is important to notice the agreement of the "measured" value of $\sim$ 50% with the calculated lower limit of that probability reported in Table 5.2. This indicates that the calculated lower limit of the probability to see both decays, of the Λ^o- and of the θ^o-particles produced in reaction (1), as quoted in Table 5.2, is very realistic.

iv) Events produced in the plates according to reaction (1).

Let us compare the observed number of events produced in the plates according to reaction (1) with the expected number if all the Λ^o- and the θ^o-particles had been produced according

TABLE 5.4

Summary of V-events from copper and carbon obtained by the CERN-Jungfraujoch group

	Copper			Carbon			Totals
	Λ^0	Θ^0	Total	Λ^0	Θ^0	Total	
Particles observed	27	26	53	10	18	28	81
Particles produced	54	54	108	19 (10)	39 (20)	58 (30)	166
Observed Charged V-particles			3			4	7

The numbers of particles produced in each materials were obtained by dividing the numbers observed by the probability of observation, as described in the text. The numbers in parenthesis relative to carbon correspond to events produced in the plate only; the others correspond to events produced in the plate and in the wedge.

to that reaction. Table 5.2 shows that for values of the momentum of the π-meson between about 1 to 3 $\frac{GeV}{c}$, the lower limit to the probability of seeing the decays of both the Λ^0- and the Θ^0-particles produced according to reaction (1) varies very little with the angular distribution of the particles in the C.M.S.; we can take that lower limit as 5% for all values of Θ^*.

Table 5.4 shows that there are 54 Λ^0- and 54 Θ^0-particles produced in the copper plate; if we assume that all of them are produced according to reaction (1) we should observe 3 or more pairs (Λ^0, Θ^0) from copper fitting the dynamics of that reaction. The same table shows that there are 10 Λ^0-particles and 20 Θ^0-particles produced in the carbon plate; on the same assumption we should expect 1 or more pairs (Λ^0 , Θ^0) from carbon fitting the dynamics of reaction (1). The observed numbers are 3 pairs from copper and none from carbon.

With such figures it is not very surprising that we do not see any pair from carbon, because of the poor statistics. In any case, we should expect to observe more events produced according to reaction (1) in copper than in carbon, because secondary π-mesons are easier produced in copper than in carbon.

The statistics are very poor, and in experiments like this we cannot calculate exactly how many pairs (Λ^0, θ^0) have been produced in copper or carbon according to reaction (1). But, if we now take into account also the two following facts :

a) according to Eisler et al.[18] the decays of $\sim$30% of the Λ^0-hyperons and of $\sim$ 15% of the θ^0-mesons are not seen because of the decay modes : $\Lambda^0 \rightarrow n + \pi^0$ and $\theta_1^0 \rightarrow \pi^0 + \pi^0$;

b) as we shall see in the next chapter, there is evidence for some of the Λ^0-hyperons originated from copperto be produced in some process of conversion of strange particles ;

we conclude that the numbers of events from the copper plate that are observed are evidence that reaction (1) occurs frequently in copper, produced by secondary π^--mesons.

3. Events in which two neutral V-particles were produced above the cloud chamber.

i) Reaction $\pi^- + p \rightarrow \Lambda^0 + \theta^0$

Table 5.1 shows that among the events produced above the illuminated volume of the cloud chamber, there are 11 events in which one of the two V^0-particles was identified as a K^0-meson, and 9 in which neither of the V^0-particles could be

identified. The 20 events were analysed in order to find out whether reaction (1) could account for their production. The measured momenta of the two V^{o}-particles and the angle ϕ between the lines of flight allowed an analysis based on diagrams 1 to 8 of Appendix I, in the same way as described in Section 2 i) for the events produced in the plates. The conclusion was that only event SG 75 fits the dynamics of reaction (1), with case c of the nucleon's Fermi momentum. The other 19 events do not fit the dynamics of this reaction. The elements of the dynamics of reaction (1) for event SG 75 are listed in Table 5.3.

There is an important characteristic of the dynamics of reaction (1) which must be emphasized at this point. When the angle ϕ between the lines of flight is small, less than, say, 40^{o}, one of the two V^{o}-particles is slow : taking into account the Fermi energy either the Λ^{o}-hyperon has momentum less than 900 MeV/c, or the K^{o}-meson has momentum less than 450 MeV/c. This can easily be seen from diagrams 1 to 8 of Appendix I.

The measurements that are reported in Table 4.4 show that in our events the angle ϕ is in general small, but both the V^{o}-particles are fast. The nucleon's Fermi momentum does not help; in diagrams 3 to 8 the extreme conditions for each

of the cases b, c and d of the nucleon's Fermi momentum were taken into account.

At first it might seem surprising that 3 out of 4 events produced in the plates fit the dynamics of reaction (1), and out of 20 produced above the illuminated volume of the cloud chamber only one does. The calculated probability of seeing both the decays of the Λ^{o}- and the Θ^{o}-particles, given in Table 5.2, show that we should expect to see very few decays of both the particles when they are produced in the lead block L_1. This probability is direct consequence of the dynamics of the reaction (1). When the reaction occurs in the lead block L_1, the Λ^{o}- and the Θ^{o}-decays are seen only when they are emitted at small angles in the L.S. As was already pointed out, in this case one of the V^{o}-particles is slow. Therefore, it has very high probability of decaying before reaching the illuminated volume of the cloud chamber.

ii) Scattering of the V^{o}-particles

The existence of hyperfragments shows that the Λ^{o}-particle interacts strongly with nucleons. We must expect that Λ^{o}-particles are frequently scattered by nucleons. This point

will be emphasized in Chapter VIII, when the spectrum of the Λ^{o}-hyperons will be discussed. We could think that the 19 events produced in L_1 and which do not follow the dynamics of reaction (1) were produced according to that reaction and then the scattering of one or both V^{o}-particles changed the original values of momenta and angles. This hypothesis is completely ruled out, because as was pointed out in i) the general reason why the events do not follow the dynamics of reaction (1) is that the V^{o}-particles are too fast for the observed angles ϕ. This cannot be explained by scattering, since scattering should produce exactly the opposite effects, i.e., should slow down the particles and give at least random angle distribution, but not systematic collimation of the lines of flight.

iii) Other possible production reaction

The following processes can account for the production of the 19 events originated above the illuminated volume of the cloud chamber which do not fit the dynamics of reaction (1).

a) Each of the two V^{o}-particles could have been produced in separate elementary interactions which occurred inside the same nucleus (in a cascade process). In this case the association of the two V^{o}-particles in the same photograph is casual.

The author developed several statistical arguments in order to calculate how many of the events correspond to casual association; in all of them so many assumptions have to be made that no reliable result can be obtained. It is worth mentioning only the following : if we assume that in the vast majority of the elementary interactions no more than 2 neutral V-particles are produced, then very few of the 19 events are cases of casual association. Otherwise we would conclude that in 50% or more of the times in which two neutral V-particles are produced in an interaction inside a nucleus, there is a second interaction inside the same nucleus which also produces two other V^{o}-particles.

b) The reactions :

$$N + N \rightarrow \Lambda^0 + \underline{K}^0 + N \qquad (2)$$

$$N + N \rightarrow K^0 + \underline{K}^0 + N + N \qquad (3)$$

$$\pi^- + N \rightarrow K^0 + \underline{K}^0 + N \qquad (4)$$

$$\pi^- + N \rightarrow \Lambda^0 + \underline{K}^0 + n\pi^- \qquad (5)$$

We shall see in the next chapters that there is evidence that reactions (2), (3) and (4) occur often in our experiment. Considering that at the energy of ç GeV the double and triple production of π^--mesons occur about as often as single production, we should expect reaction (5) to compete seriously with reaction (1) at high energies.

4. The cases of one neutral V-particle associated with one charged V-particle

The measurements made on these events are reported in Tables 4.5 and 4.6. Out of the 10 observed cases, 8 were produced above the cloud chamber, 2 in the copper plate (SL 496 and TB 249) and none in carbon. With the exception of event SL 496 in which the charged V-particle is a K-meson, probably a $K_{\mu 2}$-meson, the other nine charged V-particles listed in Table 4.5 cannot be identified.

Let us examine reaction (7).

Steinberger's groups[19] and Glaser's group[20][21] show that when $\Sigma^{\pm}$-particles are produced in π-meson-nucleon collisions according to reaction (7) the $\Sigma^{\pm}$-particle is emitted predominantly forwards in the C.M.S. In the notation used in diagrams of Appendix I, the $^{\pm}$-particle is emitted in the C.M.S. at angle $\theta^{*} < \sim 60^{\circ}$. Diagrams 9 to 16 of Appendix I show that the K-meson which is associated with the $\Sigma^{\pm}$-particle is then emitted in the L.S. at an angle between $\sim 50^{\circ}$ and $\sim 120^{\circ}$. When a θ°-meson is emitted from the plate at such an angle, the probability of seeing its decay is nearly zero. In fact, among the observed decays of all strange particles produced in the copper and carbon plates there is not one single decay of a θ°-meson or charged K-meson above the plate.

We analysed the difficulty of detecting reactions (6) and (7) when they occur in the plate. When the reactions occur above the illuminated volume of the cloud chamber the probability of seeing the decays of the particles is still smaller.

ii) Analysis of the events in terms of reactions (6) and (7)

As our charged V-particles cannot be identified, each event has to be analysed twice. First, assuming that the charged V-particle is a K-meson with the momenta quoted in Table 4.5 and trying to fit interaction (6) by using diagrams 1 to 8 of Appendix I. Secondly, assuming that the charged V-particle is a Σ -hyperon with the momenta given in Table 4.5 and trying to fit reaction (7) by comparing the values of momenta and angle ϕ with diagrams 9 to 16 of Appendix I. The conclusion is that only event SL 101 could have been produced according to reaction (6), in case c of the nucleon's Fermi momentum, and events SU 908 and SZ 984 could have been produced according to reaction (7), in case c of the nucleon's Fermi momentum.

The simplest reaction of a π^--meson with a nucleon does not explain, then, the production of the majority of these events. We cannot prove that the two particles of event SL 101 were produced according to reaction (6) nor that the particles of events SU 908 and SZ 984 were produced according to reaction (7); we can only say that the measurements made on the three events are not inconsistent with the dynamics of reactions (6) and (7); the measurements made on the other seven events listed in Table 4.5 are inconsistent with the dynamics of those two reactions.

Due to uncertainties in the identification of a charged V-particle and to the impossibility of calculating the probability for a charged V-particle to decay in the illuminated volume of the cloud chamber, these events are not so useful as the events that show two neutral V-particles. If reaction (1) occurs frequently in heavy nuclei, produced by secondary π^--mesons, we should expect reactions (6) and (7) also to occur frequently, but in our experiment we have no direct evidence for this.

5. Comments on the other events

i) Cases of three neutral V-particles

By combining two by two the three momenta and angles reported in Table 4.8, in order to see whether some combination agrees with the dynamics of reaction (1) we conclude that no combination is consistent with this reaction. As we have only two events of this type and they present no special features, we shall try not to make any further analysis of them. The number of events is very small and we should expect two or three casual associations of this type. We cannot decide whether or not they are cases of casual association or examples of "multiple production" of strange particles, as reported by Tsai-Chu and Max Morand.(70)

ii) Events of the type V^o-particle plus non-decaying K^+-meson.

There are three such events, reported in Table 4.7. Event SN 1534 is extremely important and will be described at length in the next chapter. The other two events present no special interest.

iii) Event RQ 31 ($\theta^o + \theta^o + V^-$-particle)

The result of the measurements made on this event are reported in Tables 4.10 and 4.11. Neither of the θ^o-mesons with the V^--particle satisfies the dynamics of reaction (7), under the hypothesis that the V^--particle is a Σ^--hyperon. It is remarkable that the three strange particles are associated with a shower of very high energy, certainly more than 40 GeV, containing 10 other fast particles. Table 4.10 shows that the V^--particle has momentum > 2.6 GeV/c if it is a hyperon, and one of the θ^o-mesons has momentum $(8.4^{+1.2}_{-1.8})$ GeV/c. This measurement in itself shows that the quality of the photograph is extremely good. It might be that the event is a case of associated production of a Ξ^--particle (strangeness -2) with two θ^o-mesons, similar to the event reported by Sorrels et al.[33] but we cannot prove it.

EVENT RQ 31 - A is a negative charged V-particle, B its charged secondary; C, D and E, F are the decay products of two K^{o}-mesons. The three strange particles are associated with a shower with visible energy greater than 40 GeV.

5363

6. Conclusions

The following conclusions arise from the analysis presented in this chapter.

1. Reaction (1) occurs frequently in the copper plate, produced by secondary π^--mesons originated in the plate, probably in the same nucleus where the reaction occurs.

2. The majority of the observed events which consist of two copunctual strange particles (neutral + neutral or neutral + charged) originated in the lead block L_1 are not produced in a two-body π^--meson-nucleon interaction. The Fermi energy of the nucleon was taken into account. These events are produced in some other processes in which the strange particles are produced with high energy and with the lines of flight collimated. These processes could be, for example, reactions (2) to (5) and the corresponding reactions in which the Λ^o-particle and the K^o-meson are replaced by charged hyperons and K-mesons respectively.

3. It is reasonable to assume that the same types of interactions occur in the lead block L_1 and in the copper plate. But due to lifetimes and energies of the V^o-particles at production, the pairs (Λ^o, θ^o) produced in reaction (1) are

predominantly seen when the reaction occurs in copper plate. On the contrary, the pairs (V^o, V^o) produced in other reactions are predominantly seen when they are produced in the lead block L_1; when produced in the copper plate they escape through the bottom of the cloud chamber.

* * *

CHAPTER VI

EVENTS WHICH CONSIST OF TWO IDENTIFIED K-MESONS

1. Introduction

In the Gell-Mann model of the fundamental particles there are two doublets of K-mesons: one, characterised by strangeness S = +1, is formed by the positive and a neutral K-meson; the other is the doublet consisting of the anti-particles of those K-mesons, namely the negative K-meson and the anti-neutral K-meson, and consequently has strangeness S = -1.

In all the other models of the fundamental particles there is a similar division of the K-mesons into two groups. In the Sachs model, for instance, there is a class of K-mesons with attribute a = -1, formed by the positive and a neutral K-meson; and a second class, with attribute a = +1, formed by the negative and another neutral K-meson.

If we accept conservation of strangeness in strong interactions there are two ways to prove whether K-mesons with

strangeness -1 exist : 1) one way is to observe experimentally the absorption of a neutral K-meson by a particle with strangeness zero, to produce a particle which is known to have strangeness -1; 2) the other way is to observe the associated production of a neutral K-meson with either another neutral K-meson or with a positive K-meson.

Therefore, to test the classification of the K-mesons in the acceptable models of the fundamental particles it is extremely important to observe experimentally the following cases of associated production:

two K^{o}-mesons, a K^{o}-meson with a K^{+}-meson, a K^{+} with a K^{-}-meson, in the three cases without the production of other strange particles if the reaction is produced by "ordinary" particles.

Three events interpreted as associated production of a K^{+}- with a K^{-}-meson have been found in nuclear emulsion experiments, and one event interpreted as associated production of two K^{o}-mesons was found in a diffusion cloud chamber. Among the three events found in emulsion, in one, reported by Lal et al.,[9] and in a second, reported by Friedlander et al.,[71] a K^{+}- and a K^{-}-meson emerge from a star together with many other particles. Those authors assume that both K-mesons have been produced in the same elementary collision, and do not discuss the possibility of

them being produced in different interactions inside the same n nucleus. In the third example, found by Cocarelli et al.,[72] the K^+- and the K^--mesons are produced in a simple interaction, without any other charged particle. The event interpreted as associated production of two K^o-mesons was found by Fowler et al.[73] in a hydrogen diffusion cloud chamber attached to the Bevatron: from an interaction produced by a 4.3 GeV π^--meson colliding with a proton emerge a Θ_1^o-meson, a π^--meson and a proton. Momentum and energy balance shows that another K^o-meson was produced and escaped detection.

In this chapter we shall study in detail two events obtained in the Jungfraujoch experiment, which give strong support to the idea that there are two classes of K-mesons. One event shows the associated production of two K^o-mesons, the other shows the associated production of a K^o- with a K^+-meson. The three K^o-mesons are all seen to decay.

2. Events Observed in the Jungfraujoch Experiment

During the systematic analysis of the events reported in this thesis, 6 events were found in which two "copunctual" strange particles are identified as K-mesons. In 4 of these events both K-mesons are neutral, in the other 2 one is neutral

TABLE 6.1

Measurements of the events which consist of two identified K-mesons

Event	Origin	K_a		K_b		ϕ (Deg.)	n_s	n_h	E (GeV)	ψ_a (Deg.)	ψ_b (Deg.)	ψ_{ab} (Deg.)
		Type	Momentum (GeV/C)	Type	Momentum (GeV/c							
NJ 42	Outside	K^o	2.70 ± 0.20	K^o	$5.10^{+0.20}_{-0.70}$	8 ± 2	2	0	12	20 ± 5	80 ± 2	86 ± 5
SL 496	P-Cu	K^o	$5.00^{+1.00}_{-0.50}$	K^+	0.35 ± 0.10	59 ± 4	4	4	9	10 ± 6	41 ± 9	38 ± 9
TF1561	P-Cu	K^o	1.08 ± 0.06	K^o	$1.70^{+0.10}_{-0.20}$	42 ± 1	1	3	6.5	84 ± 5	61 ± 20	28 ± 20
VB 913	W - C	K^o	$4.30^{+0.53}_{-0.30}$	K^o	2.30 ± 0.15	10 ± 2	4	0	14.5	29 ± 10	86 ± 16	56 ± 16
VB 536	P - C	K^o	1.40 ± 0.07	K^o	$2.55^{+0.32}_{-0.18}$	5 ± 1	0	1	3.9	72 ± 3	20 ± 2	55 ± 2
SN1534	P-Cu	K^o	1.09 ± 0.05	K^+	0.22 ± 0.02	69.5 ± 2	0	0	3.8	20 ± 7	-	-

The origin of event NJ 42 is outside the cloud chamber, in the lead block L_1 (figure 1.1). P, W, Cu and C stand for plate, wedge, copper and carbon respectively. The momenta of the neutral K-mesons were calculated on the assumption that they are θ_1^o-mesons. ϕ, n_s, n_h, ψ_a, ψ_b and ψ_{ab} have the same meaning as in Table 4.4. The last two events are extensively discussed in the text.

and the other is positively charged. Although the measurements made on these events are given in Tables 4.4, 4.5 and 4.7, the results of the most relevant measurements are repeated in this chapter in Table 6.1.

It might be that besides these 6 events there are others which show two neutral K-mesons, among the events of Table 4.4 in which at least one of the V^{o}-particles could not be identified.

It is worthwhile to point out that the positions of the origins of these 6 events also show how important is the study of the events produced inside the cloud chamber. Only event NJ 42 was produced outside the cloud chamber; the other five were produced inside: event VB 913 in the carbon wedge and the other four in the plates.

There is a remarkable difference in importance between events NJ 42, SL 496, TF 1561 and VB 913 on one side, and events SN 1534 and VB 536 on the other. As is shown in Table 6.1, from the interactions which produce the K-mesons of the first 4 events several other charged particles also emerge. In experiments like this it is impossible to find statistical arguments which prove that both K-mesons in any of these 4 events were produced in the same elementary act. (This remark also applies to the events found in nuclear emulsions[9][71] in which the pairs

(K^+, K^-)-mesons are associated with stars of many prongs.) However, in events VB 536 and SN 1534 the simplicity of the interaction is such that the probability of the two K-mesons being produced in one elementary act is very large.

We shall then describe in detail only events VB 536 and SN 1534. It must be emphasized that the analysis of the two events can be remarkably well done, because, besides the simplicity of the interaction, the photographs are of good quality and in both cases the interaction occurs in the middle of the plate and in the middle of the illuminated depth of the cloud chamber (see plates 3 and 4). The two events have been reported by Cooper et al.(4)

3. Event VB 536

This event shows two neutral V-particles and a single slow proton coming from an interaction in the carbon plate. The interaction is produced by a neutral particle, presumably a neutron. Plate 3 is a photograph of the event: A, B, C and D are the four charged decay products of the V^o-particles, P is the proton.

The line of flight of the proton meets the intersection of the two decay planes of the V^o-particles at a point in the

Plate 3

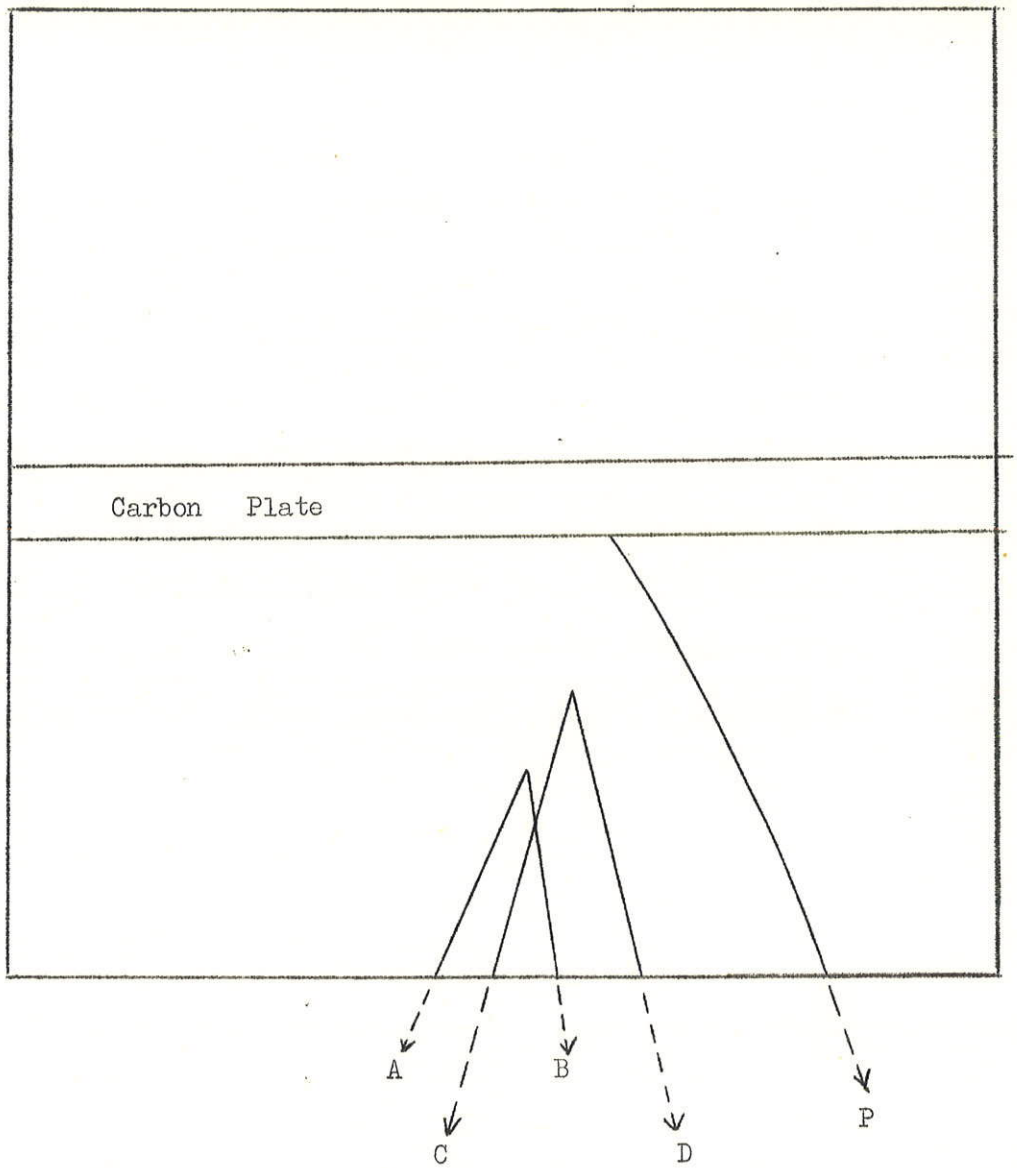

EVENT VB 536 - A, B and C, D are the decay products of the two K^{o}- mesons, P is the proton. The event is extensively discussed in the text.

TABLE 6.2

Measurements made on event VB 536

a) T r a c k s

(1) Track	(2) Sign	(3) Ionization (I_0)	(4) Length (cm)	(5) Momentum (MeV/c)	(6) Calculated Momentum (MeV/c)
A	$\pm$	< 2	8.0	> 530	540 ± 40
B	$\pm$	< 2	7.0	> 410	930 ± 50
C	$\pm$	< 2	12.5	> 1300	1450 ± 150
D	$\pm$	< 2	13.0	> 1400	1160 ± 150
P	+	3 to 6	11.5	330^{+144}_{77}	-

b) A n g l e s

(7) Tracks	(8) Angle (°)	(9) Tracks	(10) Angle (°)
A B	33.0 ± 1	C D	18.5 ± 1
V_{AB} A	20.5 ± 2	V_{CD} C	7.0 ± 3
V_{AB} B	12.5 ± 2	V_{CD} D	11.5 ± 3
V_{AB} V_{CD}	5.0 ± 1		
	Plane (AB) Plane (CD)		55 ± 2
	Plane (V_{AB} V_{CD}) Plane (AB)		72 ± 3
	Plane (V_{AB} V_{CD}) Plane (CD)		20 ± 2

(see caption over)

TABLE 6.2

(caption)

The ionisation densities given in column (3) are visual estimates. The lower limits to the momenta of particles A, B, C and D given in column (5) are the values of maximum detectable momentum corresponding to the track lengths given in column (4); they were calculated as described in the text. V_{AB} and V_{CD} stand for line of flight of V_{AB} and V^{o}_{CD} respectively. The directions of these lines of flight have been obtained on the assumption that the V^{o}-particles come from an interaction in the graphite plate located by track P and the planes of the two V-decays. The momenta in column (6) have been calculated using the angles given in the table and assuming that the two V^{o}-particles are Θ^{o}_{1}-mesons.

carbon plate. This point was considered as the point of interaction. The lines of flight of the two V^{o}-particles are the lines that join the point of interaction to the apexes of the V^{o}-decays.

The measurements made on this event are given in Table 6.2. The limits to the ionisation densities given in column (3) were established with visual estimates made independently by five observers. None of the four tracks from the neutral V-events show a measurable curvature. The lower limits to the momenta of the four particles A, B, C and D, given in column (5) are the maximum detectable momenta corresponding to the track lengths given in column (4). As explained in Chapter I, in the Jungfraujoch cloud chamber the maximum detectable momentum is 4 GeV/c for a vertical track 25 cm long, and the assumption is made that it varies with the square of the track length for lengths less than 25 cm and is constant for longer tracks.

Track P is certainly the track of a proton. Fortunately the momentum of this particle is in the range of the curve momentum versus ionisation in which a proton is easily identified.

i) Analysis of the V^o-particle which decays into A and B (V^o_{AB})

This V^o-particle cannot be a Λ^o-hyperon, because the product of the momentum of the negative secondary (P_-) by the sine of the decay angle (φ) is greater than 118 MeV/c (see Astbury[66]). As the track of particle B is shorter than the track of particle A, the lower limit to the momentum of B is less than the lower limit to the momentum of A. If we assume that particle B is the negative secondary, we have $P_- \sin\varphi > 217$ MeV/c. If we make the pessimistic assumption that the momentum of particle B is only half the maximum detectable momentum, the value of $P_- \sin\varphi$ is only greater than 108 MeV/c, allowing interpretation of V^o_{AB} as a Λ^o-particle. However, there is also the following reason why V^o_{AB} cannot be a Λ^o-particle: the angles given in column (8) of Table 6.2 allow an analysis of V^o_{AB} based on the (α , ϵ) parameters of Podolanski and Armenteros.[67] If we assume that V^o_{AB} is a Λ^o-particle, this analysis shows that the maximum value of the momentum of the proton secondary is only 350 MeV/c. A proton with such a momentum has ionisation equal to five times the minimum ionisation. This value is inconsistent with the observed ionisation of tracks A and B. Therefore, V^o_{AB} cannot be a Λ^o-hyperon. It is therefore a K^o-meson.

It would be of great value to know whether this neutral K-meson is a θ_1^o-meson, which decays into two charged π-mesons with a Q-value of (214 ± 5) MeV. Unfortunately, as tracks A and B show no measurable curvature, only lower limits to the $Q(\pi, \pi)$-value can be calculated. If the momenta of particles A and B are taken to be equal to the appropriate maximum detectable momentum the lower limit to the $Q(\pi, \pi)$-value is 106 MeV. If we make the pessimistic assumption that the momenta of both particles are, in fact, only half the maximum detectable momentum, that lower limit becomes 37 MeV.

If we assume that V_{AB}^o is a θ_1^o-meson, the momenta of particles A and B can be calculated from the angles given in column (8) of Table 6.2 with an (α, ϵ) analysis. The results are given in column (6) of that table. The corresponding momentum of V_{AB}^o, under the assumption that it is a θ_1^o-meson, is (1400 ± 70) MeV/c. On this assumption its time of flight is 1.3×10^{-10} sec.

ii) Analysis of the V^o-particle which decays into C and D (V_{CD}^o)

This V^o-particle cannot be a Λ^o-hyperon, because $P_- \sin \varphi > 390$ MeV/c. If, again, we make the pessimistic assumption that the momenta of particles C and D are only half the

maximum detectable momentum, the value of $P_{\perp} \sin\varphi$ is greater than 195 MeV/c.

Again we cannot decide whether the V^o-particle is a θ_1^o-meson, because we cannot calculate the $Q(\pi^-, \pi^-)$-value of the decay. Assuming that the momenta of particles C and D are the maximum detectable momenta given in column (5) of Table 6.2, the $Q(\pi^-, \pi^-)$-value of the decay is 236 MeV. Under the pessimistic assumption that the momenta of both particles are only half those maximum detectable momenta, the lower limit to the $Q(\pi^-, \pi^-)$-value is 77 MeV.

If we assume that V^o_{CD} is a θ_1^o-meson, the momenta of particles C and D calculated from the (α, ϵ) parameters, using the values of angles given in column (10) of Table 6.2 are quoted in column (6) of that table. The corresponding momentum of V^o_{CD} is (2550^{+320}_{-180}) MeV/c. On this assumption its time of flight is 0.4×10^{-10} sec.

iii) Final remarks

Both V^o-particles are K^o-mesons. The lower limits to the $Q(\pi^-, \pi^-)$-values of the decays of V^o_{AB} and V^o_{CD} show that it is possible that both are decays of θ_1^o-mesons, but it is also possible that they are "anomalous decays". It is worth emphasizing

that the times of flight of both V^o-particles obtained on the assumption that they are θ_1^o-mesons are consistent with the mean lifetime of the θ_1^o-meson ($\sim 1 \times 10^{-10}$ sec.). This fact does not give any direct evidence for identifying the K^o-mesons as θ_1^o-mesons. We can only say that if the K^o-mesons had a long mean lifetime, for instance $\sim 10^{-8}$ sec., the probability of observing both to decay would be extremely small.

4. Event SN 1534

In this event a neutral V-particle and a non-decaying K-meson are the only visible products of a nuclear interaction in the copper plate. The primary of the interaction is again neutral, presumably a neutron. Plate 4 is a photograph of the event : A and B are the charged secondaries of the neutral V-particle, C is the K^+-meson. Track C meets the plane of the V^o-decay at a point inside the copper plate. This point lies very close to the continuation of track B.

The measurements made on this event are given in Table 6.3.

i) Analysis of the V^o-particle

The results of the measurements which are given in Table 6.3 show that particle A, the positive secondary of the

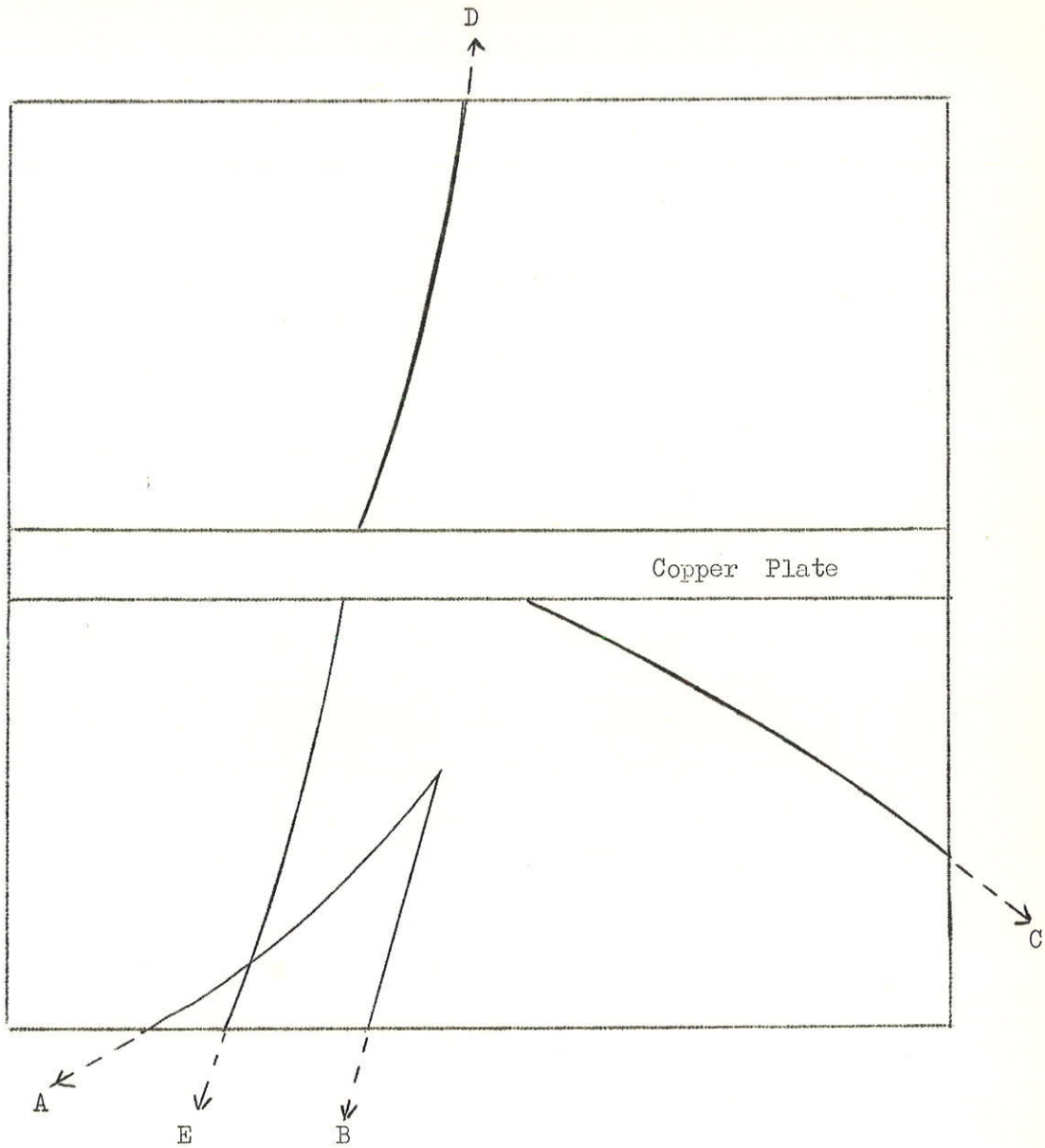

EVENT SN 1534 - A and B are the decay products of the K^{o} - meson, C is the K^{+}- meson. D is another K^{+}- meson, which stops in the plate and gives rise to the charged secondary E.

TABLE 6.3

Measurements made on event SN 1534

(1) Track	(2) Sign	(3) Ionization (I_o)	(4) Length (cm)	(5) Momentum ($\frac{MeV}{c}$)	(6) Mass (m_o)
A	+	3 to 6	13.0	64 ± 5	220 to 430
B	$\pm$	< 2	13.0	> 1080	-
C	+	3 to 6	23.0	220 ± 15	770 to 1400
D	+	4 to 8	10.0	$155 \, {}^{+34}_{-26}$	560 to 1400
E	+	< 2	19.0	188 ± 12	< 520

Angle $\widehat{AB} = 26^\circ \pm 1^\circ$ Angle $\widehat{V_{AB}C} = 69.5^\circ \pm 2^\circ$

The ionization densities given in column (3) are visual estimates. The lower limit to the momentum of track B, given in column (5), is the maximum detectable momentum corresponding to a track 13.0 cm. long in the Jungfraujoch cloud chamber. The masses of the various particles have been found by combining the estimated ionization densities with the measured momenta. V_{AB} stands for line of flight of the V^o-particle, which decays into A and B.

V^o-particle, has mass between 220 and 430 electronic masses. Particle A is then a light meson. Consequently, the V^o-particle cannot be a Λ^o-hyperon. It is a neutral K-meson.

Track B shows no curvature. Only a lower limit can be given to the momentum of particle B, equal to the maximum detectable momentum corresponding to the adequate track length. Due to this fact, only a lower limit to the $Q(\pi^-, \pi^-)$-value of the decay can be calculated. This lower limit is 225 MeV if we assume that the momentum of particle B is the maximum detectable momentum. If the momentum of particle B is taken to be half the maximum detectable momentum, the lower limit to the $Q(\pi^-,\pi^-)$-value of the decay is 106 MeV. There is then consistency with the Q-value of the decay of the θ_1^o-meson. The K^o-meson cannot be a τ^o-meson, because for this particle the $Q(\pi^-, \pi^-)$-value can never be greater than 80 MeV.

If we <u>assume</u> that the K^o-meson is a θ_1^o-meson, the momentum of particle B, calculated from the measured momentum of particle A and the Decay angle of the V^o-event is (1050 ± 40) MeV/c. The corresponding momentum of the V^o-particle, under the assumption that it is a θ_1^o-meson is (1090 ± 50) MeV/c. With these values it is found that the line of flight of the θ_1^o-meson meets track C in a point inside the copper plate. The time of flight of the

V^o-particle, on the assumption that it is a θ_1^o-meson, is 1.6×10^{-10} sec.; (This value is not in contradiction with the mean lifetime of the θ_1^o-meson).

ii) The identification of the K^+-meson

It is well known that it is difficult to identify a positive K-meson in a magnet cloud chamber when the K-meson does not decay. The reason is that due to uncertainties attached to visual estimates of ionisation, the track of a supposed K^+-meson could in fact be the track of a proton. However, two peculiarities make the identification of particle C as a K^+-meson extremely reliable.

Firstly, particle C has a momentum of only (220 ± 15) MeV/c, which is in the range of momentum in which the difference between the ionisation of a proton and that of a K-meson is very large. A proton with such a momentum has ionisation Between 9.5 and 11.5 times the minimum ionisation, which is completely out of the range 3 to 6 times the minimum ionisation estimated for particle C. This range was confirmed independently by four other observers, besides the author.

Secondly, event SN 1534 shows a second K^+-meson (particle D) which stops in the plate and gives rise to only one charged

secondary (particle E), producing a characteristic S-event. The measured momentum of particle E is (188 ± 12) MeV/c. Correcting for the energy loss in the plate, we conclude that this particle was emitted from the decay point of particle D with a momentum of (204^{+18}_{-15}) MeV/c, if E is assumed to be a μ-meson, or with a momentum of (207^{+19}_{-15}) MeV/c if it is assumed to be a π-meson. The decay is probably that of a $K_{\pi 2}$-meson ($p^* = 205$ MeV/c), but could also be the decay of a $K_{\mu 2}$-meson ($p^* = 236$ MeV/c). By comparing the measurements made on tracks C and D, which are given in Table 6.3, we conclude that if particle D is a K-meson, particle C is also a K-meson.

5. The Production Reactions

As pointed out in Section 1 of this chapter, the importance of the two events which have been described depends on the reactions in which the strange particles were produced. It will be easier to discuss at the same time the production reactions of the two events.

Assuming that strangeness is conserved in strong interactions, there are three processes in which two K-mesons may arise from a nuclear interaction.

A) First process : The first process is that in which each K-meson has strangeness +1 and is produced associated with a Λ^0- or a Σ -hyperon, both of which have strangeness -1, in a cascade process inside the nucleus. In this case the K-mesons are produced in separate elementary interactions. Let us examine first the associated production with Λ^0-hyperons.

The primary particle of the interaction of event VB 536 in presumably a neutron. The neutron can initiate a cascade process by colliding with either a neutron or a proton of the carbon nucleus. The only cascade which could give rise to only the two K^0-mesons and the proton is the following :

initial collision : $n + n \rightarrow \pi^- + n + p$ (1)

secondary collisions
$\pi^- + p \rightarrow \Lambda^0 + K^0$ (2)
$n + n \rightarrow \Lambda^0 + K^0 + n$ (3)

The primary particle of the interaction of event SN 1534 is also presumably a neutron. The only two cascades which could have been responsible for the event are the following :

initial collision : $n + N \rightarrow \pi^+ + \pi^- + n + n$ (4)

secondary collisions
$\pi^- + p \rightarrow \Lambda^0 + K^0$ (2)
$\pi^+ + n \rightarrow \Lambda^0 + K^+$ (5)

or :

$$\text{initial collision} \quad : \quad n + p \rightarrow \pi^{+} + n + n \qquad (6)$$

$$\text{secondary collisions} \begin{cases} \pi^{+} + n \rightarrow \Lambda^{o} + K^{+} & (5) \\ n + n \rightarrow \Lambda^{o} + K^{o} + n & (3) \end{cases}$$

The K^{o}- and the K^{+}-mesons would be the only particles which have been observed; all the other secondaries would escape detection. Any other initial process different from (4) and (6) would lead to the creation of more charged particles besides the K^{+}-meson.

Using the measurements made on the events and the known dynamics of reactions (2, 5) (which have been studied in Chapter III), it is possible to estimate the probability of detecting any of the hypothetical Λ^{o}-particles produced with the 4 K-mesons. In every case this probability turns out to be greater than 90%. Making allowance for possible decays of the type $\Lambda^{o} \rightarrow n + \pi^{o}$ and for nuclear scattering of the Λ^{o}-particles, this probability may be slightly but not greatly reduced. This high probability of detection is primarily due to the fact that the two interactions occur very close to the sensitive volume of the cloud chamber.

Exactly the same argument applies if the processes occur with a Σ^{o}-particle produced in place of the Λ^{o}-particle.

The very short mean lifetime of the Σ^0-particle means that the probability of detection of the Λ^0-particles is unchanged.

The high probability of detecting either Λ^0- or Σ^0-hyperons makes interpretation of the two events in terms of the reactions listed above extremely small.

If associated production of the K-mesons with charged Σ -hyperons had occurred, either the track of the Σ-particle, or the track of its charged decay product, would have been seen.

We can therefore exclude the first process as an explanation of the events.

B) Second process : The second process in which two K-mesons may arise from a nuclear interaction is the following : both K-mesons with strangeness +1 are produced associated with a Ξ^-- or a Ξ^0-particle, which have strangeness -2.

The production of a Ξ^--particle is excluded because either its track or the track of its charged secondary would have been seen.

The production of Ξ^0-particles in the reactions :

$$(\text{VB } 536) \quad n + p \rightarrow \Xi^{o} + K^{o} + K^{o} + p \qquad (7)$$

$$(\text{SN } 1534) \quad n + p \rightarrow \Xi^{o} + K^{o} + K^{+} + n \qquad (8)$$

should account for our events. The Ξ^{o}-particle would decay into a Λ^{o}-particle and a π^{o}-meson.

However, as the decay of a Ξ^{o}-particle was never observed, we cannot claim that these two reactions occurred. To claim that reactions (7) and (8) occurred is the same as to claim that we have the first two observations of a Ξ^{o}-particle. As there is no evidence for the decay of a Ξ^{o}-particle in either of the two events, we shall exclude the second process.

C) Third process : The third, and most plausible interpretation is that the events show the production of pairs of K-mesons in elementary interactions. As the interacting particles are "ordinary" particles, with strangeness equal to zero, the two K-mesons of each event must have equal and opposite strangeness, i.e. one is a "particle" and the other is an "anti-particle". In event VB 536 one of the K^{o}-mesons belong to the doublet with strangeness S = +1, and the other to the doublet of the anti-particles, with strangeness S = -1. In event SN 1534 the K^{+}-meson belongs to the doublet of the particles, and the K^{o}-meson to the doublet of the anti-particles.

The simplest reactions which could have occurred to produce the events are:

$$\text{event VB 536} = n + p \rightarrow K^{o} + \overline{K}^{o} + n + p \qquad (9)$$

$$\text{event SN 1534} = n + p \rightarrow K^{+} + \overline{K}^{o} + n + n \qquad (10)$$

In fact, event VB 536 shows, above the plate, two fast particles travelling near the vertical direction. If we assume that the direction of the neutron which produced reaction (9) is not very different from vertical, the transverse momentum of the two K^{o}-mesons and the proton do not balance, and we then have to assume that at least one more particle was produced. Assuming that reaction (9) occurred, if we make no assumption about the direction of the incident neutron it is possible to calculate a lower limit to the energy of this particle: it is 5.7 GeV. If we assume that this incident neutron is associated with the two fast particles at the top of the cloud chamber, then the dynamics of reaction (9) is determined, and the energy of the primary is uniquely determined as 7.3 GeV.

Because in event SN 1534 no other particle is seen besides the two K-mesons, only a lower limit can be set to the energy of the incident neutron which could have produced reaction (8); it is 3.8 GeV.

6. Conclusion

Due to the simplicity of the two interactions which have been described, the best interpretation for event VB 536 is that it shows the associated production of two neutral K-mesons; the best interpretation for event SN 1534 is that it shows the associated production of a neutral with a positive K-meson. If we now consider:

a) the conservation laws which hold in the Gell-Mann model;

b) that the particles which produced the interactions have strangeness zero;

we conclude that the two events are strong evidence for the existence of an anti-neutral K-meson.

As far as the author knows, these are the first examples that have been observed of $(K^{o}, \overline{K}^{o})$ and $(K^{\pm}, \overline{K}^{o})$ pairs produced in simple interactions in which the K-mesons have both been directly identified.

* * *

CHAPTER VII

EVIDENCE FROM SINGLE V^o-PARTICLES

1. Numbers of Λ^o- and θ^o-particles produced in carbon, copper and lead.

Let us call $N(\theta^o)$ and $N(\Lambda^o)$ respectively the numbers of θ^o- and Λ^o-particles produced in one experiment during the same running time. It was discovered by Blumenfeld et al.[14] and confirmed by Blumenfeld[15] that the ratio $\frac{N(\theta^o)}{N(\Lambda^o)}$ is greater for particles produced in carbon than for particles produced in lead. The same result was also found by the CERN-Jungfraujoch group,[16] which found :

$$\frac{\frac{N(\theta^o)}{N(\Lambda^o)}\ \text{Carbon}}{\frac{N(\theta^o)}{N(\Lambda^o)}\ \text{Copper}} \sim 2 : 1$$

Table 7.1 gives the values of the ratio $\frac{N(\theta^o)}{N(\Lambda^o)}$ for carbon and lead obtained by Blumenfeld, for carbon and copper obtained by the CERN-Jungfraujoch group and for lead found by Gaythor[75]. These values will be compared in section 4 of this chapter.

TABLE 7.1

Values of the ratio $\frac{N(\theta^o)}{N(\Lambda^o)}$ at production in several materials obtained in different experiments

Workers	Experiment	Carbon		Copper		Lead	
		Non cor.	Cor.	Non cor.	Cor.	Non cor.	Cor.
Blumenfeld (15)	Machine	0.82	1.2	-	-	0.26	0.4
Jungfraujoch group	Cosmic ray	2	3	1	1.5	-	-
Gaythe r (75)	" "	-	-	-	-	0.5	0.8

In Blumenfeld's experiment the incident particles were 2.0 BeV π^--mesons. The figures on the left have not been corrected for the existence of the long lived θ_2^o-meson and for neutral decay modes of the θ_1^o-meson and Λ^o-hyperon. The figures on the right have been corrected for these effects.

To explain their result, Blumenfeld et al. suggested that inside the nucleus where the strange particles are produced the following reaction should occur with great frequency:

$$\Sigma^- + N \rightarrow \Lambda^0 + N \qquad (1)$$

The reaction is allowed by conservation of strangeness. Then, Σ^--hyperons produced in association with θ^0-mesons would be absorbed inside the nucleus where they are produced and "converted" into Λ^0-particles. Because the lead nucleus contains more nucleons than the carbon nucelus, the absorption would occur more often in lead than in carbon. As a consequence, for the same number of θ^0-mesons, more Λ^0-particles would come out from lead than from carbon. The absorption of Σ^--particles has been confirmed by several experiments made with emulsions.*)

To explain the positive excess of K-mesons the CERN-Jungfraujoch group(2) suggested that the cross sections of the reactions of the type:

$$\pi + N \rightarrow Y^{+,-,0} + K^{+,0} \qquad (2)$$
$$N + N \rightarrow Y^{+,-,0} + K^{+,0} + N \qquad (3)$$
$$\pi + N \rightarrow K^{+,0} + \overline{K^{+,0}} + N \qquad (4)$$
$$N + N \rightarrow K^{+,0} + \overline{K^{+,0}} + N + N \qquad (5)$$

vary differently with energy, such that reactions (2) and (3)

---

*) Some experiments were reported at the International Conference on Mesons and Recently Discovered Particles, Padua-Venice, September (1957).

predominate at low energies, but at energies of several GeV reactions (4) and (5) become rather rapidly more important. We shall come back to this point in section 7 of the next chapter.

To explain why the ratio $\frac{N(\theta^o)}{N(\Lambda^o)}$ is greater in carbon than in copper the same group suggested that:

a) in fact reactions (4) and (5) should occur very frequently, and then there are many anti-K-mesons produced;

b) not only Ξ^--particles are absorbed according to reaction (1), but also anti-K-mesons are absorbed in reactions of the types:

$$K^- + N \rightarrow \Lambda^o + \pi^- \qquad (6)$$

$$\overline{\theta^o} + N \rightarrow \Lambda^o + \pi^- \qquad (7)$$

where strangeness is conserved. Reactions (1), (6) and (7) would then explain why, for the same number of θ^o-particles there are more Λ^o-particles coming out from copper than from carbon.

2. Normalisation of the numbers of events produced in carbon and copper.

To have a better idea about the processes of production of Λ^{o}- and θ^{o}-particles in carbon and copper, we should normalise the numbers of events in terms of a good physical quantity. But, unfortunately, this normalisation can only be exactly done if we have a clear picture of the degree of interdependence of the nucleons inside the same nucleus.

Let us try two normalisations based on two almost opposite pictures of the nucleus, namely:

a) A normalisation in terms of interaction length. This is equivalent to the assumption that the nucleus is very "opaque" and that the primary interaction of an incoming particle takes place predominantly at the periphery of the nucleus.

b) A normalisation in terms of g/cm^2. In this limit the behaviour of a single nucleon is independent of the presence of the others; the nucleus is very "transparent" and the primary interaction can occur with nucleons situated inside the nucleus.

The density of copper is 8.9 g/cm^3 and the interaction length in copper is 105 g/cm^2. About 35,000 photographs were taken with the copper plate 1.25 cm thick inside the cloud

chamber. The density of the graphite used to make our plate is 2 g/cm^3. The interaction length in carbon is 65 g/cm^2. About 19,000 photographs were taken with the graphite plate 2.5 cm thick in the cloud chamber. The normalisation in terms of interaction length corresponds to the multiplication of the number of events produced in carbon by the factor:

$$\frac{1.25 \times 8.9}{105} \times \frac{65}{2.5 \times 2} \times \frac{35000}{19000} = 2.4$$

The normalisation in terms of g/cm^2 corresponds to the multiplication of the number of events produced in carbon by the factor:

$$\frac{1.25 \times 8.9}{2.5 \times 2} \times \frac{35000}{19000} = 4$$

Taking into account the figures quoted in Table 5.4, the normalised numbers of Λ^0- and θ^0-particles are given in the following table.

	In terms of interaction length		In terms of g/cm^2	
	Cu	C	Cu	C
Λ^0	54	24	54	40
θ^0	54	48	54	80

The normalisations which we made are two extremes; the correct normalisation must be between the two. Nevertheless, the following effect appears from the figures which we obtained: from carbon to copper there is an increase in the number of Λ^{o}-hyperons and a decrease in the number of θ^{o}-mesons. The decrease in the number of θ^{o}-mesons when the normalisation is made in terms of g/cm^{2} had been found also by Blumenfeld.

3. The interactions produced by secondary π-mesons and the bias in the observation of θ^{o}-mesons.

Let us now assume that reactions of the type (2), produced by secondary π-mesons inside the nucleus where the π-meson originated, occur more frequently in heavy nuclei than in light nuclei. We shall see that on this assumption the difference in the angles of emission of the Λ^{o}- and θ^{o}-particles in the L.S. would be enough to account in great extent for the difference in the ratios $\frac{N(\theta^{o})}{N(\Lambda^{o})}$ obtained in copper, lead and carbon.

The two-body reactions produced by secondary $\bar{\pi}$-mesons which give rise to Λ^{o}- and θ^{o}-particles are:

$$\pi^- + p \rightarrow \Lambda^0 + \theta^0 \qquad (a)$$

$$\pi^+ + n \rightarrow \Lambda^0 + K^+ \qquad (b)$$

$$\pi^- + p \rightarrow \Sigma^0 + \theta^0 \qquad (c)$$

$$\pi^+ + n \rightarrow \Sigma^0 + K^+ \qquad (d)$$

$$\pi^\pm + n \rightarrow \Sigma^\pm + \theta^0 \qquad (e)$$

The dynamics of these reactions were studied in detail in chapter III.

It was shown by Eisler et al.[19] and by Brown et al.[20, 21] that when reactions (a) and (b) occur at energies not much above the threshold the Λ^0-hyperon is emitted predominantly backwards in the C.M.S. In our notation, $\theta^* > 120^\circ$. Diagrams 1 to 8 of Appendix I show that the Λ^0-hyperon and the K^+- or θ^0-meson are emitted in the L.S. at angles less than 40°. When the reaction occurs in the plate the geometrical bias for the observation of the decays of the Λ^0- or the θ^0-particle is then small.

The same authors show that when reactions (c), (d) and (e) occur the Σ-particle is emitted predominantly forwards(*) in the C.M.S., i.e. $\theta^* < 60^\circ$. Diagrams 9, 11, 13 and 15 of

(*) Brown et al. had originally reported that in the case of the Σ^0-particle, θ^* is large and in the case of the $\Sigma^\pm$-particle θ^* is small. At the Padua-Venice Conference, September 1957, those authors did not maintain this preliminary result, which was based on small numbers of events, and which is in contradiction of charge independence in the production processes.

Appendix I show that in this case the Σ^{o}-particle is emitted in the L.S. at small angle. Due to the short mean lifetime of the Σ^{o}-particle, the Λ^{o}-particle originated from its decay is also emitted in the L.S. at small angle. Diagrams 10, 12, 14 and 16 show that, on the contrary, the Θ^{o}- and the K^{+}-meson are emitted in the L.S. at an angle generally between about 60^{o} and 120^{o}; at this angle the decay of the Θ^{o}-meson is not seen, even when it is produced in the plate.

The conclusion is then the following: the geometrical bias for the observation of the Λ^{o}-hyperon produced in reactions (a), (b), (c) and (d) is small; the geometrical bias for the observation of the Θ^{o}-meson is only small when it is produced in reaction (a), but is very large when it is produced in reactions (c) and (e). As reactions (a), (b), (c), (d), and (e) should occur more often in heavy than in light nuclei, the geometrical bias tends to make the ratio $\frac{N(\Theta^{o})}{N(\Lambda^{o})}$ smaller in heavy nuclei than in light. This bias would then be enough to explain in great extent the results of each of the three experiments listed in Table 7.1 when considered individually. We shall see in the next section that when the three experiments are considered together the geometrical bias is not enough to explain the results.

4. Conclusions

The conclusions that arise from the three last sections are:

i) The increase of the absolute (normalised) number of Λ^0- hyperons from carbon to copper (or to lead) could be caused by:

a) reactions (a), (b), (c) and (d) produced by secondary π^--mesons inside the nucleus where the π^--mesons were produced; we expect these reactions to occur more often in copper than in carbon.

b) conversion processes of other strange particles with strangeness -1, such as:

$$\Xi^- + N \rightarrow \Lambda^0 + N \qquad (1)$$

$$\bar{K} + N \rightarrow \Lambda^0 + \pi^- \qquad (8)$$

ii) The decrease of the absolute (normalised) number of θ^0-mesons from carbon to copper could result from absorption processes such as:

$$\bar{\theta}^0 + N \rightarrow \Lambda^0 + \pi^- \qquad (7)$$

or from charge exchange scattering:

$$\theta^0 + p \rightarrow K^+ + n \qquad (9)$$

$$\bar{\theta}^0 + n \rightarrow K^- + p \qquad (10)$$

iii) The results of the experiments listed in Table 7.1 can be analysed in two ways:

First - the ratios $\frac{N(\theta^o)}{N(\Lambda^o)}$ for light and heavy material obtained in the same experiment can be compared.

Second - the ratios $\frac{N(\theta^o)}{N(\Lambda^o)}$ for the same material obtained in two different experiments can be compared.

Let us start with the first comparison, i.e. consider each experiment independent from the others. The difference in the ratios $\frac{N(\theta^o)}{N(\Lambda^o)}$ in carbon and copper, and in carbon and lead could then be explained by what was written in section 3; in a heavy material more secondary π-mesons are produced, more often reactions (a), (b), (c), (d) and (e) occur, and the bias against the observation of the θ^o-mesons produced in some of those reactions would make the ratio $\frac{N(\theta^o)}{N(\Lambda^o)}$ less in heavy than in light materials.

Let us make now the second comparison. We notice that for the same material the ratio $\frac{N(\theta^o)}{N(\Lambda^o)}$ is greater in cosmic ray than in the machine experiment.

The π^--mesons of Blumenfeld's experiment have an energy of only 2.0 GeV. This energy is not enough to produce as many secondary π-mesons with energy greater than 1 GeV as in cosmic ray experiments. Therefore, in cosmic ray experiments reactions (a), (b), (c), (d) and (e), produced by secondary π-mesons occur more frequently than in Blumenfeld's experiment. As there is bias against the observation of Θ^0-mesons produced in some of those reactions, the ratio $\frac{N(\Theta^0)}{N(\Lambda^0)}$ should be <u>less</u> in cosmic ray experiments than in the machine experiment. The experimental results show the opposite.

Therefore, in order to compensate the effect described above and to make the ratio $\frac{N(\Theta^0)}{N(\Lambda^0)}$ greater in the cosmic ray than in the machine experiment, there must be processes in which Θ^0- or $\overline{\Theta^0}$-mesons are produced more often in the cosmic ray experiments than in the machine experiment. The most likely explanation is the following:

The energy of 2.0 GeV of π^--mesons is not much above the threshold for the production of $(K\,\overline{K})$-pairs according to the reaction:

$$\pi + N \rightarrow K + \overline{K} + N \qquad (4)$$

Many cosmic ray particles are well above the threshold of reaction (4) and the threshold of the reaction:

$$N + N \rightarrow K + \overline{K} + N + N \qquad (5)$$

Reaction (4) occurs more frequently in the cosmic ray experiments than in the machine experiment, and reaction (5) does not occur at all in the latter. These reactions could explain the above ratios. This explanation has still stronger support in the results obtained with carbon; as the carbon nucleus is light, there is less probability of secondary interactions than in the copper or lead nucleus. The observed difference in the ratio $\frac{N(\theta^o)}{N(\Lambda^o)}$ for carbon has to lie in a difference in the primary interactions which occur in cosmic ray and the machine experiment.

The large difference in the ratios $\frac{N(\theta^o)}{N(\Lambda^o)}$ obtained in cosmic ray and machine experiments suggests that the frequency of production of pairs of $(K\,\overline{K})$-mesons is comparable with the frequency of pairs $(Y\,K)$.

The following points must be emphasized:

<u>first</u> - Reactions (7) or (10) can be important only if reactions (4) and/or (5) in which θ^o are produced, are important.

second - Reaction (1) could justify in part the fact that very few Σ-hyperons are seen from the plates. This is shown in Table 5.4.

* * *

5363

CHAPTER VIII

DISCUSSION

1. Introduction

The production of strange particles in a complex nucleus is due to three different processes:

Process 1 - The strange particles can be produced in the collision of the primary particle which enters the nucleus, i.e., in the primary collision.

This process leads to the creation of either a (Y K)-pair or a (K $\bar{K}$)-pair. The simplest reactions corresponding to process 1 are:

$$\pi + N \rightarrow Y + K \qquad (1)$$

$$N + N \rightarrow Y + K + N \qquad (2)$$

$$\pi + N \rightarrow K + \bar{K} + N \qquad (3)$$

$$N + N \rightarrow K + \bar{K} + N + N \qquad (4)$$

The following particular cases of reaction (1) will be important in the discussions presented in this chapter:

$$\pi^- + p \rightarrow \Lambda^0 + \theta^0 \qquad (1a)$$

$$\pi + N \rightarrow \Lambda^0 + K^+ \qquad (1b)$$

$$\pi + N \rightarrow \Sigma + \theta^0 \qquad (1c)$$

$$\pi + N \rightarrow \Sigma + K^+ \qquad (1d)$$

Process 2 - The strange particles can be created in interactions produced by secondary particles of the primary collision.

We know that the most numerous of these secondaries in cosmic ray experiments are π^--mesons with energy of about 1 to 2 GeV. The creation of (Y K)-pairs according to reactions (1) must be predominant in this process.

Process 3 - The strange particles can be produced by conversion of other strange particles which were created in processes 1 or 2.

The following reactions should occur:

$$\Xi^- + N \rightarrow \Lambda^0 + N \qquad (5)$$

$$\overline{\Theta^0} + N \rightarrow \Lambda^0 + \overline{\pi} \qquad (6)$$

$$K^- + N \rightarrow \Lambda^0 + \pi \qquad (7)$$

$$\Theta^0 + p \rightarrow K^+ + n \qquad (8)$$

$$\overline{\Theta^0} + n \rightarrow K^- + p \qquad (9)$$

In a cosmic ray experiment it is impossible to separate the frequency of occurrence of each of the three processes. But we shall see that there is a series of experimental facts that collected together give good evidence that, at cosmic ray energies, the creation of $(K\,\overline{K})$-pairs is as important as the creation of $(Y\,K)$-pairs. The experimental facts are the following :

1 - The number of pairs $(\Lambda^0\,\Theta^0)$ produced in the copper plate.

2 - The observation of the production of pairs $(K^+\,\overline{K^0})$ and $(K^0\,\overline{K^0})$.

3 - The ratio $\frac{N(\Theta^0)}{N(\Lambda^0)}$ for carbon, copper and lead.

4 - The spectrum of the Θ^0-meson.

5 - The spectrum of the Λ^0-hyperon.

6 - The positive excess of K-mesons.

7 - The high energy of the strange particles and the collimation of their lines of flight in most of the 47 "double" events analysed in this work.

2. The number of pairs (Λ^o θ^o) produced in the copper plate.

The analysis of the pairs (Λ^o θ^o), which was presented in chapter V, gave the following information: secondary π-mesons produced in heavy nuclei frequently interact with nucleons, inside the nuclei where the π-mesons originated, to produce (Y K)-pairs. This result was also obtained by Boldt et al.[30] who showed that this is true in the case of iron.

3. The experimental observation of the production of pairs of (K^+ $\overline{K^o}$)- and (K^o $\overline{K^o}$)-mesons.

In chapter VI two events which show the production of (K^+ $\overline{K^o}$)- and (K^o $\overline{K^o}$)-pairs were described. Reaction (4) is the

Four other events listed in chapter VI are very likely to be further examples of production of (K $\overline{K^o}$)-pairs. It is also worth mentioning that in more than half of our events which show two neutral V-particles one of the V^o-particles was identified as a K^o-meson. In many of these events the other V^o-particle could not be identified. This can be seen from Tables 4.4 and 5.1. It is then likely that among our events there are more examples of association of two K^o-mesons, besides the six events reported in chapter VI.

4. The ratio $\frac{N(\theta^o)}{N(\Lambda^o)}$ for carbon, copper and lead.

The discussion of the experiments of Blumenfeld[15], Gaythe[75] and the CERN-Jungfraujoch group, presented in chapter VII, showed the following:

A) - if each experiment is considered individually, the ratios $\frac{N(\theta^o)}{N(\Lambda^o)}$ found in each experiment can be satisfactorily explained by:

i) frequent production of pairs (Λ^o θ^o) by secondary -mesons in heavy nuclei;

ii) bias against the observation of the θ^o-meson when produced in such pairs.

B) - A comparison of the ratios $\frac{N(\theta^o)}{N(\Lambda^o)}$ for the same material, especially carbon, obtained in machine and in cosmic ray experiments, give strong evidence that the production of pairs of ($K\,\overline{K}$)-mesons is important at cosmic ray energies.

5. The spectrum of the θ^o-mesons in cosmic ray experiments.

James[74] and Gaythe[75] found that the differential momentum spectrum of the θ^o-particles produced in lead has a maximum at about 850 MeV/c. Recently the CERN-Jungfraujoch group[6] confirmed that result: the momentum spectrum of

θ^o-mesons produced in copper and carbon show that the number of such particles produced with momentum less than 700 MeV/c is only about 10% of the total number of θ^o-mesons originating from the copper and carbon targets.

The momentum spectrum of the θ^o-mesons found in cosmic ray experiments is in agreement with the following facts:

a) the θ^o-mesons which are produced in reactions (1), i.e. in the pairs (Y θ^o), when emitted forwards in the C.M.S. are emitted at small angles in the L.S. and are fast in the L.S. (see diagrams 1 to 16 of Appendix I). There is no geometrical bias against the observation of such fast θ^o-mesons.

b) the θ^o-mesons which are produced in reactions (1), when emitted backwards in the C.M.S., are slow in the L.S., but are emitted at large angle in the L.S. Therefore, there is strong geometrical bias against the observation of such slow θ^o-mesons.

The occurrence of reactions (6), (8) and (9) in "Process 3" is consistent with the non-occurrence of slow θ^o-mesons.(*)

(*) It must be kept in mind that the decay of a $\overline{\theta^o}$-meson appears in a cloud chamber as the decay of a θ^o-meson; when one of them appears isolated, we cannot distinguish one from the other.

We have no information about the θ^o- and $\overline{\theta^o}$-mesons produced in reactions (2), (3) and (4). But we can say that: either the slow ones are emitted predominantly at large angle in the L.S., in the same way as those produced in reactions (1); or θ^o- and $\overline{\theta^o}$-mesons produced in reactions (2), (3) and (4) are predominantly fast in the L.S.

6. The spectrum of the Λ^o-particles in cosmic ray experiments.

Reynolds and Treiman[37] were the first to point out that there is a very large number of slow Λ^o-particles produced in cosmic ray experiments. The author, in collaboration with G.D. James[1], determined the differential momentum spectrum of Λ^o-particles produced in lead. They found that it corresponds to a power law with exponent ~ -2 in the momentum range ~ 0.25 GeV/c to ~ 5 GeV/c. The same authors calculated the differential momentum spectrum using the data reported by Gaythor and Butler[76] relative to Λ^o-particles momenta from ~ 0.25 GeV/c to ~ 1.2 GeV/c, and found agreement with the spectrum obtained with the data of the Jungfraujoch experiment. Recently the CERN-Jungfraujoch group[6] determined the differential momentum spectrum of Λ^o-particles produced in copper and carbon and found agreement with the previous results.

All those measurements show, without any doubt, that the number of Λ^0-particles produced in nuclei increases when the energy decreases, and that there is a large number of Λ^0-particles which emerge from nuclei with momenta of the order of 300 MeV/c (kinetic energy $\sim$ 40 MeV). However, evidence for the large number of Λ^0-particles with still less energy is given by the existence of a large number of hyper-fragments, produced by Λ^0-particles bound in nuclei.

The large numbers of slow Λ^0-particles is difficult to explain only in terms of production in π-meson-nucleon or nucleon-nucleon collision, without any additional process. The reason is the following:

Reactions (1) and (2) are both endothermic. As discussed in Chapter III (pages 52 and 63) the E.R.L. represents the limit of the possibility for the Λ^0 to be produced in those reactions. The minimum momentum of the Λ^0-hyperon given in Figures 3.2 and 3.3 (or Table 3.2), are the absolute minimum of the momentum of Λ^0-hyperons produced in reactions (1) and (2); only in case b of the nucleon's Fermi momentum is this minimum as low as 65 MeV/c. This is also true if π-mesons are added to the right-hand side of equations (1) and (2).

Only two mechanisms can explain the large number of slow Λ^{o}-hyperons.

a) Scattering of the Λ^{o}-particle by nucleons inside the nucleus where it is produced. This mechanism had been suggested in the work which the author had made in collaboration with G.D. James[1].

b) Very slow Λ^{o}-hyperons can be produced in the reactions:

$$\Sigma^{-} + N \rightarrow \Lambda^{o} + N \qquad (5)$$

$$\overline{\theta^{o}} + N \rightarrow \Lambda^{o} + \overline{\pi} \qquad (6)$$

$$K^{-} + N \rightarrow \Lambda^{o} + \overline{\pi} \qquad (7)$$

Reaction (5) to produce slow ^{o}-hyperons had been suggested by Reynolds.[77]

The dynamics of reactions (6) and (7) are represented in detail in Figures 17 to 20 of Appendix I. The diagrams show clearly that when slow K^{-}-meson or $\overline{\theta^{o}}$-meson interact with a nucleon to produce a Λ^{o}-particle, the Λ^{o}-particle can also be slow. Reactions (6) and (7) are both exothermic; some of their characteristics have been emphasized in Chapter III.

7. The positive excess of K-mesons

It is well known that there is an excess of the positive over the negative charged K-mesons, observed in cosmic ray experiments with cloud chambers and with nuclear emulsions, and in experiments made at the Bevatron with nuclear emulsions. The G-stack groups[78] give a ratio of 10 : 1 for the number of positive to number of negative, Chupp et al.[79] give 100 : 1, and the CERN - Jungfraujoch group [2] gives 3.4 : 1 as an average of all cosmic ray experiments with magnet cloud chambers.

If reactions (1b) and (1d) occur often in heavy nuclei, produced by π-mesons, inside the nucleus where the π-mesons are produced, they account in great extent for the positive excess of K-mesons. The reason is that most of those π-mesons have energy well above the threshold energy of reactions (1b) and (1d). Due to conservation of strangeness, in reactions (1b) and (1d), only positive K-mesons can be produced, the negative can not.

Besson et al.[23] made an experiment to study the production of K-mesons in nuclear emulsions by 4.3 GeV π^--mesons of the Bevatron. They conclude that: a) the majority of the K^--mesons were produced in primary interactions of the type of reaction (3), produced by the incident π^--mesons; b) the majority

of the K^+-mesons were not produced in the primary interaction, but were produced associated with a hyperon, in an interaction of a secondary π-meson (i.e. reactions (1b) and (1d)).

As had been suggested by the CERN-Jungfraujoch group, the large occurrence of reactions (3) and (4) at cosmic ray energies contribute to the positive excess of K-mesons.

8. The high energy of the Jungfraujoch "double" events

It has been mentioned in Chapter V, but it is important to emphasize again at this point, that the events which have been analysed in this thesis, which show two neutral V-particles, or one neutral and one charged V-particle, are in general fast and collimated (see Tables 4.4 to 4.11). The high energy of both the V-particles of each event is not consistent with them being produced in reaction (1), but is consistent with them being produced according to reactions (2), (3) or (4).

* * *

CHAPTER IX

CONCLUSIONS

The conclusions of this work can be summarized in the following way:

1) The work shows strong evidence for the existence of an anti-K^0-meson, as had been predicted by Pais, Gell-Mann and Nishijima. As far as the author knows, the two events presented in chapter VI, showing the production of $(K, \bar{K})$-meson pairs, are the only two cases of this kind which have been reported up to this time.

2) The process:

$$\pi + N \rightarrow Y + K \qquad (1)$$

is well established from machine experiments using free π-mesons. This thesis provides strong evidence that secondary π-mesons produced inside a heavy nucleus frequently produce reaction (1) in interactions with further nucleons in the same nucleus.

The difference in the frequence of this reaction observed with events produced inside and outside the cloud chamber is due to bias in observation.

3) It is known that strange particles produced in a nucleus may convert, in further interactions in the nucleus of production, into strange particles with the same strangeness; as for instance in the processes:

$$\pi^- + N \rightarrow \Lambda^0 + N \qquad (2)$$

$$\bar{K} + N \rightarrow \Lambda^0 + \pi \qquad (3)$$

In a heavy nucleus, reaction (1) produced by secondary π-mesons in the nucleus where the π-meson was produced, and reactions (2) and (3) are certainly of importance. The problem is too complex to allow a quantitative evaluation of the number of pairs (Y K) and (K $\bar{K}$) produced in primary interactions compared to the number of pairs (Y K) produced by secondary π-mesons, or to allow an estimate of the frequency of the conversion processes (2) and (3). Nevertheless, the two following conclusions arise:

A) A large frequency of reaction (1), produced by secondary π^--mesons is enough to account in great extent for the following experimental facts:

a) the positive excess of K-mesons;

b) the ratio $\frac{N(\theta^o)}{N(\Lambda^o)}$ in copper, lead and carbon in each of the three experiments listed in Table 7.1;

c) the spectrum of the θ^o-meson;

d) the spectrum of the Λ^o-hyperon above $\sim$40 MeV; the explanation of this spectrum below 40 MeV in terms of reaction (1) only would require that Λ^o-hyperons with kinetic energy of that order has large probability of being scattered inside the nucleus where it was produced.

A large frequency of reaction (1) does not account for the facts:

e) the ratios $\frac{N(\theta^o)}{N(\Lambda^o)}$ for the same material are greater in cosmic ray experiments than in the machine experiment;

f) the high energy of the strange particles and collimation of their lines of flight in the Jungfraujoch "double" events.

B) Frequent production of pairs of ($K\bar{K}$)-mesons at cosmic ray energies has as consequences:

i) - it completes the explanations of facts a), b), c) and d) if we assume that reactions (2) and (3) are also frequent;

ii) - it accounts for facts e) and f).

4) One of the most important conclusions of this work is to show that reactions leading to pairs of ($K\bar{K}$)-mesons are, at cosmic ray energies, of comparable importance to those leading to the production of (Y K)-pairs.

5) The detailed study of the dynamics of some reactions in which K-mesons and hyperons are produced, and the diagrams presented in Appendix I proved to be useful in the analysis of cosmic ray experiments.

* * *

APPENDIX I

DIAGRAMS RELATIVE TO THE REACTIONS $\pi + B \rightarrow Y + K$ AND $K + N \rightarrow Y + \pi$

The diagrams that follow represent the dynamical quantities, in the C.M.S. and in the L.S., relative to the following reactions:

$\pi + N \rightarrow \Lambda^{\circ} + K$	(1)	Figures 1 to 8
$\pi + N \rightarrow \Sigma + K$	(2)	" 9 to 16
$K + N \rightarrow \Lambda^{\circ} + \pi$	(3)	" 17 to 20
$K + N \rightarrow \Sigma + \pi$	(4)	" 21 to 24

The dynamics of these reactions were studied in detail in chapter III. Each reaction was considered four times, corresponding to the four cases a, b, c and d of the nucleon's Fermi momentum, as described in chapter III.

It is important to notice that in the diagrams relative to the hyperons and also in those relative to the K-mesons, the dotted lines are curves of constant angle of

emission of the hyperon in the C.M.S., θ^*. The full lines are curves of constant momentum of the incident particle in the L.S. (π-meson in reactions (1) and (2), k-meson in reactions (3) and (4)).

In all diagrams the vertical axis represents the angle of emission of the particle and the horizontal axis represents its momentum, in the L.S. For the calculations the following values of the masses have been used:

		MeV c^2
π-meson	139.5	
K-meson	493.4	"
nucleon	938.2	"
Λ^0-particle	1115.0	"
Σ-particle	1190.0	"

* * *

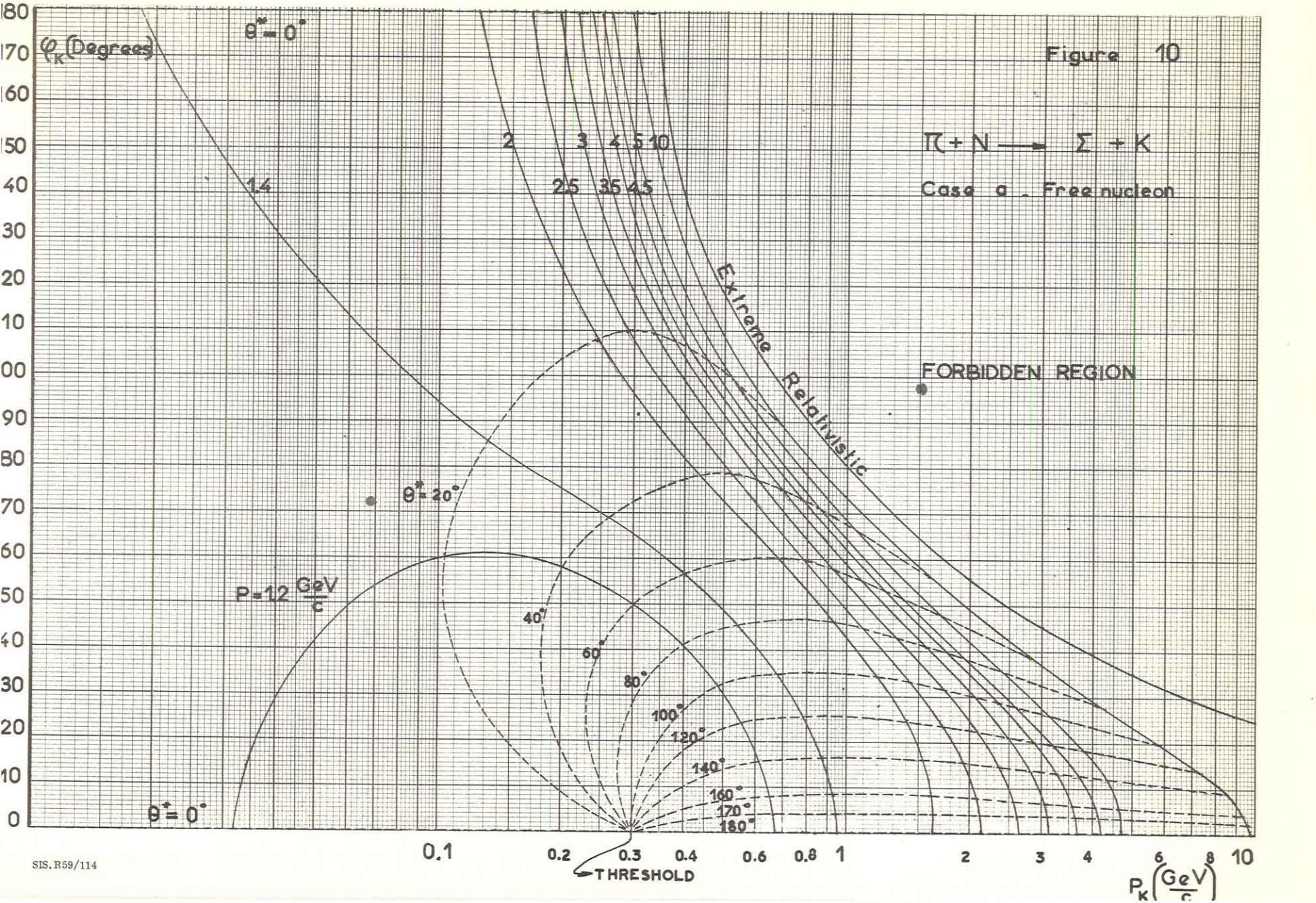
Figure 10
$\pi^- + N \longrightarrow \Sigma^- + K^+$
Case a - Free nucleon
φ_K (Degrees)
$\theta^* = 0^\circ$
1.4
2
3
4
5
10
2.5
3.5
4.5
Extreme Relativistic
FORBIDDEN REGION
$\theta^* = 20^\circ$
$P = 1.2 \frac{GeV}{c}$
40°
60°
80°
100°
120°
140°
160°
170°
180°
$\theta^* = 0^\circ$
THRESHOLD
$P_K \left(\frac{GeV}{c}\right)$
0.1
0.2
0.3
0.4
0.6
0.8
1
2
3
4
6
8
10
0
10
20
30
40
50
60
70
80
90
100
110
120
130
140
150
160
170
180

SIS.R59/114

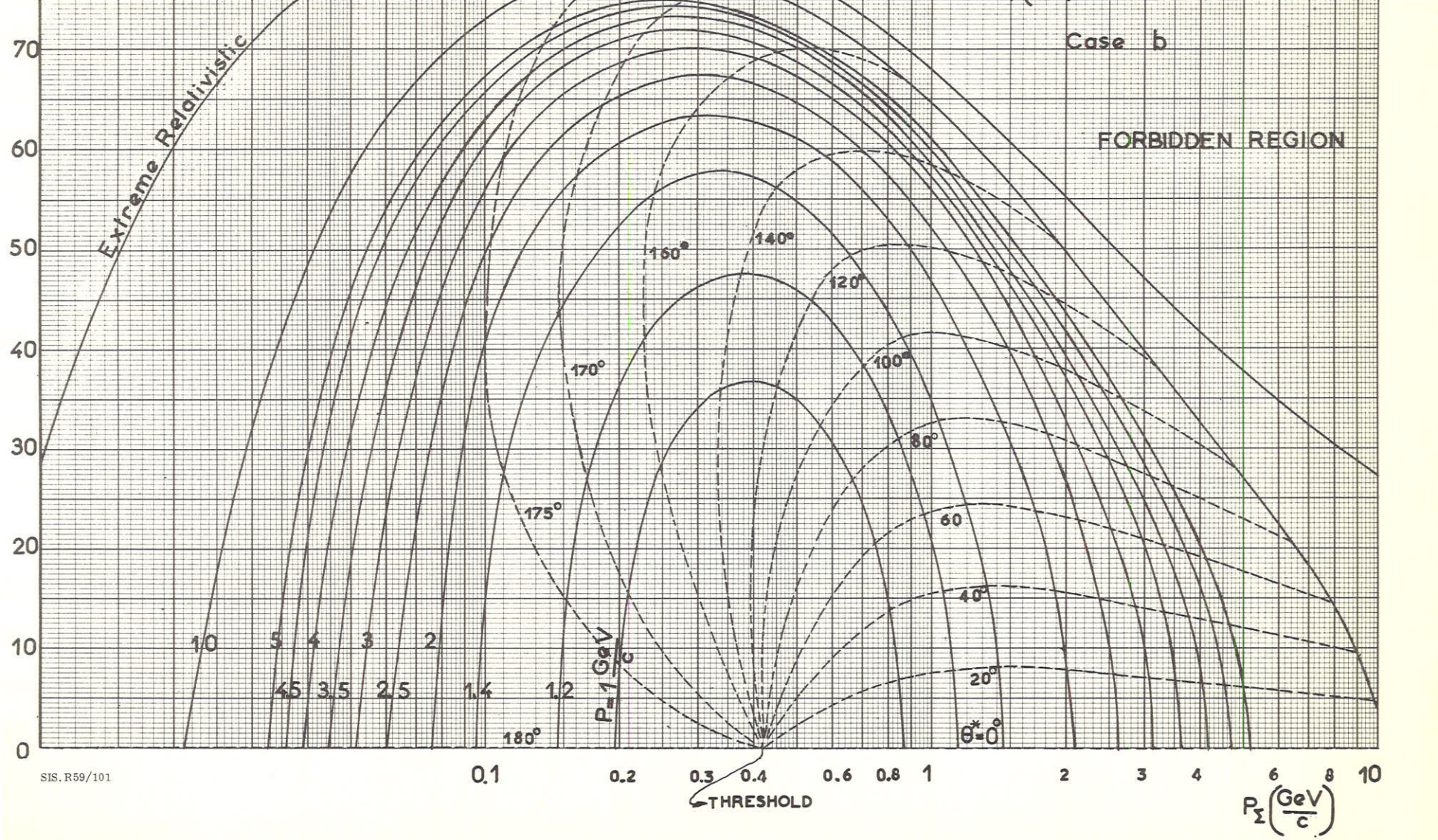
Case b
FORBIDDEN REGION
Extreme Relativistic
160°
140°
120°
100°
80°
60
40°
20°
170°
175°
180°
θ*=0°
P=1 GeV/c
1.0
5
4
3
2
4.5
3.5
2.5
1.4
1.2
0
10
20
30
40
50
60
70
0.1
0.2
0.3
0.4
0.6
0.8
1
2
3
4
6
8
10
THRESHOLD
$P_\Sigma\left(\frac{GeV}{c}\right)$

SIS. R59/101

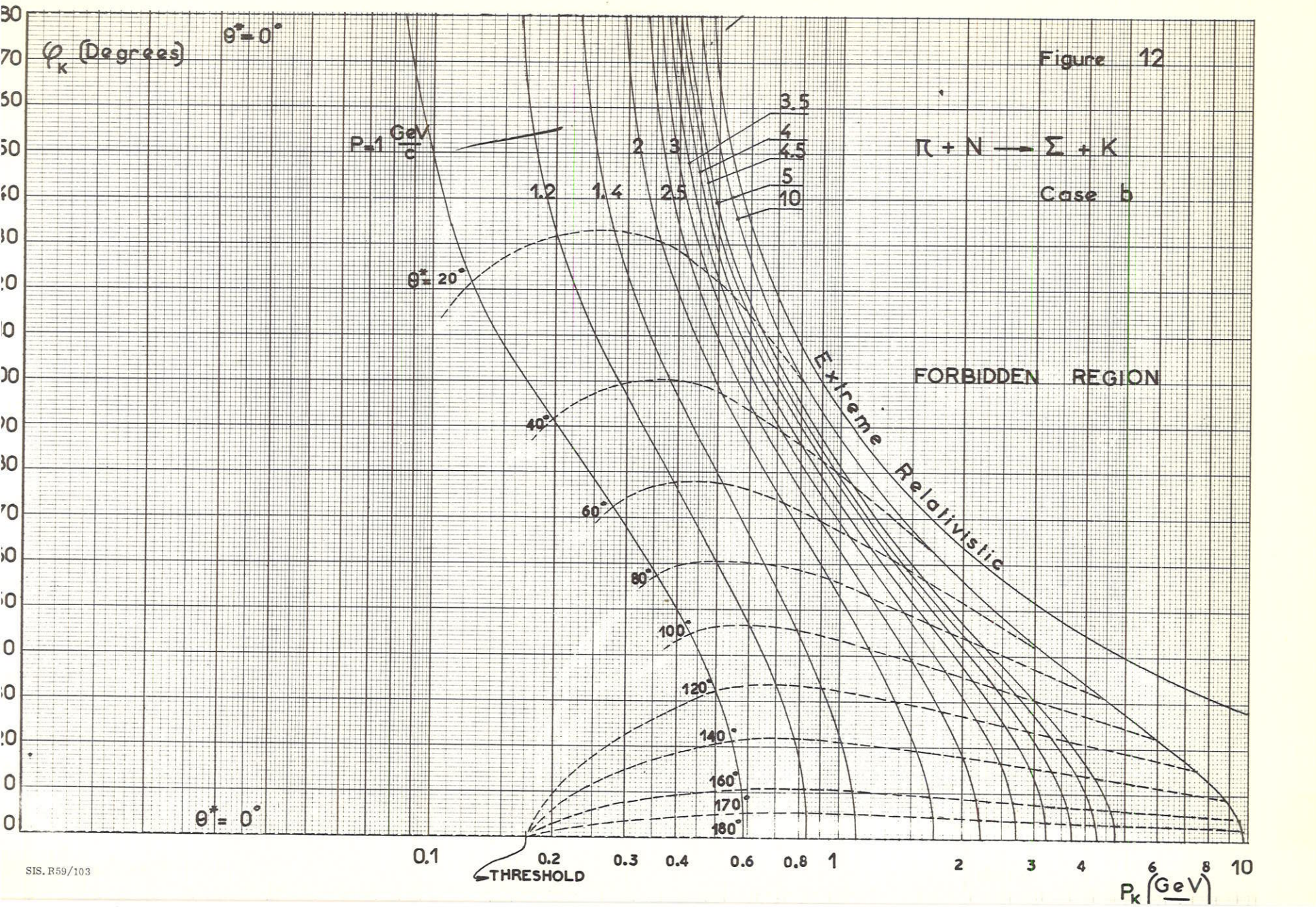
Figure 12
φ_k (Degrees)
$\theta^* = 0^\circ$
P = 1 GeV/c
2
3
3.5
4
4.5
5
10
1.2
1.4
2.5
$\pi + N \longrightarrow \Sigma + K$
Case b
$\theta^* = 20^\circ$
40°
60°
80°
100°
120°
140°
160°
170°
180°
Extreme Relativistic
FORBIDDEN REGION
$\theta^* = 0^\circ$
0.1
0.2
THRESHOLD
0.3
0.4
0.6
0.8
1
2
3
4
6
8
10
P_k (GeV)

SIS. R59/103

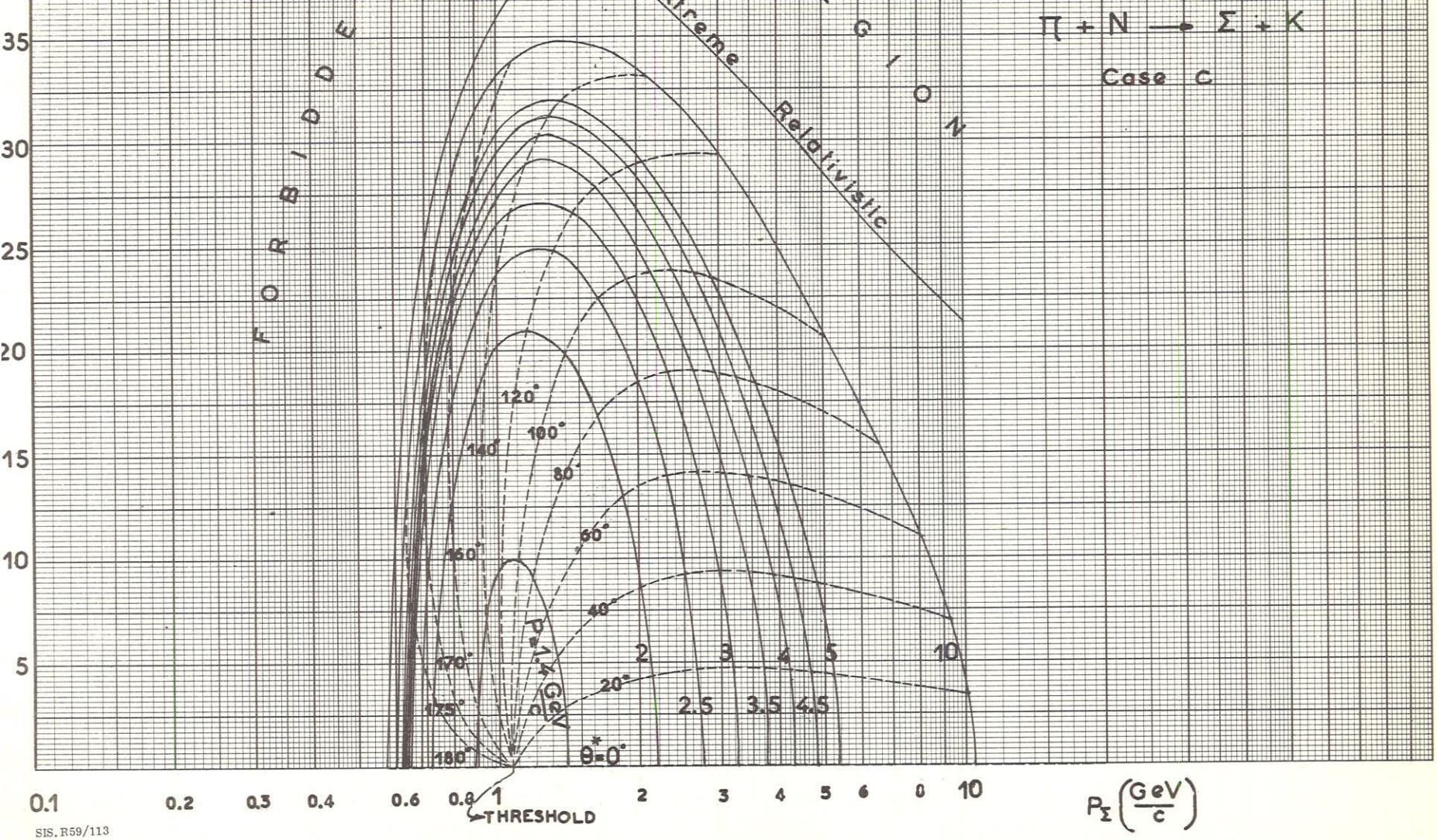
Extreme Relativistic
REGION
$\pi + N \longrightarrow \Sigma + K$
Case C
120°
100°
140°
80°
160°
60°
40°
20°
170°
175°
180°
$\theta^* = 0°$
$P_K = 1.4$ GeV/c
2
3
4
5
10
2.5
3.5
4.5
35
30
25
20
15
10
5
0.1
0.2
0.3
0.4
0.6
0.8
1
THRESHOLD
2
3
4
5
6
8
10
$P_\Sigma \left(\frac{GeV}{c}\right)$

SIS. R59/113

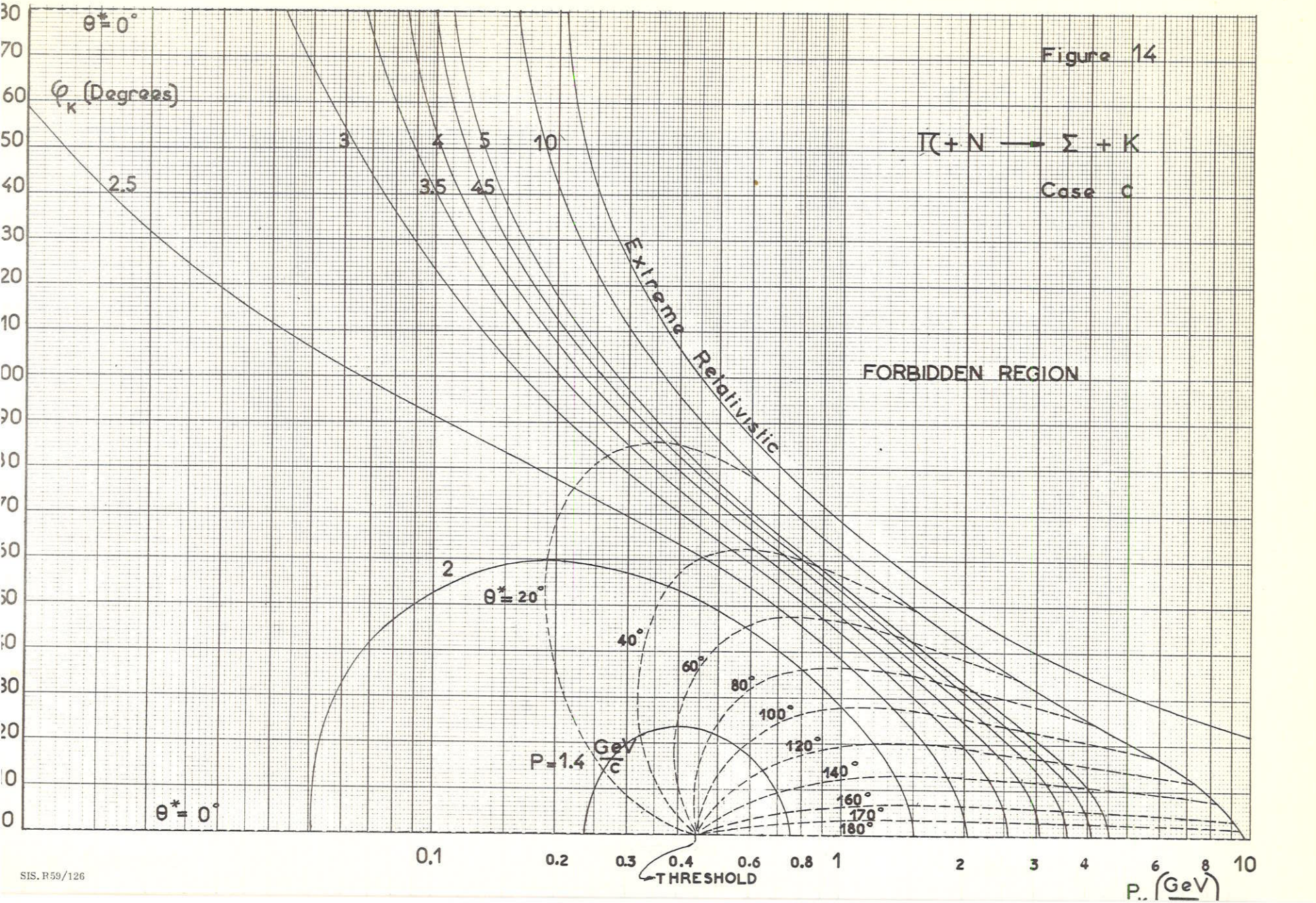
Figure 14
$\pi^- + N \longrightarrow \Sigma + K$
Case C
φ_K (Degrees)
$\theta^* = 0°$
2.5
3
3.5
4
4.5
5
10
Extreme Relativistic
FORBIDDEN REGION
2
$\theta^* = 20°$
40°
60°
80°
100°
120°
140°
160°
170°
180°
P = 1.4 GeV/c
$\theta^* = 0°$
0.1
0.2
0.3
0.4
0.6
0.8
1
2
3
4
6
8
10
THRESHOLD
P_π (GeV)

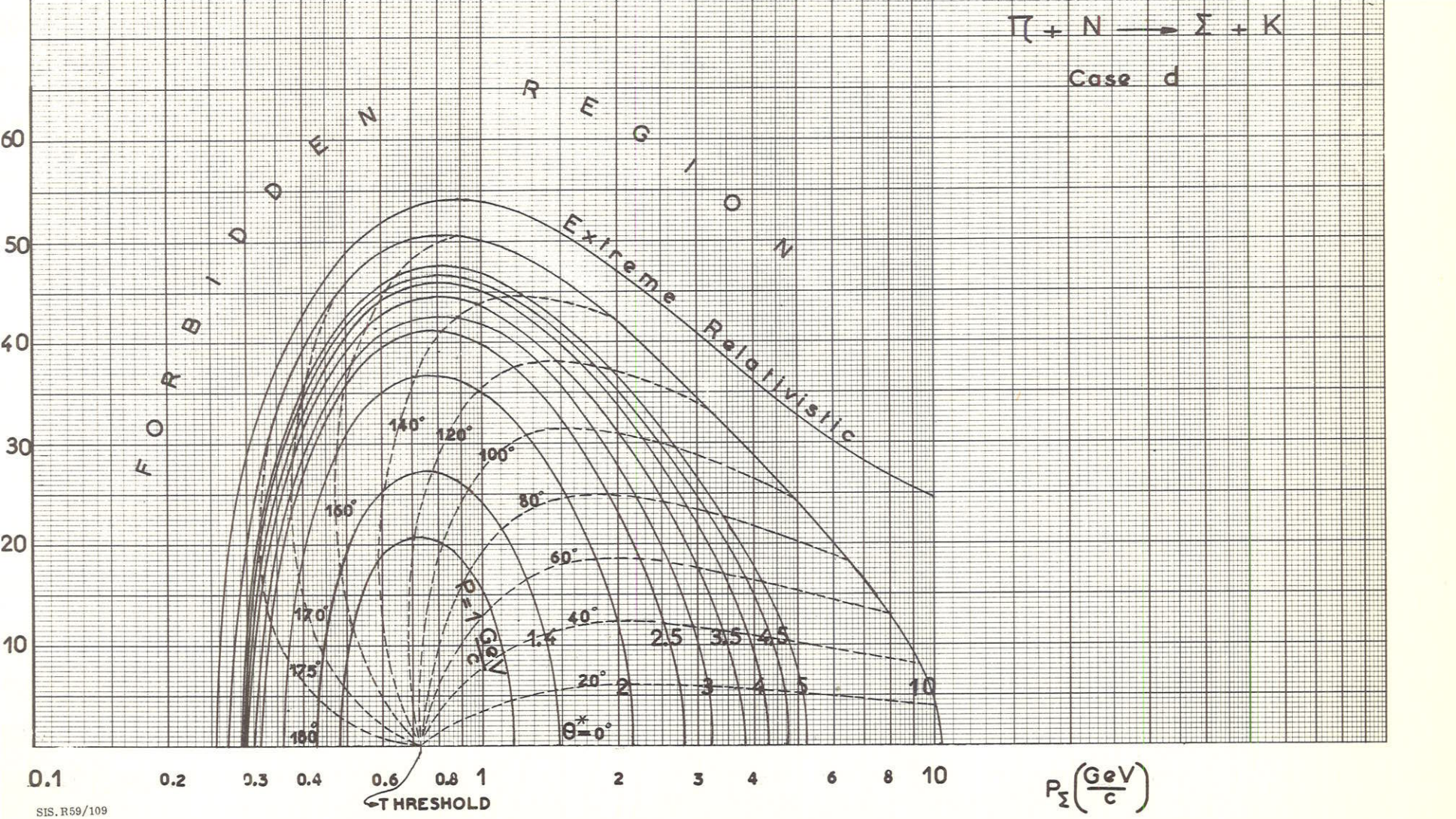
$\pi^- + N \longrightarrow \Sigma^- + K^+$
Case d
FORBIDDEN REGION
Extreme Relativistic
140°
120°
100°
80°
160°
60°
170°
40°
175°
20°
180°
θ*=0°
1.4 GeV/c
1.5
2.5
3.5
4.5
2
3
4
5
10
60
50
40
30
20
10
0.1
0.2
0.3
0.4
0.6
0.8
1
2
3
4
6
8
10
THRESHOLD
$P_\Sigma \left(\frac{GeV}{c}\right)$

SIS. R59/109

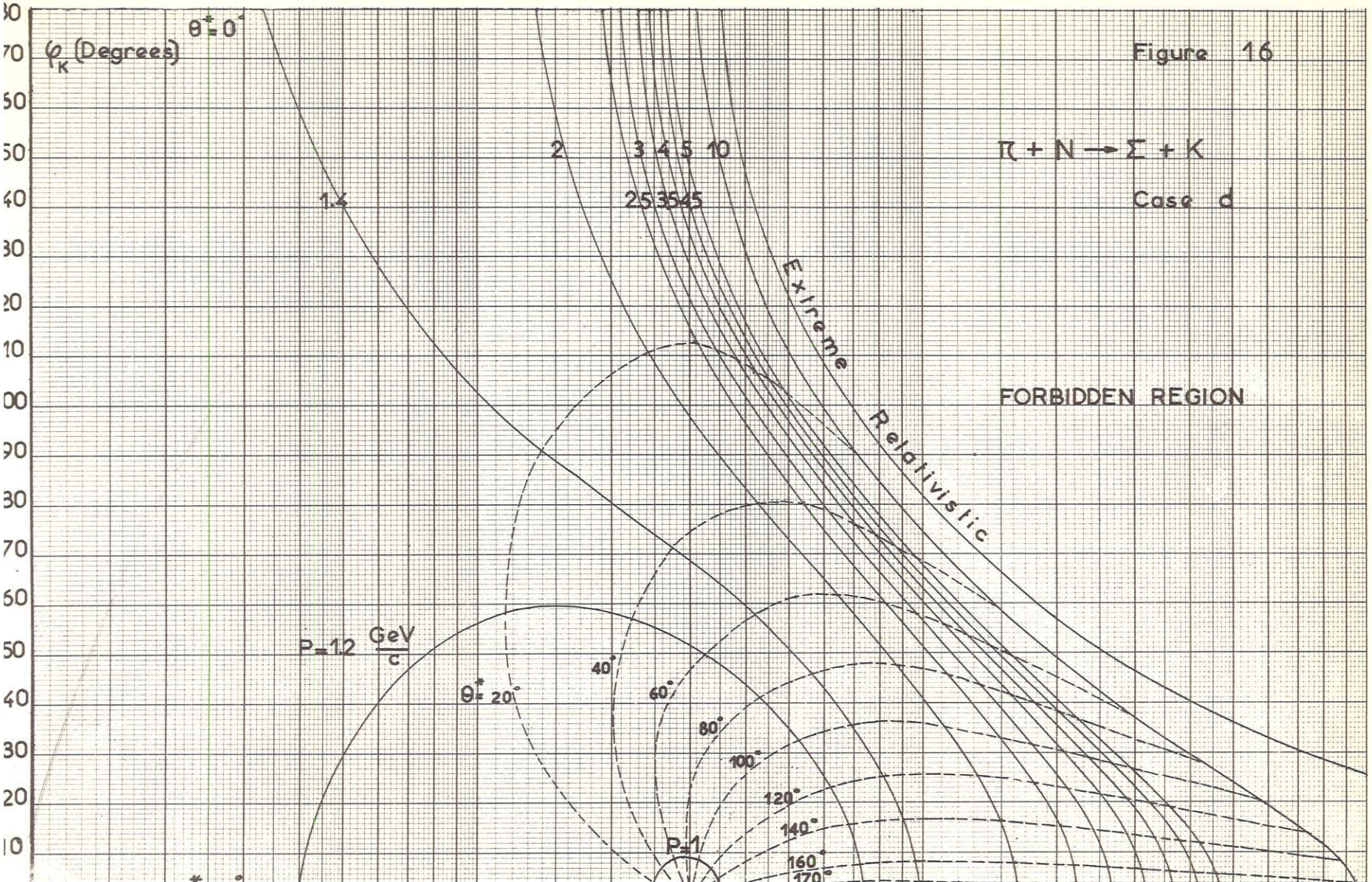
Figure 16
$\pi + N \rightarrow \Sigma + K$
Case d
φ_K (Degrees)
$\theta^* = 0^\circ$
1.4
2
3 4 5 10
2 5 3 5 4 5
Extreme Relativistic
FORBIDDEN REGION
P=1.2 GeV/c
$\theta^* = 20^\circ$
40°
60°
80°
100°
120°
140°
160°
170°
P=1

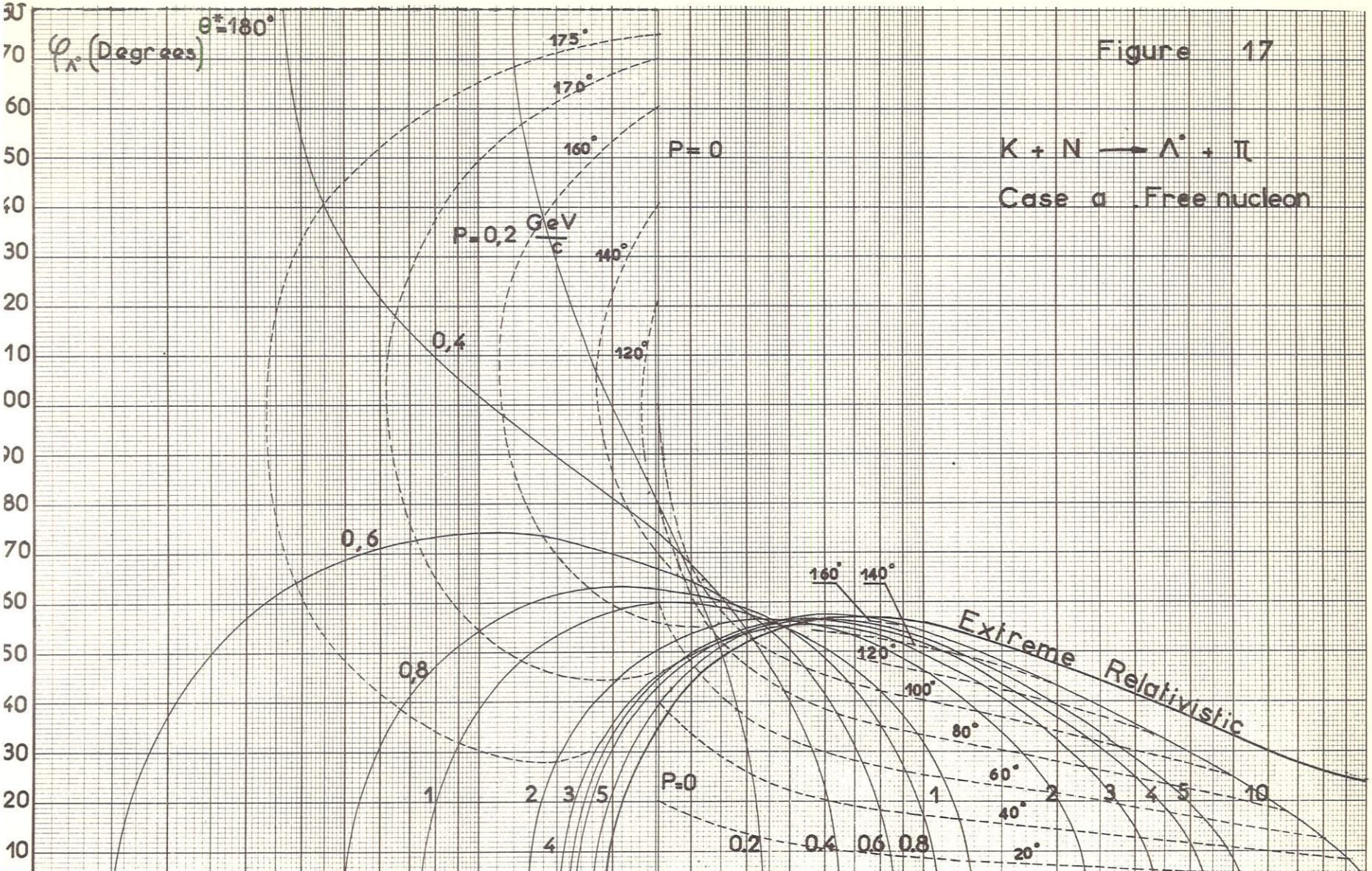
Figure 17
$K + N \longrightarrow \Lambda^{\circ} + \pi$
Case a Free nucleon
$\varphi_{\Lambda^{\circ}}$ (Degrees)
$\theta^{*}_{\Lambda^{\circ}} = 180^{\circ}$
P = 0
P = 0,2 GeV/c
Extreme Relativistic
175°
170°
160°
140°
120°
100°
80°
60°
40°
20°
0,4
0,6
0,8
1
2
3
4
5
10
0.2
0.4
0.6
0.8

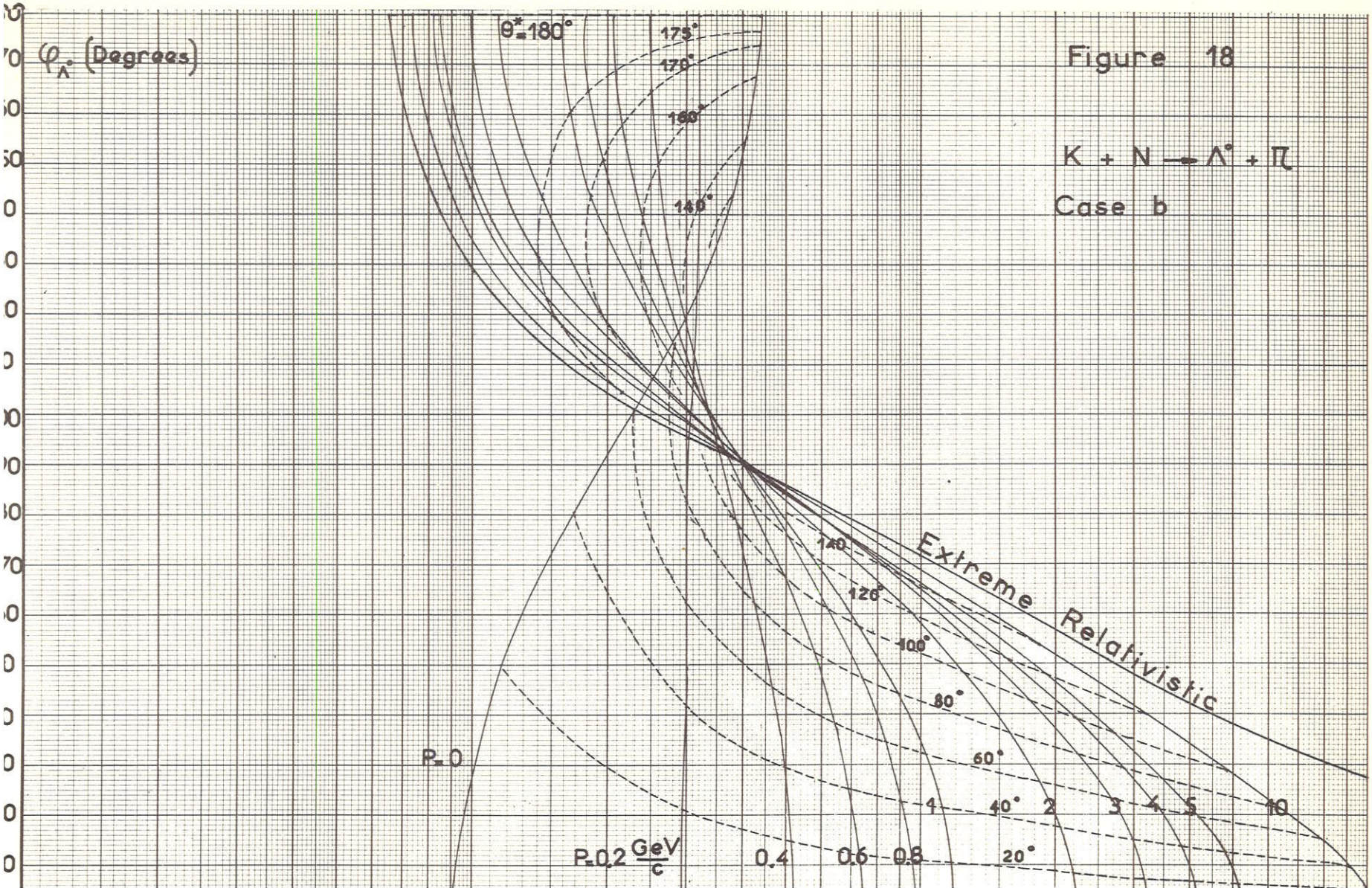
φ_{Λ° (Degrees)
$\theta^*=180^\circ$
175°
170°
160°
140°
140°
126°
100°
80°
60°
40°
20°
Extreme Relativistic
P=0
P=0.2 GeV/c
0.4
0.6
0.8
1
2
3
4
5
10
Figure 18
K + N → Λ° + π
Case b

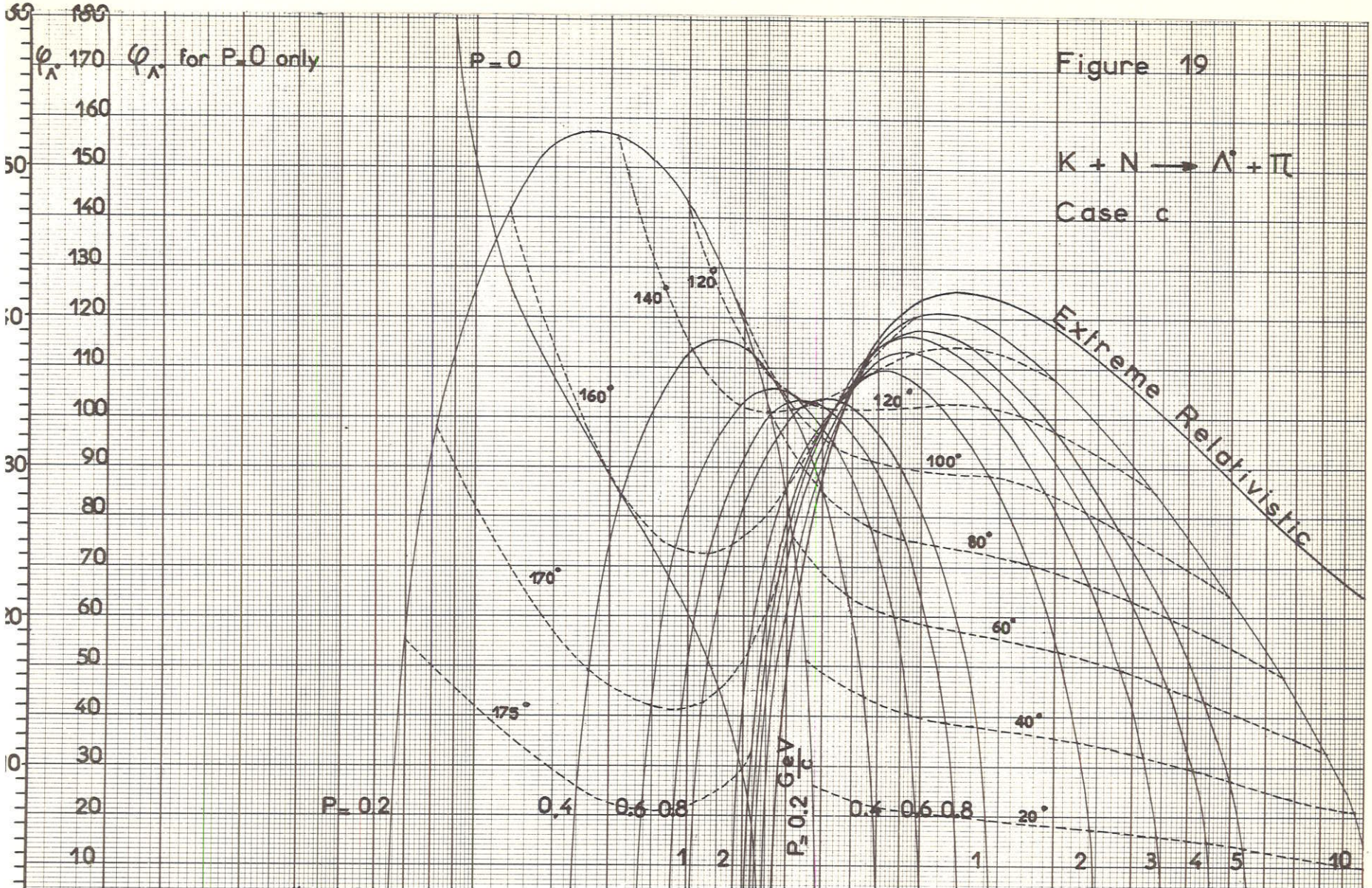
Figure 19
K + N → Λ° + π
Case c
Extreme Relativistic
P = 0
φ_{Λ° for P = 0 only
φ_{Λ°
P = 0.2 GeV/c
P = 0.2
140°
120°
160°
120°
100°
80°
170°
60°
175°
40°
20°
0.4
0.6
0.8
1
2
3
4
5
10

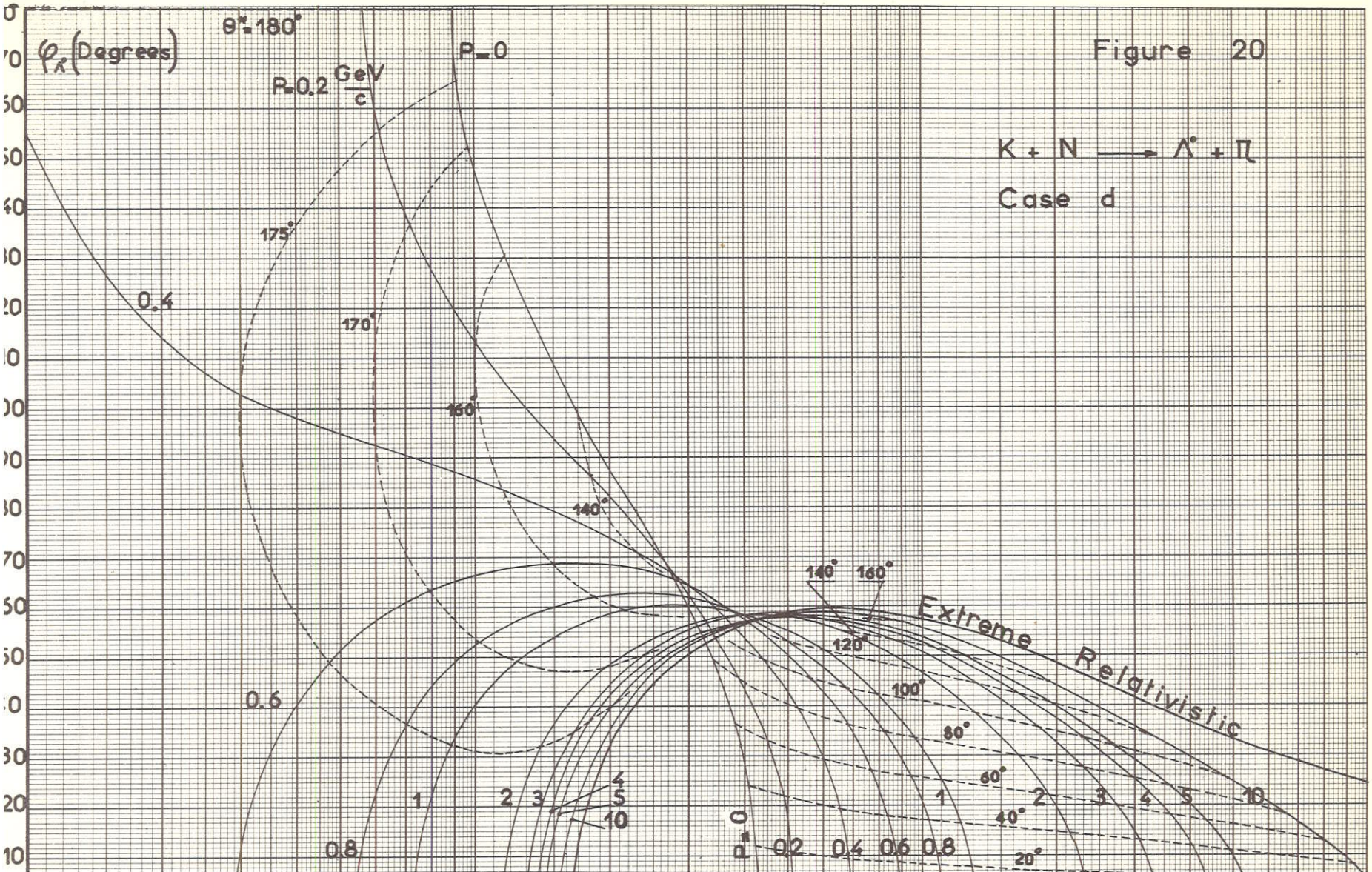
Figure 20
K + N ⟶ Λ° + π
Case d
θ*=180°
P=0
R=0.2 GeV/c
φ* (Degrees)
175°
170°
160°
140°
120°
100°
80°
60°
40°
20°
0°
0.4
0.6
0.8
1
2
3
4
5
10
Extreme Relativistic
n
0
02
0.4
0.6
0.8

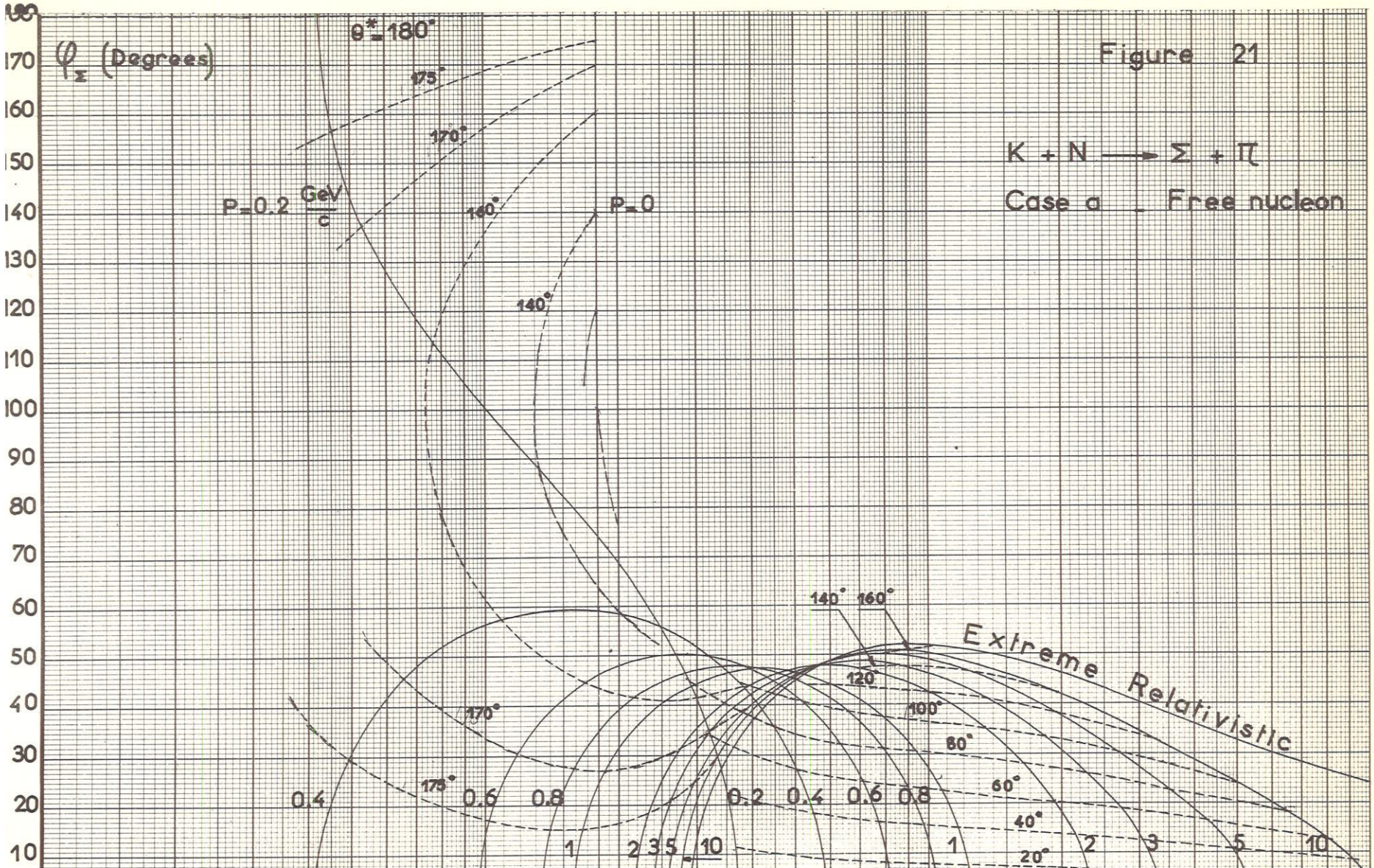
Figure 21
$K + N \longrightarrow \Sigma + \pi$
Case a - Free nucleon
φ_Σ (Degrees)
$\theta^*_\pi = 180°$
P=0.2 GeV/c
P=0
Extreme Relativistic
175°
170°
160°
140°
120°
100°
80°
60°
40°
20°
0.4
0.6
0.8
0.2
1
2
3
5
10

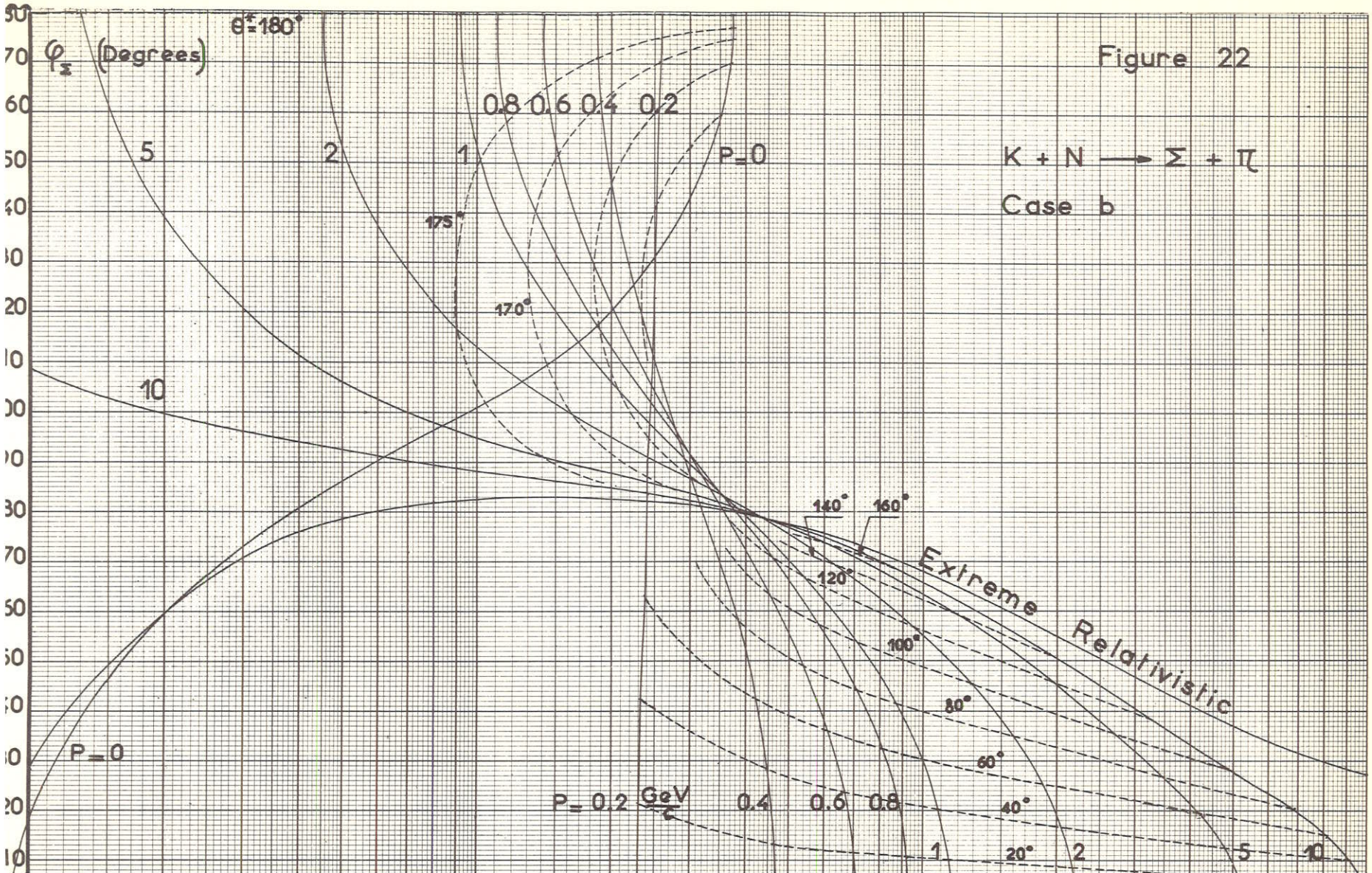
Figure 22
K + N ⟶ Σ + π
Case b
φ_Σ (Degrees)
$\theta^*=180^\circ$
0.8 0.6 0.4 0.2
5
2
1
P=0
175°
170°
10
140°
160°
120°
100°
80°
60°
40°
20°
Extreme Relativistic
P=0
P= 0.2 GeV/c
0.4
0.6
0.8
1
2
5
10

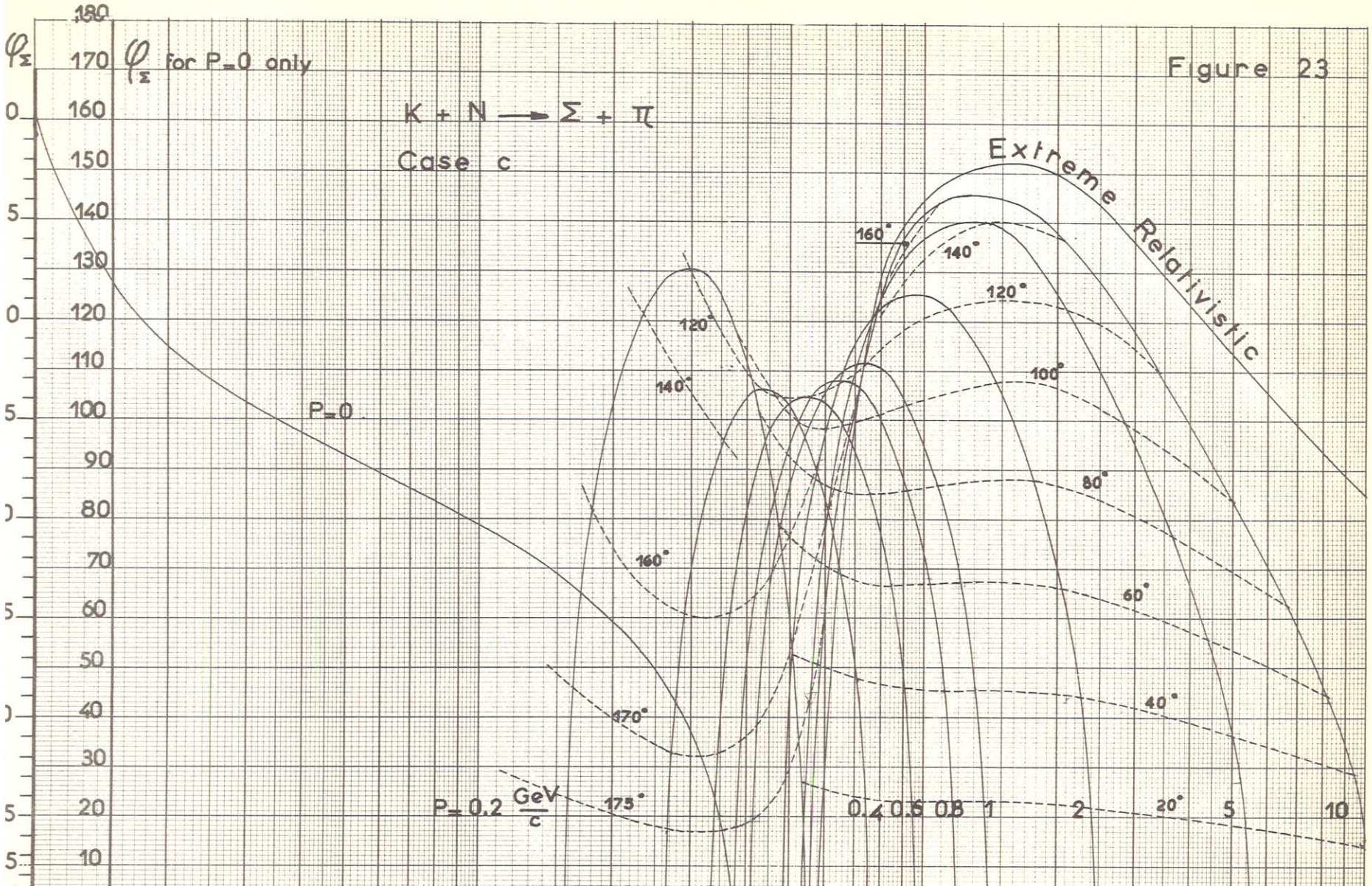
Figure 23
$K + N \longrightarrow \Sigma + \pi$
Case c
φ_Σ for P=0 only
φ_Σ
180
170
160
150
140
130
120
110
100
90
80
70
60
50
40
30
20
10
P=0
P= 0.2 GeV/c
175°
170°
160°
140°
120°
160°
140°
120°
100°
80°
60°
40°
20°
Extreme Relativistic
0.4 0.6 0.8 1 2 5 10

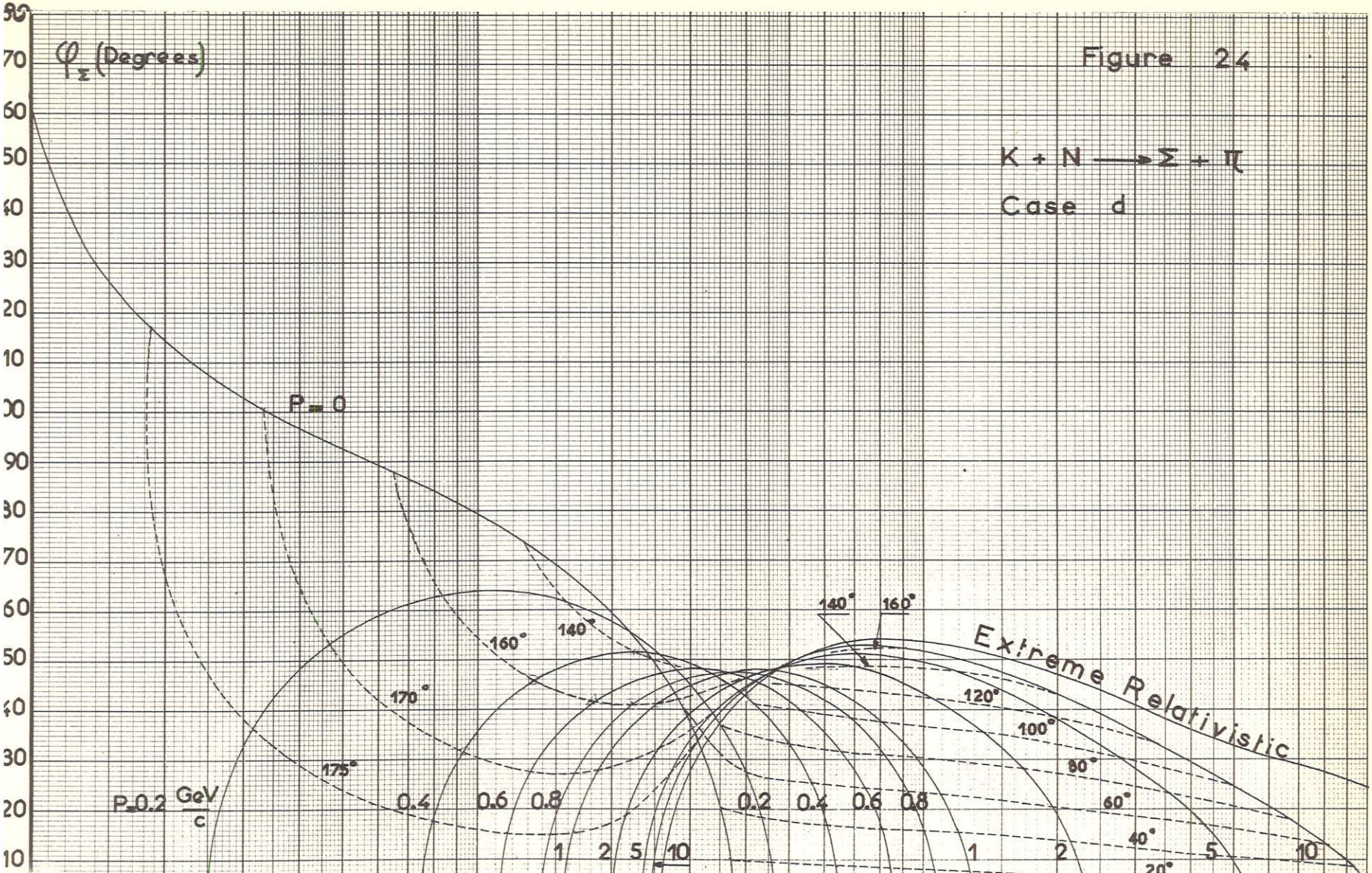
φ_Σ (Degrees)
Figure 24
K + N ⟶ Σ + π
Case d
P = 0
160°
140°
170°
175°
120°
100°
80°
60°
40°
20°
Extreme Relativistic
P=0.2 GeV/c
0.4
0.6
0.8
1
2
5
10
0.2
0.4
0.6
0.8
1
2
5
10

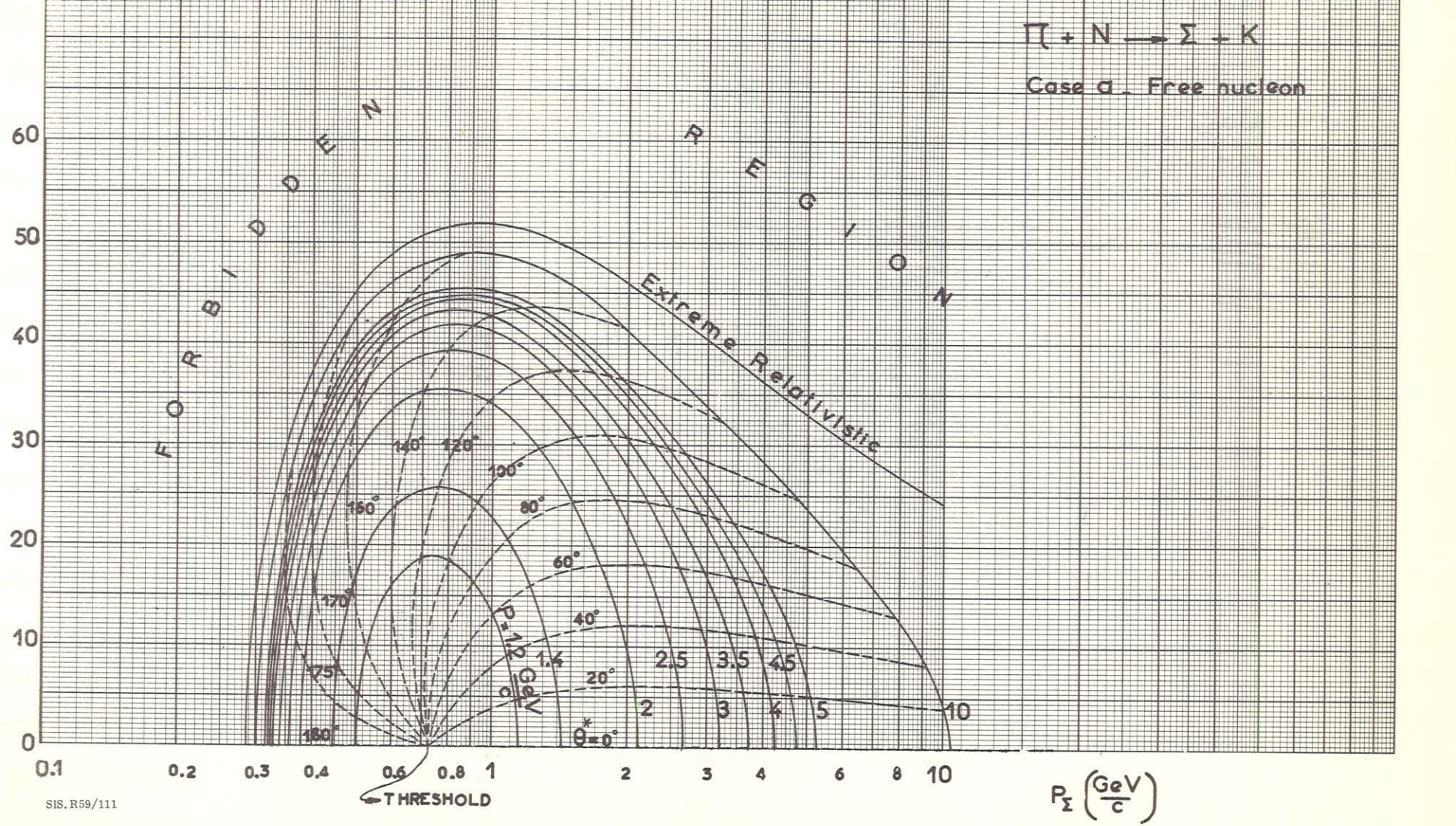
$\pi^- + N \rightarrow \Sigma + K$
Case a. Free nucleon
FORBIDDEN REGION
Extreme Relativistic
140°
120°
100°
80°
160°
60°
170°
40°
175°
20°
180°
P=1.2 GeV/c
1.4
2.5
3.5
4.5
2
3
4
5
10
θ*=0°
60
50
40
30
20
10
0
0.1
0.2
0.3
0.4
0.6
0.8
1
2
3
4
6
8
10
THRESHOLD
$P_\Sigma \left(\frac{GeV}{c}\right)$

SIS. R59/111

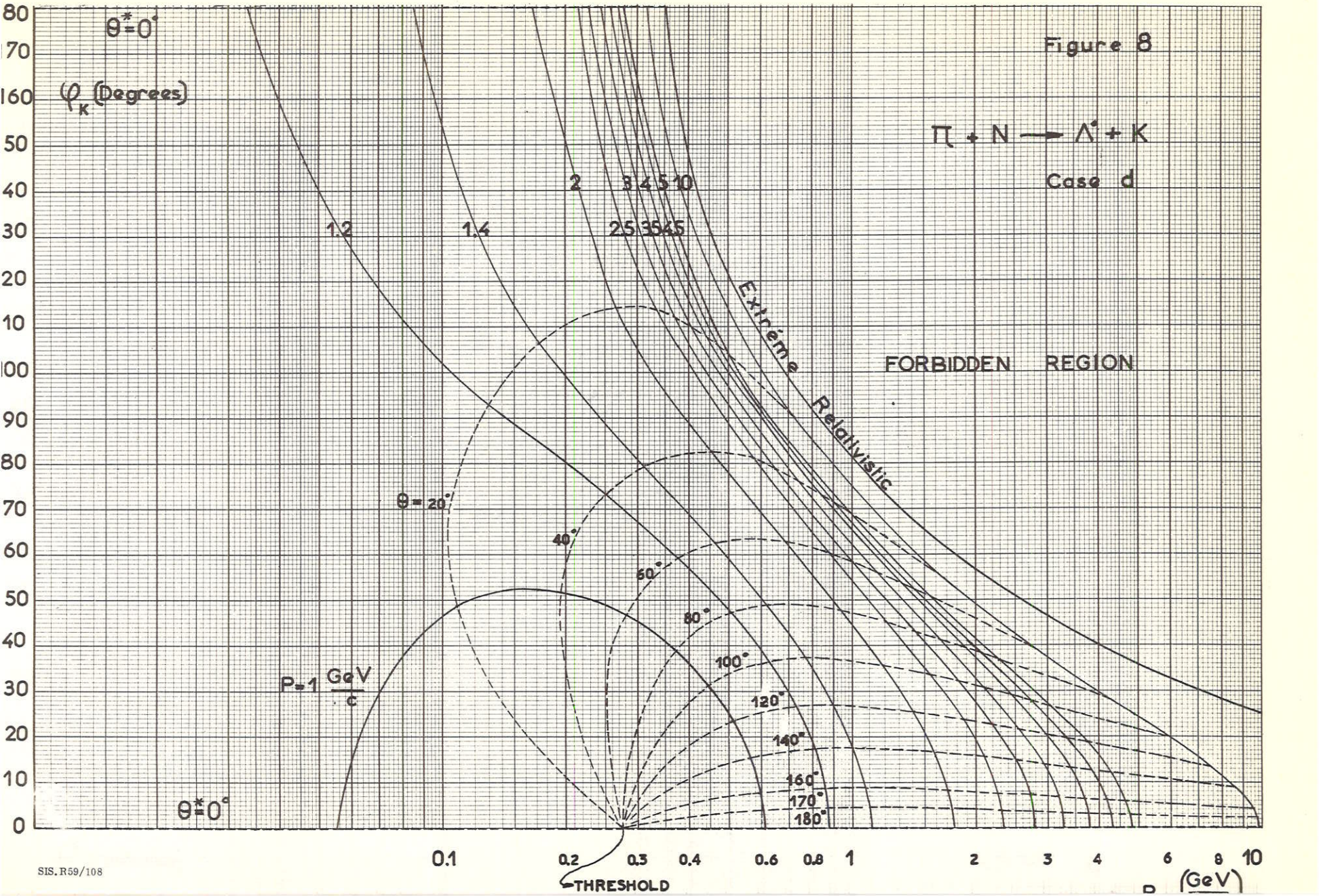
Figure 8
$\pi + N \rightarrow \Lambda^{\circ} + K$
Case d
$\theta^{*}=0^{\circ}$
φ_K (Degrees)
1.2
1.4
2
3 4 5 10
25 35 45
Extreme Relativistic
FORBIDDEN REGION
$\theta = 20^{\circ}$
40°
60°
80°
100°
120°
140°
160°
170°
180°
P = 1 GeV/c
$\theta^{*}=0^{\circ}$
0.1
0.2
0.3
0.4
0.6
0.8
1
2
3
4
6
8
10
THRESHOLD
P (GeV)

SIS. R59/108

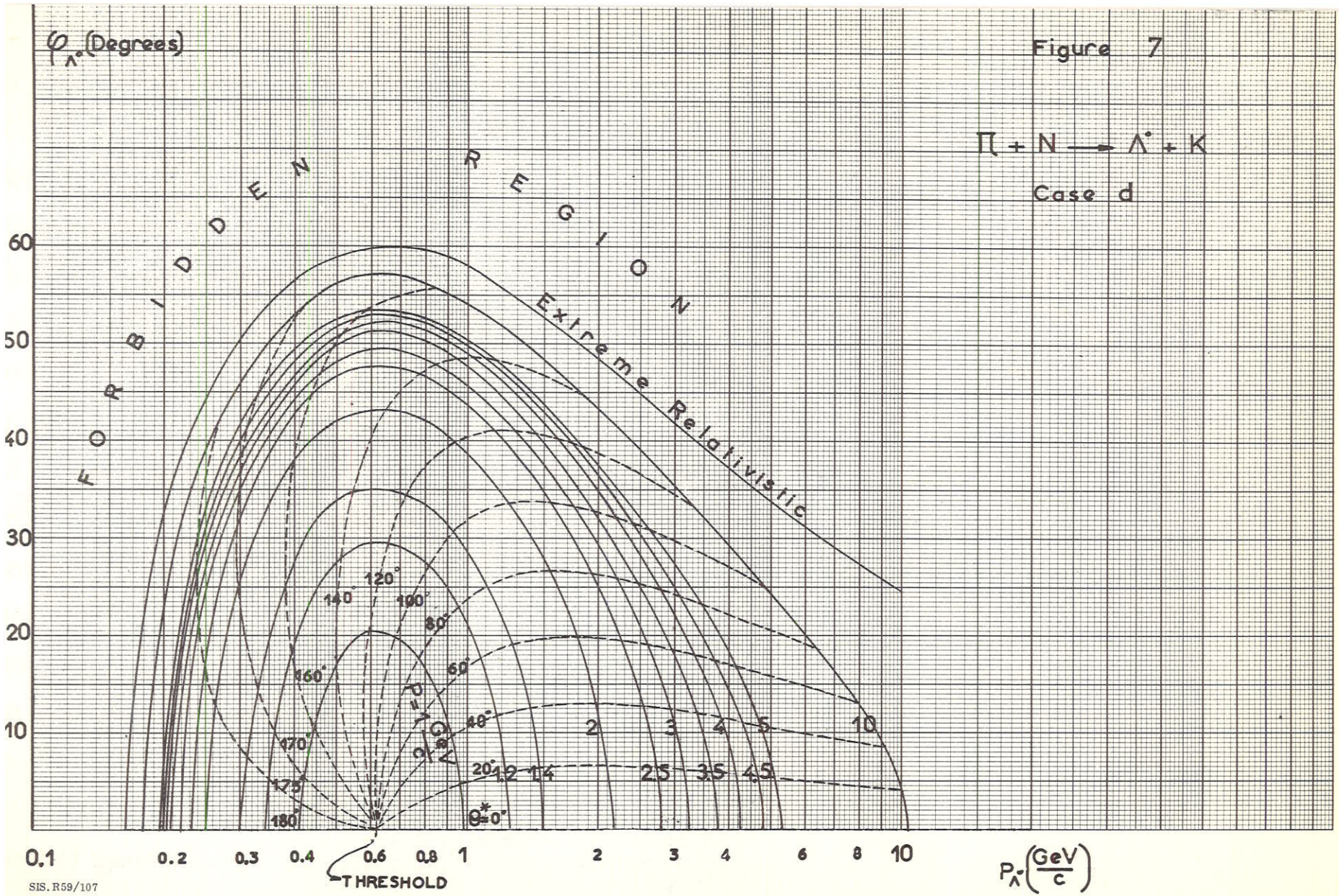
φ_{Λ° (Degrees)
Figure 7
$\pi^- + N \longrightarrow \Lambda^\circ + K$
Case d
FORBIDDEN REGION
Extreme Relativistic
60
50
40
30
20
10
120°
140°
100°
80°
160°
60°
40°
170°
20°
175°
180°
$\theta^*=0°$
2
3
4
5
10
1.2
1.4
2.5
3.5
4.5
0.1
0.2
0.3
0.4
0.6
0.8
1
2
3
4
6
8
10
THRESHOLD
$P_{\Lambda^\circ}\left(\frac{GeV}{c}\right)$

SIS. R59/107

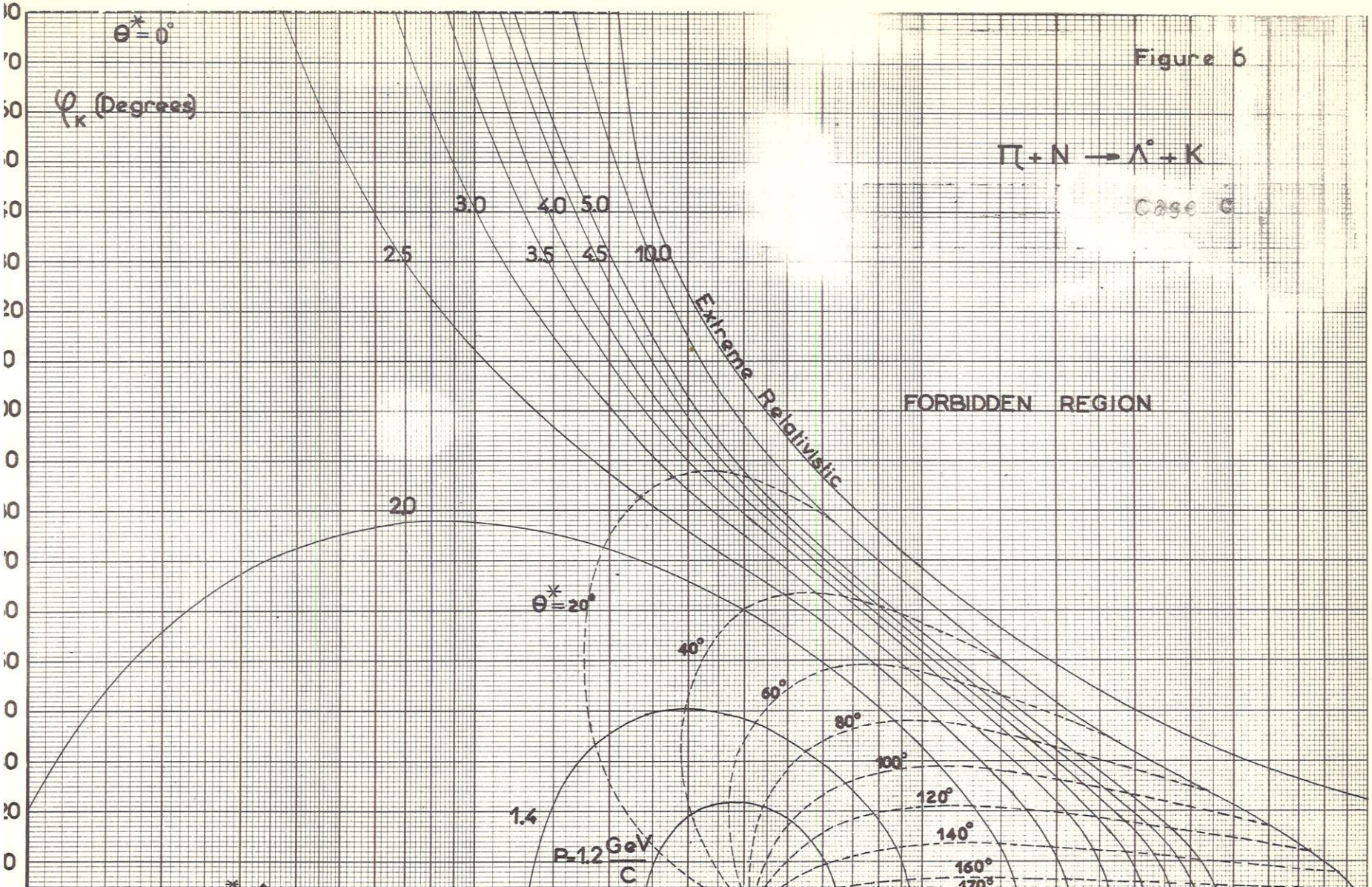
Figure 6
$\pi^- + N \rightarrow \Lambda^\circ + K$
Case C
$\theta^* = 0^\circ$
φ_K (Degrees)
3.0
4.0
5.0
2.5
3.5
4.5
10.0
Extreme Relativistic
FORBIDDEN REGION
2.0
$\theta^* = 20^\circ$
40°
60°
80°
100°
120°
140°
160°
170°
1.4
P=1.2 GeV/C

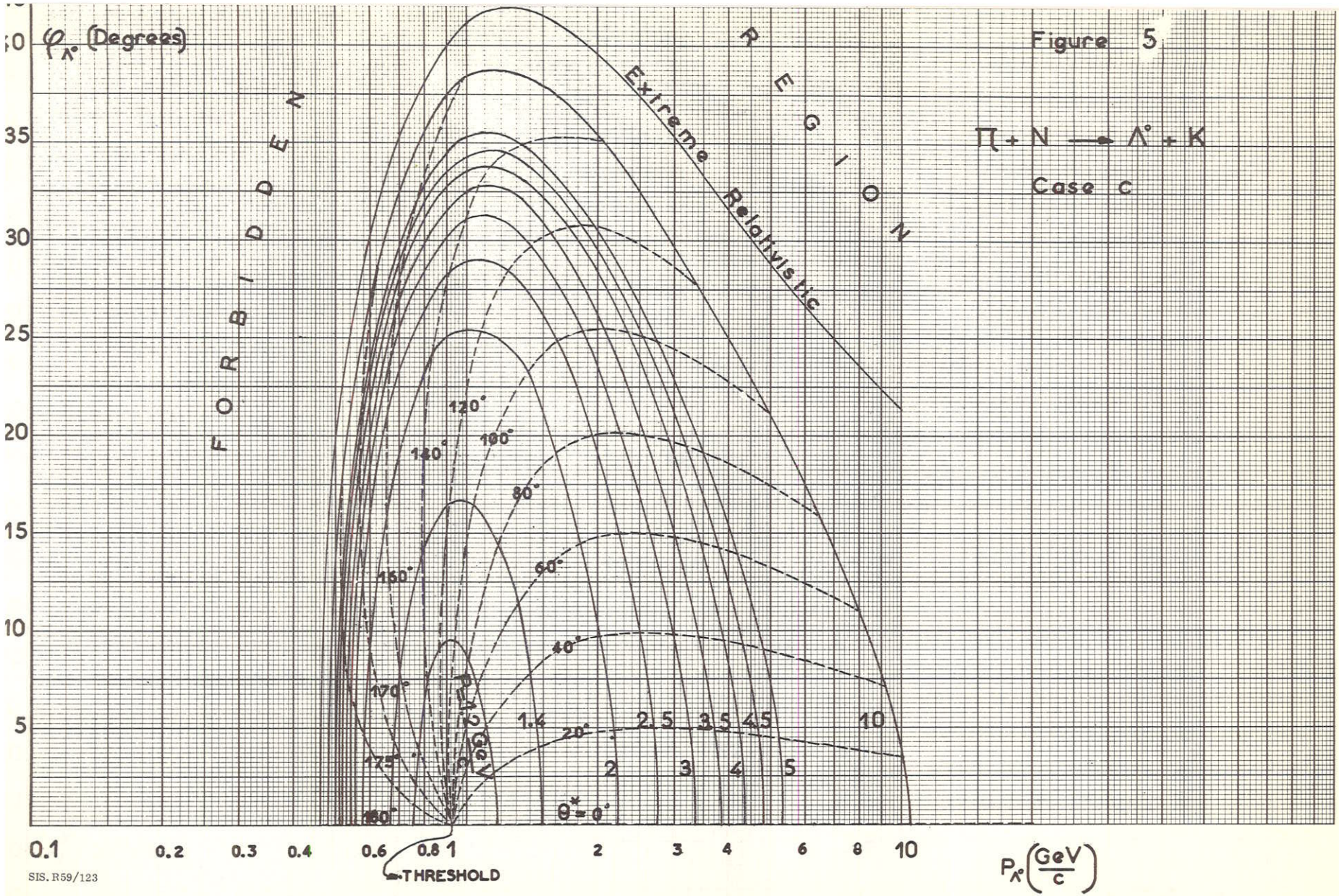

Figure 5

$\pi^- + N \longrightarrow \Lambda^\circ + K$

Case c

SIS. R59/123

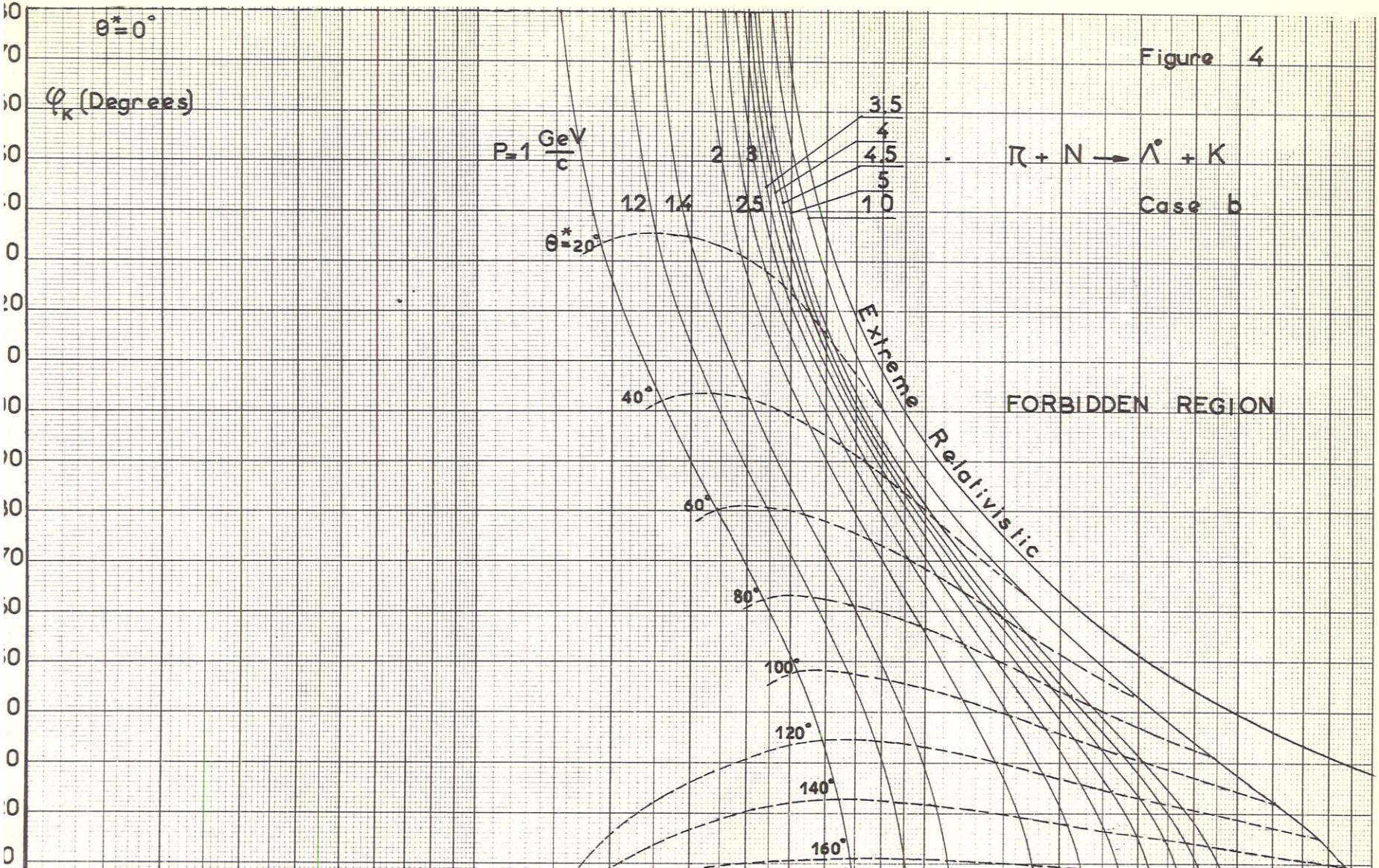
Figure 4
$\theta^*=0^\circ$
φ_K (Degrees)
$P=1\ \frac{GeV}{c}$
2
3
3.5
4
4.5
5
10
1.2
1.4
2.5
$\pi + N \rightarrow \Lambda^\circ + K$
Case b
$\theta^*=20^\circ$
40°
60°
80°
100°
120°
140°
160°
Extreme Relativistic
FORBIDDEN REGION

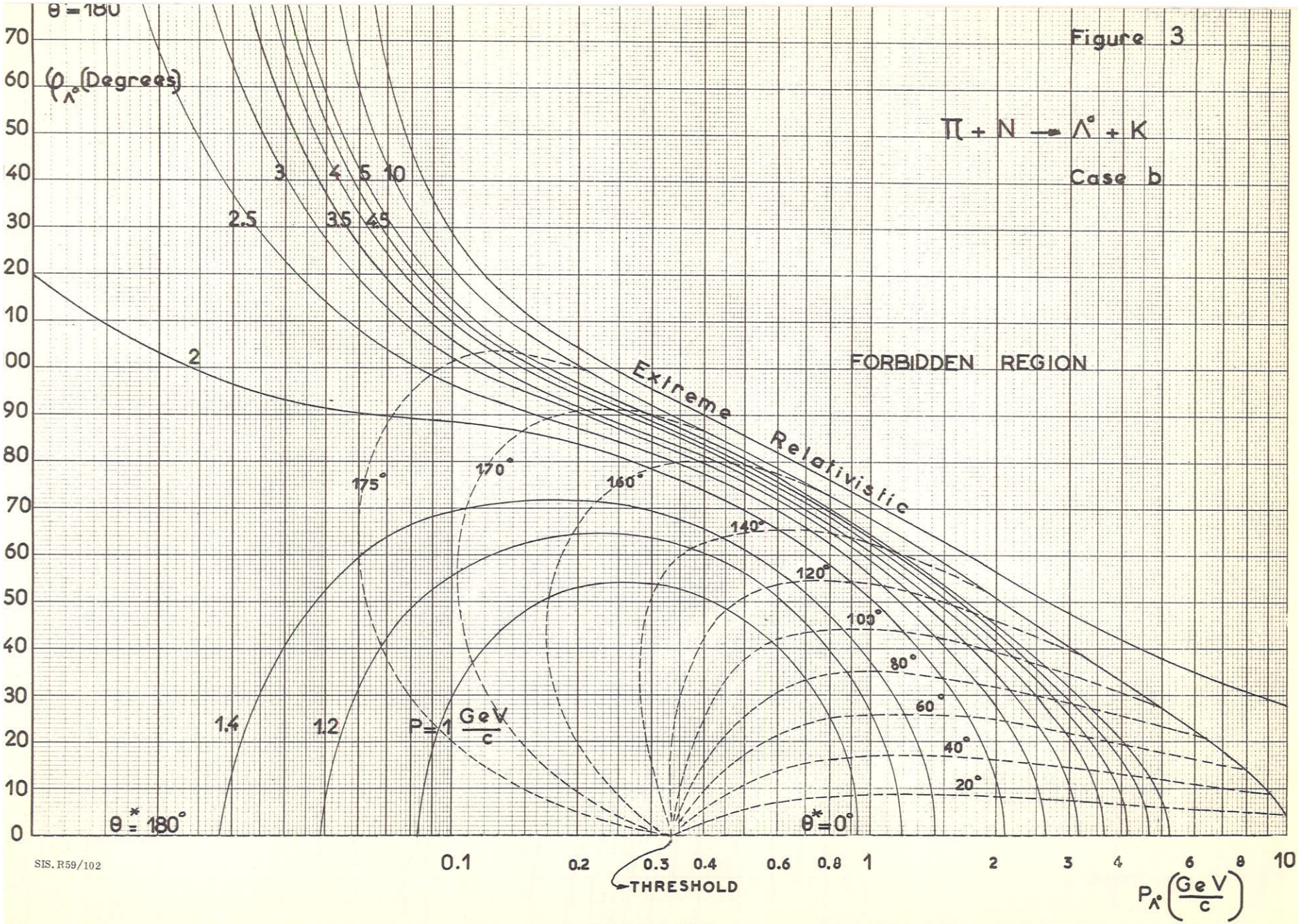
Figure 3
$\pi + N \rightarrow \Lambda^\circ + K$
Case b
$\theta = 180$
θ_{Λ° (Degrees)
FORBIDDEN REGION
Extreme Relativistic
2
2.5
3
3.5
4
4.5
5
10
175°
170°
160°
140°
120°
100°
80°
60°
40°
20°
1.4
1.2
P = 1 GeV/c
$\theta^* = 180°$
$\theta^* = 0°$
THRESHOLD
P_{Λ° (GeV/c)
SIS. R59/102

Figure 2

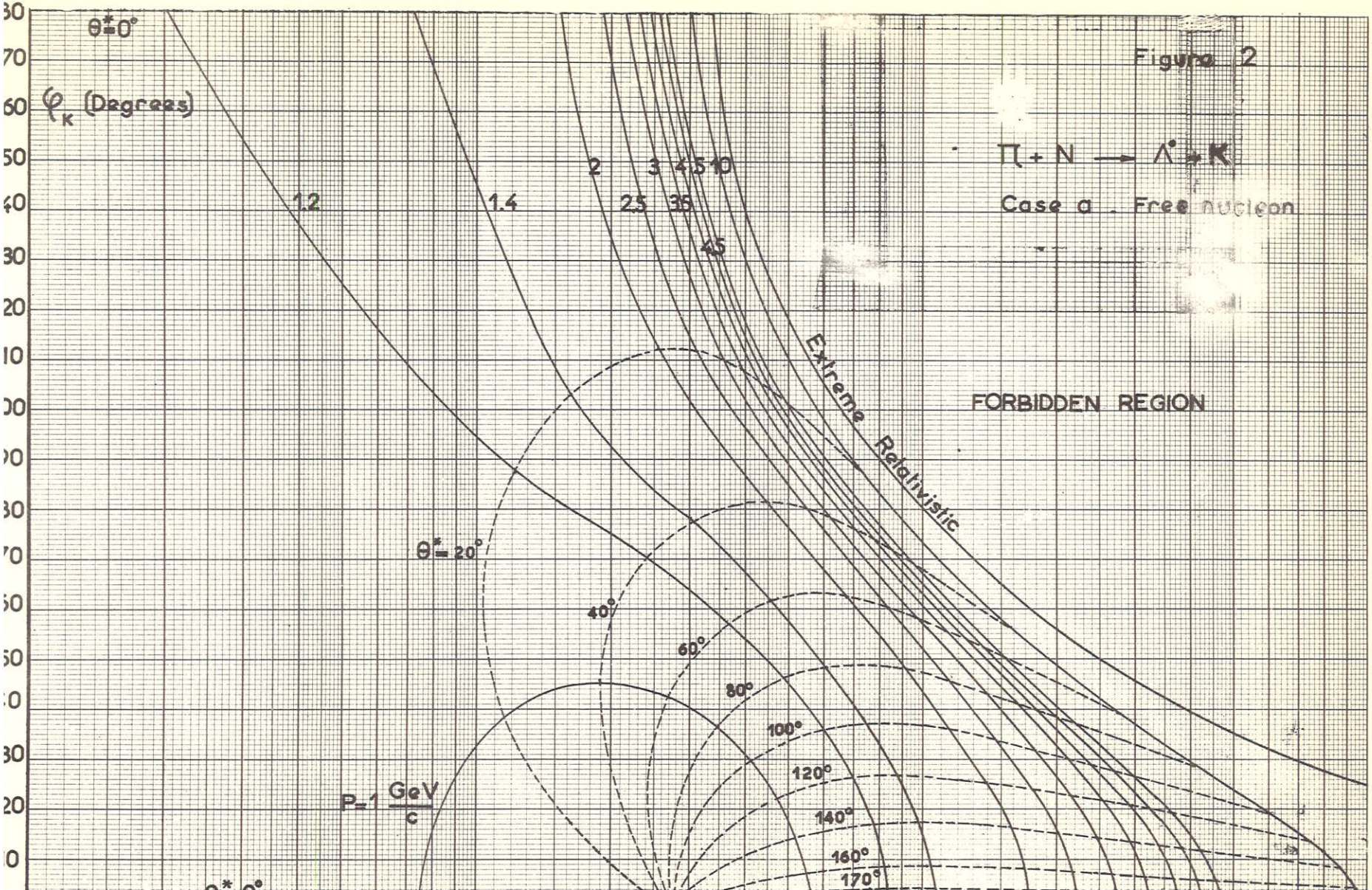
$\pi^- + N \rightarrow \Lambda^\circ + K^+$
Case a . Free nucleon
φ_K (Degrees)
$\theta^*=0°$
$\theta^*=20°$
1.2
1.4
2
2.5
3
3.5
4
5
10
15
Extreme Relativistic
FORBIDDEN REGION
40°
60°
80°
100°
120°
140°
160°
170°
P=1 GeV/c

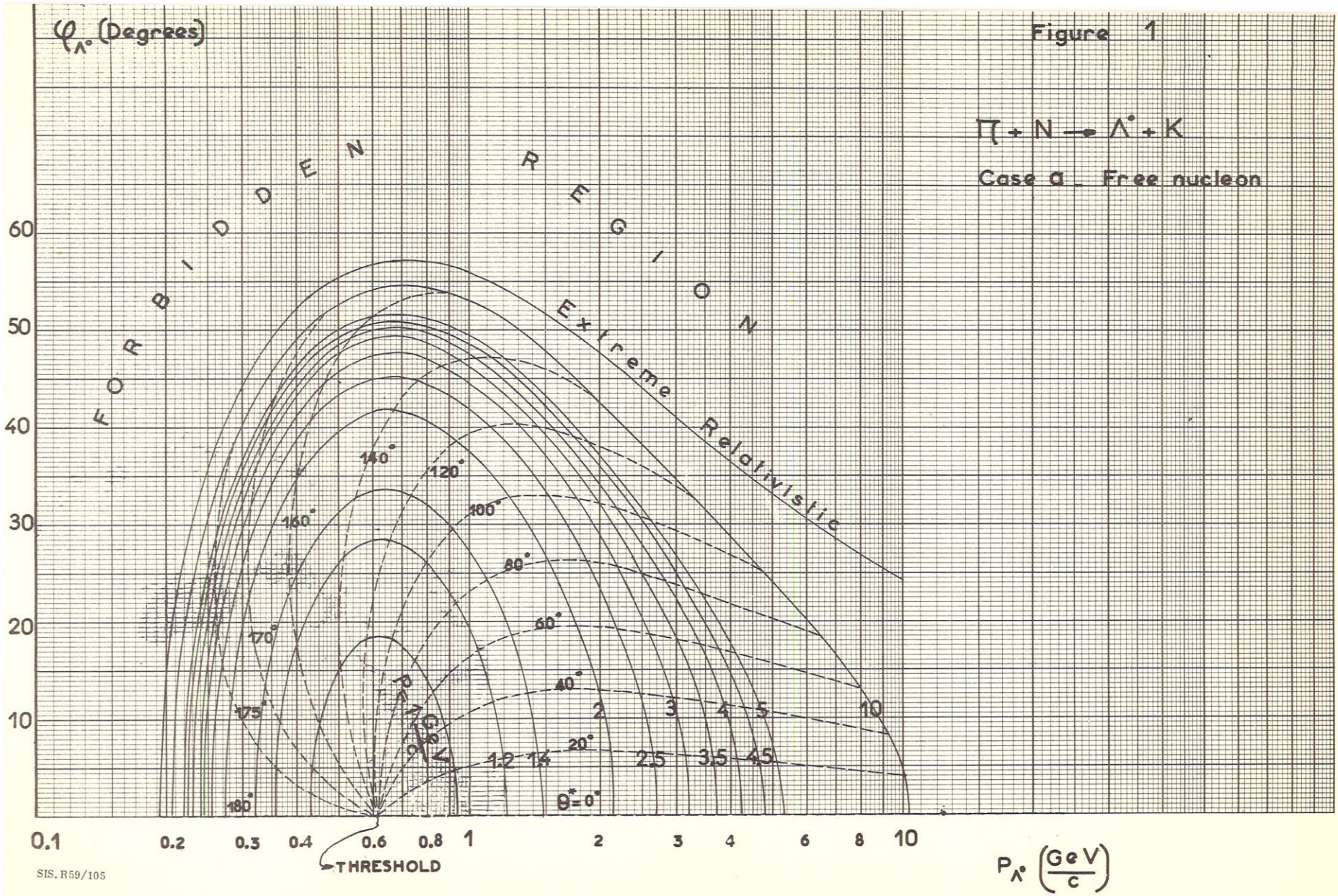
φ_{Λ° (Degrees)
Figure 1
$\pi^+ + N \rightarrow \Lambda^\circ + K$
Case a _ Free nucleon
FORBIDDEN REGION
Extreme Relativistic
60
50
40
30
20
10
140°
120°
160°
100°
80°
170°
60°
40°
175°
20°
180°
$\theta^*=0°$
1.2
1.4
2
2.5
3
3.5
4
4.5
5
10
0.1
0.2
0.3
0.4
0.6
0.8
1
2
3
4
6
8
10
THRESHOLD
P_{Λ° $\left(\frac{GeV}{c}\right)$
SIS. R59/105

APPENDIX II

ABSENCE OF ANGULAR CORRELATION BETWEEN PLANES

As was explained in chapter IV, the angle between the planes of the two V-decays and the angles between these two planes and the plane determined by the two lines of flight were measured for each event. The results are given in Tables 4.4 to 4.11. Although it is a negative result, it is worth mentioning that several combinations were tried with these angles but no correlation was found.

* * *

A C K N O W L E D G E M E N T S

The author is very grateful to Professors P.M.S. Blackett and G.D. Rochester for their interest and for the facilities provided to the author's work at the Physics Department of the Manchester University.

The author wishes to thank Mr. J.A. Newth for continuous encouragement and help, and for many discussions during the period when this work was being prepared. The author is indebted to Professor H.S. Bridge for the interest devoted in reading the manuscript and for many stimulating criticisms.

Thanks are due to Dr. A. Zichichi for having kindly helped with some measurements and to Mr. L. Montanet for assistance with some of the drawings of Appendix I. Other members of the team contemporary with the author have been J.S. Buchanan, A.H. Chapman, W.A. Cooper, G.D. James, S.O. Larson, E.G. Michaelis, D.D. Millar, D.I. Page, B. Powell, H. Steiner and H. Filthuth, L. Montanet, G. Petrucci and A. Zichichi. To the last four and to J.A. Newth, the author is grateful for having spared him from some of the team work during part of the time when this work was done.

* * *

REFERENCES

In the references the abbreviation : I.C.M.R.D.P. (1957) will stand for "International Conference on Mesons and Recently Discovered Particles, Padua-Venice, September 1957 - Mimeographed Report."

1) G.D. James andR.A. Salmeron: Phil. Mag. 46, 571 (1955).

2) W.A. Cooper, R. Filthuth, J.A. Newth and R.A. Salmeron: Il Nuovo Cimento, 4, 390 (1956).

3) W.A. Cooper, H. Filthuth, J.A. Newth, G. Petrucci, R.A. Salmeron and A. Zichichi: Il Nuovo Cimento, 4, 1433 (1956).

4) W.A. Cooper, H. Filthuth, J.A. Newth, G. Petrucci, R.A. Salmeron and A. Zichichi: Il Nuovo Cimento, 5, 1388 (1957).

5) J.A. Newth and R.A. Salmeron: Experiments, Supplementum VI, 36 (1957).

6) W.A. Cooper, H. Filthuth, L. Montanet, J.A. Newth, G. Petrucci, R.A. Salmeron and A. Zichichi: "Neutral V-particles from Copper and Carbon", Il Nuovo Cimento (in the press).

7) G.D. Rochester and C.C. Butler: Nature, 160, 855 (1947).

8) Y. Nambu, K. Nishijima and Y. Yanaguchi: Prog. Theor. Phys., 6, 615 (1951).

9) D. Lal, Y. Pal and B. Peters: Proc. In . Acad. Sci., 38, 398 (1953).

10) W.B. Fowler, R.P. Shutt, A.M. Thorndike and W.L. Whittemore: Phys.Rev., 91, 128 (1953); Ibid., 93, 861 (1954); Ibid., 98, 121 (1955).

11) C. Dahanayake, P.E. François, Y. Fujimoto, P. Iredale, C.J. Waddington and M. Yasin: Phil.Mag., 45, 855 (1954).

12) A. Debenedetti, C.M. Garelli, L. Tallone and M. Vigone: Il Nuovo Cimento, 12, 369 (1954); Ibid. 12, 466 (1954).

13) R.W. Thompson, J.R. Burwell, R.W. Huggett and C.J. Karzmark: Phys.Rev. 95, 1576 (1954).

14) H. Blumenfeld, E.T. Booth, L.M. Lederman, W. Chinowsky: Bull.Am.Phys.Soc.Ser.II, 1, 63 (1956).

15) H. Blumenfeld: Ph.D. Thesis, Columbia University (1957).

16) W. Chinowsky, K. Lande and L.M. Lederman: I.C.M.R.D.P. (1957).

17) R. Budde, M. Chretien, J. Leitner, N.P. Samios, M. Schwartz and J. Steinberger: Phys.Rev., 103, 1827 (1956).

18) F. Eisler, R. Plano, N. Samios, M. Schwartz and J. Steinberger: Il Nuovo Cimento, 5, 1700 (1957).

19) F.R. Eisler, R. Plano, N. Samios, M. Schwartz, J. Steinberger, P. Bassi, V. Borelli, N. Tanaka, P. Waloshek, A. Zoboli, M. Conversi, P. Franzini, I. Mannelli, R. Santangelo and V. Silvestrini: I.C.M.R.D.P. (1957).

20) J.L. Brown, J. Cronin, S. de Benedetti, D.A. Glaser, D.I. Meyer, M.L. Perl and J. van der Velde: I.C.M.R.D.P. (1957).

21) J.L. Brown, D.A. Glaser, C. Groves and M.L. Perl: I.C.M.R.D.P. (1957).

22) P. Baumel, G. Harris, J. Orear and S. Taylor: I.C.M.R.D.P. (1957).

23) C. Besson, J. Crussard, V. Fouché, J. Hennessy, G. Kayas, V.P. Parikh and G. Trilling: Il Nuovo Cimento, 6, 1168 (1957).

24) E. Boldt, H.S. Bridge, D.O. Caldwell and Y. Pal: I.C.M.R.D.P. (1957).

25) V.L. Fitch, W.K.F. Panofsky, R. Motley and W. Chestnut: I.C.M.R.D.P. (1957).

26) A. Silverman, R.R. Wilson and W.M. Woodward: I.C.M.R.D.P. (1957).

27) Staff, California Institute of Technology Synchrotron: I.C.M.R.D.P. (1957).

28) G. Maenchen, W.B. Fowler, W.M. Powell, G. Saphir, R.W. Wright: Phys.Rev., 100, 1802 (1955).

29) E. Amaldi, C.D. Anderson, P.M.S. Blackett, W.B. Fretter, L. Leprince-Ringuet, B. Peters, C.F. Powell, G.D. Rochester, B. Rossi and R.W. Thompson: Nature, 173, 123 (1954).

30) E. Boldt, H.S. Bridge, D.O. Caldwell and Y. Pal: I.C.M.R.D.P. (1957).

31) R. Armenteros, A. Astier, C. d'Andlau, B. Grégory, A. Hendel, J. Hennessy, A. Lagarrigue, L. Leprince-Ringuet, F. Muller, Ch. Peyrou and R.R. Rau: Suppl. Il Nuovo Cimento, 4, 541 (1956).

32) M.M. Block, E.M. Harth, W.B. Fowler, R.P. Shutt, A.M. Thorndike and W.L. Whittemore: Phys.Rev., 99, 261 (1955).

33) J.D. Sorrels, R.B. Leighton and C.D. Anderson : Phys. Rev. 100, 1457 (1955).

34) W.B. Fowler, G. Maenchen, W.M. Powell, G. Saphir and R. Wright: Phys.Rev. 103, 208 (1956).

35) J. Ballam, D.R. Harris, A.L. Hodson, R.R. Rau, G.T. Reynolds, S.B. Treiman and M. Vidale: Phys. Rev., 91, 1019 (1953).

36) G.H. Trilling and R.B. Leighton: Phys.Rev., 104, 1703 (1956).

37) G.T. Reynolds and S.B. Treiman: Phys.Rev., 94, 207 (1954).

38) J.A. Newth: Suppl. Il Nuovo Cimento, 11, 297 (1954).

39) R. Armenteros, K.H. Barker, C.C. Butler, A. Cachon and A.H. Chapman: Nature, 167, 501 (1951).

40) J.S. Buchanan: Journ.Sci.Instr., 31, 136 (1954).

41) J.S. Buchanan: Ph.D. Thesis, Manchester University (1954).

55) M. Goldhaber: Phys.Rev., 101, 433 (1956).

56) A. Salam and J.C. Polkinghorne : Il Nuovo Cimento, 2, 685 (1955).

57) J. Schwinger: Phys.Rev., 104, 1164 (1956).

58) D.C. Peaslee: Phys.Rev., 86, 127 (1952).

59) T.D. Lee and C.N. Yang: Phys.Rev., 104, 254 (1956).

60) C.S. Wu, E. Ambler, R.W. Hayward, D.D. Hoppes and R.P. Hudson: Phys.Rev., 105, 1413 (1957).

61) R.L. Garwin, L.M. Lederman and M. Weinrich: Phys.Rev. 105, 1415 (1957).

62) B. Rossi: "High Energy Particles", p. 358 (Prentice - Hall Incorporated, New York, 1952).

63) C. d'Andlau, R. Armenteros, A. Astier, H.C. Destaebler, B.P. Gregory, L. Leprince-Ringuet, F. Muller, C. Peyrou and J.H. Tinlot: Il Nuovo Cimento, 5, 1135 (1957).

64) K. Lande, E.T. Booth, J. Impeduglia, L.M. Lederman and W. Chinowsky: Phys.Rev., 103, 1901 (1956).

65) M. Gell-Mann and A. Pais: Phys.Rev., 97, 1387 (1955).

66) J.P. Astbury: Il Nuovo Cimento, 12, 387 (1954).

67) J. Podolanski and R. Armenteros: Phil.Mag., 45, 13 (1954).

68) H.S. White: University of California, Radiation Laboratory - Report No. 3514 (1956).